



National Library
of Canada

Bibliothèque nationale
du Canada

Canadian Theses Service

Service des thèses canadiennes

Ottawa, Canada
K1A 0N4

NOTICE

The quality of this microform is heavily dependent upon the quality of the original thesis submitted for microfilming. Every effort has been made to ensure the highest quality of reproduction possible.

If pages are missing, contact the university which granted the degree.

Some pages may have indistinct print especially if the original pages were typed with a poor typewriter ribbon or if the university sent us an inferior photocopy.

Reproduction in full or in part of this microform is governed by the Canadian Copyright Act, R.S.C. 1970, c. C-30, and subsequent amendments.

AVIS

La qualité de cette microforme dépend grandement de la qualité de la thèse soumise au microfilmage. Nous avons tout fait pour assurer une qualité supérieure de reproduction.

S'il manque des pages, veuillez communiquer avec l'université qui a conféré le grade.

La qualité d'impression de certaines pages peut laisser à désirer, surtout si les pages originales ont été dactylographiées à l'aide d'un ruban usé ou si l'université nous a fait parvenir une photocopie de qualité inférieure.

La reproduction, même partielle, de cette microforme est soumise à la Loi canadienne sur le droit d'auteur, SRC 1970, c. C-30, et ses amendements subséquents.



National Library
of Canada

Bibliothèque nationale
du Canada

Canadian Theses Service Service des thèses canadiennes

Ottawa, Canada
K1A 0N4

The author has granted an irrevocable non-exclusive licence allowing the National Library of Canada to reproduce, loan, distribute or sell copies of his/her thesis by any means and in any form or format, making this thesis available to interested persons.

The author retains ownership of the copyright in his/her thesis. Neither the thesis nor substantial extracts from it may be printed or otherwise reproduced without his/her permission.

L'auteur a accordé une licence irrévocable et non exclusive permettant à la Bibliothèque nationale du Canada de reproduire, prêter, distribuer ou vendre des copies de sa thèse de quelque manière et sous quelque forme que ce soit pour mettre des exemplaires de cette thèse à la disposition des personnes intéressées.

L'auteur conserve la propriété du droit d'auteur qui protège sa thèse. Ni la thèse ni des extraits substantiels de celle-ci ne doivent être imprimés ou autrement reproduits sans son autorisation.

ISBN 0-315-55563-7

Canada

THE UNIVERSITY OF ALBERTA

**ESTIMATION OF FAULT LOCATION
USING CURVE FITTING TECHNIQUES**

BY

SALWA S. FOU DA

A THESIS

SUBMITTED TO THE FACULTY OF GRADUATE STUDIES AND RESEARCH
IN PARTIAL FULFILMENT OF THE REQUIREMENTS FOR THE DEGREE
OF MASTER OF SCIENCE

DEPARTMENT OF ELECTRICAL ENGINEERING

EDMONTON, ALBERTA

FALL 1989

The UNIVERSITY OF ALBERTA

RELEASE FORM

NAME OF AUTHOR: SALWA S. FOUDA

TITLE OF THESIS: ESTIMATION OF FAULT LOCATION USING CURVE
FITTING TECHNIQUES

DEGREE FOR WHICH THESIS WAS PRESENTED: MASTER OF SCIENCE

YEAR THIS DEGREE GRANTED: FALL 1989

Permission is hereby granted to THE UNIVERSITY OF ALBERTA LIBRARY to reproduce single copies of this thesis and to lend or sell such copies for private, scholarly or scientific research purposes only.

The author reserves other publication rights, and neither the thesis nor extensive extracts from it may be printed or otherwise reproduced without the author's written permission.

(SIGNED) Salwa Foude

PERMANENT ADDRESS:

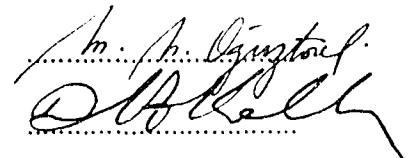
DATED May 26th 19 89

THE UNIVERSITY OF ALBERTA
FACULTY OF GRADUATE STUDIES AND RESEARCH

The undersigned certify that they have read, and recommend to the Faculty of Graduate Studies and Research, for acceptance, a thesis entitled ESTIMATION OF FAULT LOCATION USING CURVE FITTING TECHNIQUES submitted by SALWA S. FOUDA in partial fulfilment of the requirements for the degree of MASTER OF SCIENCE.


.....

Supervisor


.....

DATE May 24-89.

اِهْدَايِ..

إلى والدتي ووالدي

"To my mother and father"

ABSTRACT

Two methods involving curve fitting techniques for locating transmission line faults are studied and tested. The first method is based on the least error square approach, while the second is based on the least absolute value approach.

Using the above methods, a simulation program is developed in order to determine the fault location on a transmission line. Two power system models are used. The first model is a single phase power system, while the second one is a three phase power system model. Only the symmetrical three-phase fault is tested in the three-phase power system model. The effect of the fault resistance as well as the shunt capacitance on the accuracy of both techniques is studied. Also the effect of using different orders of low-pass filter is investigated. As well, a comparison between these two techniques is conducted.

ACKNOWLEDGEMENT

I would like to thank my supervisor, Professor G.S.Christensen. His effort and patience have been most appreciated.

iv thanks are due to Dr. S.A.Soliman. His comments and advice were a great help to me.

The financial support that has been provided by the Department of Electrical Engineering at the University of Alberta, as well as the Natural Sciences and Engineering Research Council of Canada is greatly appreciated.

Last, but not least, to my husband, Hossam, for his encouragement and help throughout my studies, for which words of appreciation simply do not suffice.

TABLE OF CONTENTS

| | |
|--|----|
| <i>Chapter 1: Introduction</i> | 1 |
| <i>Chapter 2: Theory of Fault Location Algorithm</i> | 8 |
| 2.1 Curve Fitting Techniques..... | 8 |
| 2.1.1 Least Error Square Technique..... | 9 |
| 2.1.2 Least Absolute Value Technique..... | 13 |
| 2.2 Application of Curve Fitting Techniques..... | 15 |
| 2.2.1 Impedance Calculation..... | 15 |
| 2.2.2 Least Error Square Solution..... | 22 |
| 2.2.3 Least Absolute Value Technique..... | 25 |
| 2.3 Determination of the Fault Location from the Impedance.... | 28 |
| 2.4 Advantages of LSV and LAV Techniques..... | 29 |
| <i>Chapter 3: The Transmission Line Model</i> | 31 |
| 3.1 Modelling of The Systems..... | 31 |
| 3.1.1 Single-Phase Power System..... | 31 |
| 3.1.2 Three-Phase Power System..... | 34 |
| 3.1.2.1 Pre-Fault Circuit..... | 35 |
| 3.1.2.2 Post-Fault Circuit..... | 36 |

| | |
|---|------------|
| 3.2 Design of Low-Pass Digital Filters..... | 40 |
| <i>Chapter 4: Numerical Results From The Fault Location Techniques.....</i> | <i>53</i> |
| 4.1 Numerical Results of Single-Phase Power System..... | 54 |
| 4.1.1 Effect of Sampling Rate..... | 55 |
| 4.1.2 Effect of Time Reference..... | 60 |
| 4.1.3 Effect of Varying The Number of Equations..... | 62 |
| 4.2 Numerical Results of The Three Phase Power System..... | 67 |
| 4.2.1 Effect of The Low-Pass Filter..... | 68 |
| 4.2.1.1 Effect of The Order of The Filter..... | 68 |
| 4.2.1.2 Effect of Time Delay..... | 69 |
| 4.2.1.3 A Comparison Between The LAV and LSV Tech- niques..... | 69 |
| 4.2.2 Effect of Line Shunt Capacitance..... | 70 |
| 4.2.3 Effect of Fault Resistance..... | 71 |
| <i>Chapter 5: Conclusion.....</i> | <i>118</i> |
| 5.1 Summary..... | 118 |
| 5.2 Future Work..... | 118 |
| 5.3 Concluding Remarks..... | 119 |
| <i>References.....</i> | <i>121</i> |
| <i>Appendix A: Single-Phase Power System Parameters.....</i> | <i>124</i> |

| | |
|--|-----|
| <i>Appendix B: Three-Phase Power System Parameters</i> | 126 |
| <i>Appendix C: Synthesizing The Digital Filters</i> | 127 |
| <i>Appendix D: Computer Implementation</i> | 135 |
| <i>Appendix E: Pseudoinverse</i> | 145 |
| <i>Appendix F: -</i> | 147 |

List of Tables

| | | |
|------|--|----|
| 4.1 | The Estimates of Fault Location at Different Values of Sampling Rate | 73 |
| 4.2 | The Estimates of Fault Location at Different Values of Sampling Rate | 74 |
| 4.3 | The Estimates of Fault Location at Different Values of Sampling Rate | 75 |
| 4.4 | The Estimates of Fault Location at Different Values of Sampling Rate | 76 |
| 4.5 | The Estimates of Fault Location at Different Values of Sampling Rate | 77 |
| 4.6 | The Estimates of Fault Location at Different Values of Sampling Rate | 78 |
| 4.7 | Estimates of Fault Location at Different Values of Time Reference | 79 |
| 4.8 | Estimates of Fault Location at Different Values of Time Reference | 80 |
| 4.9 | Estimates of Fault Location at Different Values of Time Reference | 81 |
| 4.10 | Estimates of Fault Location at Different Values of Time Reference | 82 |
| 4.11 | Estimates of Fault Location at Different Values of Time Reference | 83 |
| 4.12 | Estimates of Fault Location at Different Values of Time Reference | 84 |
| 4.13 | The Error of Estimated Fault Location at Different Number of Equations | 85 |
| 4.14 | The Error of Estimated Fault Location at Different Number of Equations | 86 |

List of Figures

| | | |
|------|---|----|
| 3.1 | Single Phase Power System model..... | 44 |
| 3.2 | Pre-fault Equivalent Circuit of The Single Phase model..... | 45 |
| 3.3 | Pre-Fault Converted Circuit of a Single Phase Model..... | 46 |
| 3.4 | Post-Fault Circuit of The Single-Phase Model..... | 47 |
| 3.5 | One Line diagram of The Three Phase System..... | 48 |
| 3.6 | Pre-Fault Single-Phase Equivalent Circuit..... | 49 |
| 3.7 | The Equivalent Post-Fault Circuit When Fault Occurs at A..... | 50 |
| 3.8 | The Equivalent Post-Fault Circuit When Fault Occurs at A..... | 50 |
| 3.9 | The Equivalent Post-Fault Circuit When Fault Occurs at B..... | 51 |
| 3.10 | Amplitude Characteristic of an Ideal Digital Low-Pass Filter..... | 52 |
| 4.1 | Impedance of a single phase system..... | 87 |
| 4.2 | Impedance of a single phase system using LSV..... | 88 |
| 4.3 | Impedance of a single phase system using LSV..... | 89 |
| 4.4 | Impedance of a single phase system using LSV..... | 90 |
| 4.5 | Impedance of a single phase system using LSV..... | 91 |
| 4.6 | Impedance of a single phase system using LSV..... | 92 |
| 4.7 | Impedance of a single phase system using LSV..... | 93 |
| 4.8 | Impedance of a single phase system using LSV..... | 94 |
| 4.9 | The error of distance versus the fault resistance..... | 95 |
| 4.10 | The error of distance versus the fault resistance..... | 96 |

| | | |
|------|--|-----|
| 4.11 | The error of distance versus the fault resistance..... | 97 |
| 4.12 | Estimated distance versus time delay..... | 98 |
| 4.13 | Estimated distance versus time delay..... | 99 |
| 4.14 | Estimated distance versus time delay..... | 100 |
| 4.15 | Estimated distance versus time delay..... | 101 |
| 4.16 | Estimated distance versus time delay..... | 102 |
| 4.17 | Estimated distance versus time delay..... | 103 |
| 4.18 | Impedance of the line using LSV technique..... | 104 |
| 4.19 | Impedance of the line using LAV technique..... | 105 |
| 4.20 | Impedance of the line using LSV technique..... | 106 |
| 4.21 | Impedance of the line using LAV technique..... | 107 |
| 4.22 | Impedance of the line using LSV technique..... | 108 |
| 4.23 | Impedance of the line using LAV technique..... | 109 |
| 4.24 | Impedance of the line using LSV technique..... | 110 |
| 4.25 | Impedance of the line using LAV technique..... | 111 |
| 4.26 | Impedance of the line using LSV technique..... | 112 |
| 4.27 | Impedance of the line using LAV technique..... | 113 |
| 4.28 | Impedance of the line using LSV technique..... | 114 |
| 4.29 | Impedance of the line using LAV technique..... | 115 |
| 4.30 | Estimated distance versus time delay using LSV technique..... | 116 |
| 4.31 | Estimated distance versus time delay using LAV technique..... | 117 |
| D.1 | A block diagram shows how the three programs are linked together | 139 |

| | | |
|-----|---|-----|
| D.2 | A block diagram for program 2..... | 140 |
| D.3 | Program 1, the flow chart of the pseudoinverse program..... | 141 |
| D.4 | Flow chart to determine the unfiltered voltage and current..... | 142 |
| D.5 | Flow chart of low-pass digital filter routine..... | 143 |
| D.6 | Flow chart for the main program..... | 144 |

List of Symbols and Abbreviations

Symbols

| | |
|-----------------|----------------------------------|
| \underline{R} | is the measurement vector |
| \underline{X} | is the unknown vector |
| e | error symbol |
| A^+ | is pseudoinverse of A |
| A^{-1} | is inverse of A |
| R | is the resistance |
| X | is the reactance |
| Z | is the impedance of the line |
| V | is voltage phasor |
| I | is current phasor |
| Y | length in miles |
| v | is instantaneous voltage |
| i | is instantaneous current |
| L | is the inductance |
| C | is the capacitance |
| ω | is fundamental angular frequency |
| τ | time constant |

Superscripts

T transpose of matrix

o pre-fault quantity

f post-fault quantity

Subscripts

k kth component

f fault quantity

L line quantity

Abbreviations

Re is the real part of complex quantity

Im is the imaginary part of complex quantity

fs is the sampling frequency

fc is the cutoff frequency

dB decibel

CHAPTER 1

INTRODUCTION

Transmission lines are a critical part of a power system. They are exposed to different environmental conditions and are spread over a large geographical area. As a result, they experience more faults than other power system components. Hence a line protection scheme is essential to any electric power network. The types of line faults are mainly classified as short circuit and open circuit. Short circuits are mainly due to insulation failures, human error, lightning and storm damage [1]. Open circuits may occur for a variety of reasons, including broken conductors and malfunctions of circuit breakers. The detection, location and removal of line faults in the shortest time possible is of the utmost importance in the design of line protection.

The prime concern of every power utility from economical and safety considerations is the fast and accurate fault location of short-circuited transmission lines.

In the past few years, new short-circuit fault location algorithms based on modern techniques have been developed. These methods employing measured electrical quantities at one or more points on the transmission line can be divided into four categories.

The first method is based on the distributed parameter line model in which the fault location is deduced by analyzing voltage and current travelling wave measurements. Vitins [2] presented a correlation method for transmission line protection. He suggested that the transient phenomena initiated by the occurrence of a fault on a power transmis-

sion line can be described by the telegraph equation. It was shown that the fault distance appears as a time delay between the instantaneous value of the forward travelling wave and the backward travelling wave at the measurement site. Filtering is a necessary step for this method. The presence of the fault resistance has been taken into account in the development of the algorithm. However, a lossless transmission line has been assumed and the computational effort to analyze is rather large the wave phenomenon.

Kohlas [3] used the telegraph equation to represent a line model (as Vitins did), however, he approached the problem differently. In his method, a voltage profile is used to estimate the location of the fault. The measured data from one end of the transmission line enables the instantaneous profile of the line voltage to be obtained using the wave or telegraph equation. A major drawback of this approach is that the effect of a non-zero fault resistance is neglected. The disadvantage of the above two methods is that their complexity and accuracy rely heavily on the extent of simplification of the overall system configuration.

The second method is based on solving a non-linear equation using the Newton-Raphson technique. The Newton-Raphson method is a well known iterative method for solving non-linear systems of equations and it has been successfully applied to many power system problems [4]. Takagi, Yamakoshi, Baba, Uemura and Sakaguchi [5] proposed a new type of fault location algorithm using the Fourier transformation method. In this algorithm non-linear algebraic equations, which contain the unknown variable corresponding to the fault distance, are formulated by applying the law of superposition to the faulted transmission line. Fourier analysis is used to extract the fundamental

frequency components from the measurements available at the sending end of the line. The extracted components are required by the Newton- Raphson method in solving the set of non-linear equations. No communications channels are required between the two ends of the line, and the algorithm is able to locate the fault accurately without being affected by non-zero fault resistance. The disadvantages of this method are that an unrealistic lossless line is assumed and the type of source impedance at the sending and receiving end must be carefully studied to ensure the algorithm is applicable.

Another iterative approach to fault location for power transmission lines was presented by Westlin and Bubenko [6]. This approach is based on sampled voltage and current at the sending end. A set of non-linear equations is formulated by using a suitable Thevenin equivalent model for the receiving end of the line. Each type of fault results in a different set of equations. The fault distance, receiving end current and the fault resistance can be determined from the solution of the receiving end equations using the Newton-Raphson method. A low-pass filter is required to eliminate any high frequency component present in the post-fault transient waveforms. The algorithm is readily applied to situations where the fault resistance cannot be neglected. The disadvantages of this approach is that the Thevenin equivalent circuit at the receiving end of the line must be known prior to the calculation of the fault distance. Also, the iteration process is time consuming and hence extensive computational time is needed to locate the fault accurately.

The third method is based on treating the fault location problem as a dynamic system parameter estimation problem [7,8]. Richards and Tan [8] introduced a lumped-parameter

mathematical model to compare its response with that of the real physical system during the occurrence of the fault. The fault location, fault resistance and transformer saturation parameters were computed by varying the model's parameters until an adequate match is obtained between the real system and the model response. The accuracy of the algorithm is not affected by the presence of a fault resistance. Different types of fault result in different configurations of the reference model*, which increases the complexity of the analysis. The disadvantages of this approach are that the sequence model can be very complicated in the presence of simultaneous faults. In addition, a time consuming iterative approach is employed in estimating the parameters and hence the proposed algorithm is not suitable for on-line applications.

The fourth method is based on calculating the complex impedance of a transmission line in the direction of the fault as seen from the measurement site, after which fault distance is to be deduced. Different algorithms were developed to determine the impedance accurately. One algorithm suggested by Mann and Marrison [10] used the fact that the peak magnitude of a sinusoid can be determined from its value and its rate of change at any arbitrary sampling rate. The impedance as seen from the measurement site is equal to the ratio of the voltage and the current sinusoidals at the measuring location. The values of the derivatives at any instant are approximated by the effect of the presence of a fault resistance and the decaying dc components alter the accuracy of the calculated impedance. Also, a very small sampling time is required in order to have an accurate approximation for the difference equations.

* The symmetrical component transformation was used to formulate the reference mathematical model.

Gilcrest, Rockefeller and Urden [11] introduced a slightly different approach. In their approach, the authors used the first and the second derivatives to calculate the instantaneous values and the first derivative to calculate the peak magnitude of the sinusoidal waveforms instead of using the instantaneous values and the first derivatives [10]. Three sets of sampled current and voltage values are required by the algorithm to determine the complex impedance of the faulted line. The advantage of this approach is that the decaying dc components presence in the samples does not affect the accuracy of the algorithm. The disadvantage of this approach is that the high frequency components introduce errors into the final result and thus the fault location is subject to inaccuracies.

Breingan, Gallen and Chen [12] proposed an algorithm to locate the fault for a lumped-parameter transmission line model in which the shunt capacitance is neglected. The advantage of this approach is that the decaying dc component is implicitly taken into account by the series R-L model of the transmission line. The disadvantage of this method is that it is only for short transmission lines in which the shunt capacitance can be neglected.

Another algorithm suggested by Brooks [13] used the least square estimation technique, with the assumption that the voltage and the current waveforms contain at most a constant plus a fundamental harmonic. In general, the distorted waveforms, after the occurrence of a fault, contain a decaying dc component and components of the fundamental plus higher harmonic frequencies. Sachdev and Baribeau [14] took these transient phenomena into account and came up with a different algorithm to calculate the impedance of a transmission line. The authors calculated the impedance based on the

current and the voltage measurements at the sending end of a power transmission line. No special line coupling is required between the two ends of the line. The fault distance is determined by assuming that the line reactance is proportional to the line length between the measuring point and the fault points [15,16]. The advantage of this method is that the existence of the fault resistance or shunt capacitance does not affect the accuracy of the algorithm, the dc component does not affect the accuracy of the fault either and there is no iteration which require less computation time.

Soliman and Christensen [17] proposed the least absolute value curve fitting technique which has the same advantages as the least square value technique introduced by Sachdev and Baribeau [14] and on top it is more accurate than the least square value technique.

The objective of this work is to implement an existing fault location algorithm based on current and voltage measurements at the sending end of a transmission line. The least absolute value technique is used. The fault distance is determined by assuming that the line reactance is proportional to the line length between the measuring and the fault point.

A comparison between the least absolute value and the least square value techniques will be made.

Chapter 2 presents both techniques suggested in [14,17]. The mathematical background of each technique is presented and how each technique can be implemented to determine the fault location based on the voltage and the current measurements at the sending end.

Chapter 3 describes the two transmission line models that are used to implement the least absolute value technique as well as the least square value technique. The design of a low-pass filter is also presented.

Chapter 4 gives the numerical results of both techniques. A comparison between the least absolute value technique and the least square value technique is made. The effect of the fault resistance as well as shunt capacitance is also presented.

Finally, chapter 5 presents the conclusions to be drawn from this work, as well as some directions for the future.

CHAPTER 2

THEORY OF THE FAULT LOCATION ALGORITHM

The mathematical theory and how the curve fitting technique can be used to determine the fault location of a power system will be shown in this chapter. Since the impedance of a transmission line is proportional to its length, this chapter will show how to apply curve fitting techniques to determine the impedance of a transmission line.

2.1 Curve Fitting Techniques

Two techniques will be studied in this section, the least square value technique (LSV) and the least absolute value technique (LAV). The problem is to find a functional relationship between a series of values 'a' and their corresponding functional values 'r'. This relationships could be linear, quadratic etc. Of concern here are linear relationship which generally have the form below [14].

$$r_i = a_{1i}x_1 + a_{2i}x_2 + \dots + a_{ni}x_n \quad (2.1)$$

Where,

$$i = 1, 2, \dots, n$$

a_{1i}, \dots, a_{ni} , r are the known variables,

x_1, \dots, x_n are the unknown parameters.

Given r_i and x_i for $1 \leq i \leq n$, equation (2.1) can be put in matrix form as shown below:

$$\begin{bmatrix} r_1 \\ r_2 \\ \cdot \\ \cdot \\ \cdot \\ r_n \end{bmatrix} = \begin{bmatrix} a_{11} & a_{12} & \cdot & \cdot & a_{1n} \\ a_{21} & a_{22} & \cdot & \cdot & a_{2n} \\ \cdot & \cdot & \cdot & \cdot & \cdot \\ \cdot & \cdot & \cdot & \cdot & \cdot \\ \cdot & \cdot & \cdot & \cdot & \cdot \\ a_{n1} & a_{n2} & \cdot & \cdot & a_{nn} \end{bmatrix} \begin{bmatrix} x_1 \\ x_2 \\ \cdot \\ \cdot \\ \cdot \\ x_n \end{bmatrix} \quad (2.2)$$

$$\underline{R} = \underline{A} \underline{X} \quad (2.3)$$

where,

\underline{R} is an $n \times 1$ column vector

\underline{A} is an $n \times n$ square matrix

\underline{X} is an $n \times 1$ column matrix

If \underline{A} is non-singular, then from equation (2.3)

$$\underline{X} = \underline{A}^{-1} \underline{R} \quad (2.4)$$

Using (2.4), the unknown vector \underline{X} is determined. However, in practice the number of known variables \underline{R} is usually greater than the number of unknown variables \underline{X} . Such a system is said to be overdetermined. Therefore, the matrix \underline{A} , being rectangular, is singular and, therefore (2.4) is not usable. To overcome this problem, the curve fitting approach is used.

The two sections following show the use of curve fitting techniques in overcoming this problem.

2.1.1 Least Error Square Technique

The least error square curve fitting technique is based on minimizing the sum of the square of the residuals. In equation (2.3) the error between the estimated value and the measured one can be written as:

$$e_i = r_i - a_{ij} x_j \quad (2.5)$$

Where,

$$i=1,\dots,m$$

$$j=1,\dots,n$$

The error square expression is:

$$e_i^2 = (r_i - a_{ij} x_j)^2$$

The sum of all the errors square is given by:

$$\sum_{i=1}^m e_i^2 = e_1^2 + e_2^2 + \dots + e_m^2 \quad (2.6)$$

By differentiating (2.6) with respect to x_i for $i=1,2,\dots,n$; and equating the result to zero,

the set of equations in (2.7) is obtained.

$$\begin{bmatrix} \frac{\partial \sum_{i=1}^m e_i^2}{\partial x_1} \\ \frac{\partial \sum_{i=1}^m e_i^2}{\partial x_2} \\ \vdots \\ \frac{\partial \sum_{i=1}^m e_i^2}{\partial x_n} \end{bmatrix} = \begin{bmatrix} 0 \\ \vdots \\ 0 \\ \vdots \\ \vdots \\ \vdots \\ \vdots \\ \vdots \\ 0 \end{bmatrix} \quad (2.7)$$

By substituting equations (2.5) and (2.6) in (2.7) and rearranging the terms the normal equations [6] below are obtained:

$$\begin{bmatrix} \sum_{i=1}^m r_i a_{i1} \\ \sum_{i=1}^m r_i a_{i2} \\ . \\ . \\ \sum_{i=1}^m r_i a_{in} \end{bmatrix} = \begin{bmatrix} \sum_{i=1}^m a_{i1}^2 & \sum_{i=1}^m a_{i1} a_{i2} & \dots & \sum_{i=1}^m a_{i1} a_{in} \\ \sum_{i=1}^m a_{i2} a_{i1} & \sum_{i=1}^m a_{i2}^2 & \dots & \sum_{i=1}^m a_{i2} a_{in} \\ . & . & \dots & . \\ . & . & \dots & . \\ \sum_{i=1}^m a_{in} a_{i1} & \sum_{i=1}^m a_{in} a_{i2} & \dots & \sum_{i=1}^m a_{in}^2 \end{bmatrix} \begin{bmatrix} x_1 \\ x_2 \\ . \\ . \\ x_n \end{bmatrix} \quad (2.8)$$

(2.8) can be written as

$$\underline{\bar{R}} = \underline{\bar{A}} \underline{X} \quad (2.9)$$

Where,

$\underline{\bar{R}}$ is an $n \times 1$ column vector

$\underline{\bar{A}}$ is an $n \times n$ square matrix

\underline{X} is an $n \times 1$ column vector

It should be noted that $\underline{\bar{R}}$ in (2.9) could be written as:

$$\underline{\bar{R}} = \begin{bmatrix} \sum_{i=1}^m r_i a_{i1} \\ \sum_{i=1}^m r_i a_{i2} \\ \vdots \\ \sum_{i=1}^m r_i a_{in} \end{bmatrix} = \begin{bmatrix} a_{11} & a_{21} & \dots & a_{m1} \\ a_{12} & a_{22} & \dots & a_{m2} \\ \vdots & \vdots & \ddots & \vdots \\ a_{1n} & a_{2n} & \dots & a_{mn} \end{bmatrix} \begin{bmatrix} r_1 \\ r_2 \\ \vdots \\ r_m \end{bmatrix}$$

$$\underline{\bar{A}}^T \underline{\bar{R}} = \underline{\bar{A}}^T \underline{\bar{X}} \quad (2.10)$$

Substituting (2.10) in (2.9) gives

$$\underline{A}^T \underline{R} = \underline{\bar{A}}^T \underline{X} \quad (2.11)$$

Substituting (2.3) into (2.11) gives

$$\underline{A}^T \underline{A} \underline{X} = \underline{\bar{A}}^T \underline{X}$$

Or,

$$\underline{A}^T \underline{A} = \underline{\bar{A}} \quad (2.12)$$

By substituting (2.10) and (2.12) into equation (2.9), then

$$\underline{A}^T \underline{R} = \underline{A}^T \underline{A} \underline{X} \quad (2.13)$$

Premultiplying by the inverse* of $(\underline{A}^T \underline{A})$, equation (2.13) becomes:

* Matrix A must have a rank of n to ensure that $\underline{A}^T \underline{A}$ is non-singular [10].

$$\underline{X} = (\underline{A}^T \underline{A})^{-1} \underline{A}^T \underline{R} \quad (2.14)$$

$(\underline{A}^T \underline{A})^{-1} \underline{A}^T$ is called the left *pseudoinverse* of matrix \underline{A} [14], (for more details see appendix E).

It is shown above how to estimate the state \underline{X} using the least square error technique, in the next section it will be shown how to estimate the state \underline{X} using the least absolute value.

2.1.2. Least Absolute Value Technique

The least absolute value technique is obtained by minimizing the sum of the absolute values of the residuals. That is, by first finding the least square error optimal solution, secondly determining the residuals of the least square error estimate, thirdly select n measurements corresponding to the smallest residuals and then solve equation (2.4) to get the optimal solution of least absolute value technique. This section below shows how the least absolute value technique is used.

In m -dimensions the norm of a vector \underline{E} is defined as:

$$||\underline{E}|| = \left(\sum_{i=1}^m |E_i|^p \right)^{1/p} \quad p \geq 1 \quad (2.15)$$

If $p=1$, then equation (2.15) is:

$$||\underline{E}|| = \sum_{i=1}^m |E_i| \quad (2.16)$$

According to the norm axioms, we have

$$\| \underline{E} \| = 0 \quad \text{if and only if } e_i = 0 \quad i=1,2,\dots,m$$

Then, the best least absolute value estimation is given by:

$$\underline{R} = \underline{A} \underline{X} \quad (2.17)$$

Using the least square error technique equation (2.17) is solved* and the best estimate \underline{X}^* is given by:

$$\underline{X}^* = (\underline{A}^T \underline{A})^{-1} (\underline{A}^T \underline{R}) \quad (2.18)$$

Calculating the residuals of \underline{X}^* using the absolute value of equation (2.5) and rearranging the residuals such that the points with smallest residual will be at the top of the vector \underline{E}^{**} [17], and it could written as:

$$\underline{E} = \begin{bmatrix} \hat{\underline{E}} \\ \dots \\ \underline{E}^+ \end{bmatrix}$$

and

$$\underline{A} = \begin{bmatrix} \hat{\underline{A}} \\ \dots \\ \underline{A}^+ \end{bmatrix}$$

* equation (2.17) is overdetermined.

** \underline{E} = the residual in equation form, i.e
 $\underline{E} = \underline{R} - (\underline{A}^T \underline{A})^{-1} \underline{A}^T \underline{R}$

Where,

$\underline{\hat{E}}$ is an $n \times 1$ vector containing the smallest n residuals

\underline{E}^+ is an $(m-n) \times 1$ vector containing the remainder of the residuals

$\underline{\hat{A}}$ is an $n \times n$ matrix with rank n and containing elements corresponding to $\underline{\hat{R}}$

\underline{A}^+ is an $(m-n) \times n$ matrix containing the elements corresponding to \underline{R}^+

Then using $\underline{\hat{E}}$ and $\underline{\hat{A}}$ equation (2.17) can be solved* for \underline{X}^{**} as:

$$\underline{X}^{**} = \underline{\hat{A}}^{-1} \underline{\hat{E}} \quad (2.19)$$

Equation (2.19) is the best estimate using the least absolute value technique.

2.2 Application of Curve Fitting Techniques

The impedance relay is one of the relays used to protect transmission lines. If the relay is located at the sending end, the impedance can be determined from the knowledge of the voltage and current at this end. The fact that the impedance is proportional to the distance from the fault location to the relay location, can be used to determine whether the fault is in a protection zone or not. The next section will show how to determine this impedance using the current and voltage at sending end.

2.2.1 Impedance Calculation

* $\underline{\hat{A}}$ a square matrix with rank n (i.e non-singular).

During a short-circuit fault, the current and the voltage waveforms at the sending end of a transmission line, are composed of decaying dc components and many harmonic components. The voltage and the current at time t are represented by equations (2.20) and (2.21) respectively:

$$v = k_{0v} e^{-t/\tau} + \sum_{n=1}^N k_{nv} \sin(n\omega_0 t + \theta_{nv}) \quad (2.20)$$

$$i = k_{0i} e^{-t/\tau} + \sum_{n=1}^N k_{ni} \sin(n\omega_0 t + \theta_{ni}) \quad (2.21)$$

where,

v is the instantaneous voltage at time t

i is the instantaneous current at time t

τ is the time constant of the decaying d.c. component

N is the highest order of the harmonic component present in the signal

ω_0 is the fundamental frequency of the system

k_{0v} is the magnitude of the d.c. voltage component at $t=0$

k_{0i} is the magnitude of the d.c. current component at $t=0$

k_{nv} is the peak value of the n^{th} voltage harmonic component

k_{ni} is the peak value of the n^{th} current harmonic component

θ_{nv} is the phase angle of the n^{th} voltage harmonic component

θ_{ni} is the phase angle of the n^{th} current harmonic component

Not only does the time constant τ depend on the ratio of the reactance to the resistance, X/R , but also on the resistance of the arc at the point of the fault.

By expanding $e^{-t/\tau}$ using Taylor series, we have

$$e^{-t/\tau} = 1 - \left(\frac{1}{\tau}\right)t + \left(\frac{1}{2!\tau^2}\right)t^2 - \left(\frac{1}{3!\tau^3}\right)t^3 + \left(\frac{1}{4!\tau^4}\right)t^4 + \dots \quad (2.22)$$

We assume that all the fifth and higher harmonics present in the waveform have been eliminated by either a low-pass analog or digital filter. Also assume that the post-fault current and voltage signals do not contain of even harmonic components. By using (2.22), equation (2.20) and (2.21) become:

$$\begin{aligned} v = & k_{0v} - \left(\frac{k_{0v}}{\tau}\right)t + \left(\frac{k_{0v}}{2\tau^2}\right)t^2 - \left(\frac{k_{0v}}{6\tau^3}\right)t^3 \\ & + k_{1v} \sin(\omega_0 t + \theta_{1v}) + k_{3v} \sin(3\omega_0 t + \theta_{3v}) \end{aligned} \quad (2.23)$$

$$\begin{aligned} i = & k_{0i} - \left(\frac{k_{0i}}{\tau}\right)t + \left(\frac{k_{0i}}{2\tau^2}\right)t^2 - \left(\frac{k_{0i}}{6\tau^3}\right)t^3 \\ & + k_{1i} \sin(\omega_0 t + \theta_{1i}) + k_{3i} \sin(3\omega_0 t + \theta_{3i}) \end{aligned} \quad (2.24)$$

The two sinusoidal terms in equations (2.23) and (2.24) can be expanded as follows:

$$k_{1v} \sin(\omega_0 t + \theta_{1v}) = k_{1v} \sin(\omega_0 t) \cos(\theta_{1v}) + k_{1v} \cos(\omega_0 t) \sin(\theta_{1v}) \quad (2.25)$$

$$k_{3v} \sin(3\omega_0 t + \theta_{3v}) = k_{3v} \sin(3\omega_0 t) \cos(\theta_{3v}) + k_{3v} \cos(3\omega_0 t) \sin(\theta_{3v}) \quad (2.26)$$

$$k_{1i} \sin(\omega_0 t + \theta_{1i}) = k_{1i} \sin(\omega_0 t) \cos(\theta_{1i}) + k_{1i} \cos(\omega_0 t) \sin(\theta_{1i}) \quad (2.27)$$

$$k_{3i} \sin(3\omega_0 t + \theta_{3i}) = k_{3i} \sin(3\omega_0 t) \cos(\theta_{3i}) + k_{3i} \cos(3\omega_0 t) \sin(\theta_{3i}) \quad (2.28)$$

Substituting (2.25) and (2.26) in (2.23), and (2.27) and (2.28) in (2.24), v and i could be respectively rewritten as:

$$\begin{aligned} v = & k_{0v} + \left(-\frac{k_{0v}}{\tau}\right)t + \left(\frac{k_{0v}}{2\tau^2}\right)t^2 + \left(\frac{-k_{0v}}{6\tau^3}\right)t^3 \\ & + k_{1v} \sin(\omega_0 t) \cos(\theta_{1v}) + k_{1v} \cos(\omega_0 t) \sin(\theta_{1v}) \\ & + k_{3v} \sin(3\omega_0 t) \cos(\theta_{3v}) \end{aligned} \quad (2.29)$$

$$\begin{aligned} i = & k_{0i} + \left(-\frac{k_{0i}}{\tau}\right)t + \left(\frac{k_{0i}}{2\tau^2}\right)t^2 + \left(\frac{-k_{0i}}{6\tau^3}\right)t^3 \\ & + k_{1i} \sin(\omega_0 t) \cos(\theta_{1i}) + k_{1i} \cos(\omega_0 t) \sin(\theta_{1i}) \\ & + k_{3i} \sin(3\omega_0 t) \cos(\theta_{3i}) \end{aligned} \quad (2.30)$$

The voltage and the current are sampled at $t = t_1, t_2, \dots, t_m$

where,

$$t_2 = t_1 + \Delta t,$$

$$t_3 = t_1 + 2\Delta t,$$

.

.

.

$$t_m = t_1 + (m-1)\Delta t$$

$m \geq 7$ is the number of sampling times,

and Δt is the sampling interval.

By defining the coefficients and states as follows:

$$\begin{aligned}
 a_{j1}(t) &= 1 & x_{1v} &= k_{0v} & x_{1i} &= k_{0i} \\
 a_{j2}(t) &= t & x_{2v} &= \frac{-k_{0v}}{\tau} & x_{2i} &= \frac{-k_{0i}}{\tau} \\
 a_{j3}(t) &= t^2 & x_{3v} &= \frac{k_{0v}}{2\tau^2} & x_{3i} &= \frac{k_{0i}}{2\tau^2} \\
 a_{j4}(t) &= t^3 & x_{4v} &= \frac{-k_{0v}}{6\tau^3} & x_{4i} &= \frac{-k_{0i}}{6\tau^3} \\
 a_{j5}(t) &= \sin w_0 t & x_{5v} &= k_{1v} \cos \theta_{1v} & x_{5i} &= k_{1i} \cos \theta_{1i} \\
 a_{j6}(t) &= \cos w_0 t & x_{6v} &= k_{1v} \sin \theta_{1v} & x_{6i} &= k_{1i} \sin \theta_{1i} \\
 a_{j7}(t) &= \sin 3w_0 t & x_{7v} &= k_{3v} \cos \theta_{3v} & x_{7i} &= k_{3i} \cos \theta_{3i} \\
 a_{j8}(t) &= \cos 3w_0 t & x_{8v} &= k_{3v} \sin \theta_{3v} & x_{8i} &= k_{3i} \sin \theta_{3i}
 \end{aligned} \tag{2.31}$$

Where,

$$j = 1, 2, \dots, m$$

Equations (2.29) and (2.30) can be written as:

$$\begin{aligned} v(t_j) = & a_{j1}(t)x_{1v} + a_{j2}(t)x_{2v} + a_{j3}(t)x_{3v} + a_{j4}(t)x_{4v} \\ & + a_{j5}(t)x_{5v} + a_{j6}(t)x_{6v} + a_{j7}(t)x_{7v} \end{aligned} \quad (2.32)$$

$$\begin{aligned} i(t_j) = & a_{j1}(t)x_{1i} + a_{j2}(t)x_{2i} + a_{j3}(t)x_{3i} + a_{j4}(t)x_{4i} \\ & + a_{j5}(t)x_{5i} + a_{j6}(t)x_{6i} + a_{j7}(t)x_{7i} \end{aligned} \quad (2.33)$$

In matrix form

$$\begin{bmatrix} v(t_1) \\ v(t_2) \\ \cdot \\ \cdot \\ \cdot \\ v(t_m) \end{bmatrix} = \begin{bmatrix} a_{11}(t_1) & a_{12}(t_1) & \cdot & \cdot & \cdot & a_{17}(t_1) \\ a_{21}(t_2) & a_{22}(t_2) & \cdot & \cdot & \cdot & a_{27}(t_2) \\ \cdot & \cdot & \cdot & \cdot & \cdot & \cdot \\ \cdot & \cdot & \cdot & \cdot & \cdot & \cdot \\ \cdot & \cdot & \cdot & \cdot & \cdot & \cdot \\ a_{m2}(t_m) & a_{m2}(t_m) & \cdot & \cdot & \cdot & a_{m7}(t_m) \end{bmatrix} \begin{bmatrix} x_{1v} \\ x_{2v} \\ \cdot \\ \cdot \\ \cdot \\ x_{7v} \end{bmatrix} \quad (2.34)$$

Or,

$$\underline{Z}_v(t) = \underline{A}(t)\underline{X}_v \quad (2.35)$$

$$\begin{bmatrix} i(t_1) \\ i(t_2) \\ \cdot \\ \cdot \\ \cdot \\ i(t_m) \end{bmatrix} = \begin{bmatrix} a_{11}(t_1) & a_{12}(t_1) & \cdot & \cdot & \cdot & a_{17}(t_1) \\ a_{21}(t_2) & a_{22}(t_2) & \cdot & \cdot & \cdot & a_{27}(t_2) \\ \cdot & \cdot & \cdot & \cdot & \cdot & \cdot \\ \cdot & \cdot & \cdot & \cdot & \cdot & \cdot \\ \cdot & \cdot & \cdot & \cdot & \cdot & \cdot \\ a_{m2}(t_m) & a_{m2}(t_m) & \cdot & \cdot & \cdot & a_{m7}(t_m) \end{bmatrix} \begin{bmatrix} x_{1i} \\ x_{2i} \\ \cdot \\ \cdot \\ \cdot \\ x_{7i} \end{bmatrix} \quad (2.36)$$

Or,

$$\underline{Z}_i(t) = \underline{A}(t)\underline{X}_i \quad (2.37)$$

where,

$\underline{Z}_v(t)$ is an $m \times 1$ voltage vector measurement

$\underline{Z}_i(t)$ is an $m \times 1$ current vector measurement

\underline{X}_v is an 7×1 unknown vector

\underline{X}_i is an 7×1 unknown vector

$\underline{A}(t)$ is an $m \times 7$ matrix

The elements of the matrix \underline{A} depend on the time reference and the sampling rate used and can be predetermined off-line. To find the impedance at the sending end, the fundamental components of the voltage and current will be defined as:

$$V_1 = k_{1v} e^{j\theta_{1v}} \quad (2.38)$$

$$I_1 = k_{1i} e^{j\theta_{1i}} \quad (2.39)$$

By expanding $e^{j\theta}$ equation (2.38) and (2.39) will be:

$$V_1 = k_{1v} \cos_{1v} + jk_{1v} \sin\theta_{1v} \quad (2.40)$$

$$I_1 = k_{1i} \cos_{1i} + jk_{1i} \sin\theta_{1i} \quad (2.41)$$

Using equation (2.31), equation (2.40) and (2.41) can be written as:

$$V_1 = x_{5v} + jx_{6v} \quad (2.42)$$

$$I_1 = x_{5i} + jx_{6i} \quad (2.43)$$

The impedance Z is given by:

$$Z = \frac{V_1}{I_1}$$

Which is,

$$Z = \frac{x_{5v} + jx_{6v}}{x_{5i} + jx_{6i}} \quad (2.44)$$

From (2.44) the real and imaginary components of Z are:

$$Re(Z) = \frac{x_{5v}x_{5i} + x_{6v}x_{6i}}{x_{5i}x_{5i} + x_{6i}x_{6i}} \quad (2.45)$$

$$Im(Z) = \frac{x_{5i}x_{6v} - x_{5v}x_{6i}}{x_{5i}x_{5i} + x_{6i}x_{6i}} \quad (2.46)$$

Now, the objective is to solve for the impedance, i.e solve (2.45) and (2.46). The two sections following describe the use of curve fitting techniques to solve these equations.

2.2.2 Least Error Square Solution

In the previous section, we discussed how to get the impedance at the relay location. In this section we will discuss how to solve for the impedance using the least square error technique.

Recall, the least error square technique is used when the inverse of a rectangular matrix \underline{A} has to be obtained to solve a set of equations (i.e $\underline{R} = \underline{A} \underline{X}$, \underline{A} is rectangular matrix), in this case the pseudo inverse of matrix \underline{A} has to be obtained solving for the unknown \underline{X} .

$$\underline{X} = (\underline{A}^T \underline{A})^{-1} \underline{A}^T \underline{R}$$

Here, the matrix $\underline{A}(t)$ in equation (2.35) and (2.37) is a rectangular matrix with m rows and 7 columns where $m > 7$, using the least error square technique, the sum of the squares of the errors is minimized as:

$$J_v = (\underline{Z}_v(t) - \underline{A}(t)\underline{X}_v)^T (\underline{Z}_v(t) - \underline{A}(t)\underline{X}_v) \quad (2.47)$$

$$J_i = (\underline{Z}_i(t) - \underline{A}(t)\underline{X}_i)^T (\underline{Z}_i(t) - \underline{A}(t)\underline{X}_i) \quad (2.48)$$

By differentiating equations (2.47) and (2.48) with respect to \underline{X}_v and \underline{X}_i , we respectively have:

$$\frac{\partial J_v}{\partial \underline{X}_v} = \underline{A}^T(t)(\underline{Z}_v(t) - \underline{A}(t)\underline{X}_v) \quad (2.49)$$

$$\frac{\partial J_i}{\partial \underline{X}_i} = \underline{A}^T(t)(\underline{Z}_i(t) - \underline{A}(t)\underline{X}_i) \quad (2.50)$$

By equating (2.49) and (2.50) to zero to get the minimum of J:

$$\frac{\partial J_v}{\partial \underline{X}_v} = 0 \quad \frac{\partial J_i}{\partial \underline{X}_i} = 0$$

$$\underline{A}^T(t)(\underline{Z}_v(t) - \underline{A}(t)\underline{X}_v) = 0 \quad (2.51)$$

$$\underline{A}^T(t)(\underline{Z}_i(t) - \underline{A}(t)\underline{X}_i) = 0 \quad (2.52)$$

Or,

$$\underline{X}_v^* = [\underline{A}^T(t)\underline{A}(t)]^{-1}\underline{A}^T(t)\underline{Z}_v(t) \quad (2.53)$$

$$\underline{X}_i^* = [\underline{A}^T(t)\underline{A}(t)]^{-1}\underline{A}^T(t)\underline{Z}_i(t) \quad (2.54)$$

Where $[\underline{A}^T(t)\underline{A}(t)]^{-1}\underline{A}^T(t)$ is the left pseudoinverse of $\underline{A}(t)$ and is defined as:

$$\underline{A}^{+}(t) = [\underline{A}^T(t)\underline{A}(t)]^{-1}\underline{A}^T(t) \quad (2.55)$$

Substitution of (2.55) in equations (2.53) and (2.54) yields:

$$\underline{X}_v^* = [\underline{A}(t)]^{+}\underline{Z}_v(t) \quad (2.56)$$

$$\underline{X}_i^* = [\underline{A}(t)]^{+}\underline{Z}_i(t) \quad (2.57)$$

By calculating \underline{X}_v^* and \underline{X}_i^* , the impedance can be determined.

The disadvantage of this technique, however, is that it is not suitable when the measurement vector $\underline{Z}(t)$ contains "bad data points", which is the case in practice. In general, the least square error technique gives best estimate when the set of measurement has a Gaussian error distribution, otherwise the result is not that accurate.

In the next section, the least absolute value technique will be illustrated. In this technique, if the measurement vector contains some bad data points, including points of

interest, the estimator will reject these bad data points, fitting only the good ones, and subsequently generates correct values for the bad data points.

2.2.3 Least Absolute Value Solution

The main idea here is to minimize the cost function which is the absolute value of the error. If the error is defined as:

$$\underline{E} = \underline{Z}(t) - \underline{A}(t)\underline{X} \quad (2.58)$$

the cost function to be minimized is:

$$J = |\underline{Z}(t) - \underline{A}(t)\underline{X}| \quad (2.59)$$

Here the cost function of the current and the voltage are to be minimized. Equation (2.60) and (2.61) will define the cost function for the voltage and current respectively.

$$J_v = |\underline{Z}_v(t) - \underline{A}(t)\underline{X}_v| \quad (2.60)$$

$$J_i = |\underline{Z}_i(t) - \underline{A}(t)\underline{X}_i| \quad (2.61)$$

According to equation (2.16) and the norm axioms, the best least absolute value estimation is given by:

$$\underline{Z}_v(t) = \underline{A}(t)\underline{X}_v \quad (2.62)$$

$$\underline{Z}_i(t) = \underline{A}(t)\underline{X}_i \quad (2.63)$$

Since this system is overdetermined, the left pseudoinverse (i.e. LSV technique) has to be used. For convenience, equation (2.14) is rewritten below:

$$\underline{X}^* = [\underline{A}^T(t)\underline{A}(t)]^{-1}\underline{A}^T(t)\underline{Z}(t) \quad (2.14)$$

Solving for \underline{X}_v^* and \underline{X}_i^* yields:

$$\underline{X}_v^* = [\underline{A}^T(t)\underline{A}(t)]^{-1}\underline{A}^T(t)\underline{Z}_v(t)$$

Or,

$$\underline{X}_v^* = [\underline{A}(t)]^+\underline{Z}_v(t) \quad (2.64)$$

$$\underline{X}_i^* = [\underline{A}^T(t)\underline{A}(t)]^{-1}\underline{A}^T(t)\underline{Z}_i(t)$$

Or,

$$\underline{X}_i^* = [\underline{A}(t)]^+\underline{Z}_i(t) \quad (2.65)$$

Substituting (2.64) into (2.58) to get the minimum voltage residual yields:

$$\underline{E}_v^* = \underline{Z}_v(t) - \underline{A}(t)[\underline{A}(t)]^+\underline{Z}_v(t) \quad (2.66)$$

Substituting (2.65) into (2.58) to get the minimum current residual yields:

$$\underline{E}_i^* = \underline{Z}_i(t) - \underline{A}(t)[\underline{A}(t)]^+ \underline{Z}_i(t) \quad (2.67)$$

Rearranging the elements in the residual matrix such that the points with smallest residual will be at the top of the vector \underline{E}^* , could be written as:

$$\underline{E}^* = \begin{bmatrix} \underline{\hat{E}} \\ \dots \\ \underline{E}^+ \end{bmatrix} \quad (2.68)$$

$$\underline{Z}^* = \begin{bmatrix} \underline{\hat{Z}} \\ \dots \\ \underline{Z}^+ \end{bmatrix} \quad (2.69)$$

and,

$$\underline{A}^* = \begin{bmatrix} \underline{\hat{A}} \\ \dots \\ \underline{A}^+ \end{bmatrix} \quad (2.70)$$

Where,

$\underline{\hat{E}}$ is an $n \times 1$ vector containing smallest residuals

\underline{E}^+ is an $(m-n) \times 1$ vector containing the remainder of the residuals

$\underline{\hat{Z}}$ is an $n \times 1$ measurements vector corresponding to the smallest residuals

\underline{Z}^+ is an $(m-n) \times 1$ vector containing the remainder of the measurements

$\underline{\hat{A}}$ is an $n \times n$ matrix corresponding to the smallest residuals

\underline{A}^+ is an $(m-n) \times n$ matrix containing the remainder of the elements of $\underline{A}(t)$

These matrices and vectors will be used to solve for the optimal solution of $\hat{X}_v(t)$ and

$\hat{\underline{X}}_i(t)$ in equation (2.64) and (2.65) respectively*, which gives:

$$\hat{\underline{X}}_v^*(t) = [\hat{\underline{A}}(t)]^{-1} \hat{\underline{Z}}_v(t) \quad (2.71)$$

$$\hat{\underline{X}}_i^*(t) = [\hat{\underline{A}}(t)]^{-1} \hat{\underline{Z}}_i(t) \quad (2.72)$$

By using (2.71), (2.72), (2.45), and (2.46) the solution of the impedance is obtained. Equations (2.73) and (2.74) gives the real and imaginary part of the impedance respectively as:

$$R = \frac{\hat{x}_{5v} \cdot \hat{x}_{5i} + \hat{x}_{6v} \hat{x}_{6i}}{\hat{x}_{5i} \hat{x}_{5i} + \hat{x}_{6i} \hat{x}_{6i}} \quad (2.73)$$

and,

$$X = \frac{\hat{x}_{5i} \hat{x}_{6v} + \hat{x}_{5v} \hat{x}_{6i}}{\hat{x}_{5i} \hat{x}_{5i} + \hat{x}_{6i} \hat{x}_{6i}} \quad (2.74)$$

As alluded from the discussion above, this method is more accurate than the least square error method, and we expect it to give more accurate results.

2.3 Determination of The Fault Location from The Impedance

Because the line length is proportional to the line reactance [14], the calculated reactive component of the apparent impedance using (2.74) is used to locate the short circuit

* The matrix $\hat{\underline{A}}(t)$ is a square matrix (i.e non-singular)

fault. Fault distance Y_f is determined by the following relationship:

$$Y_f = X_f Y_t / X_t \quad (2.75)$$

where,

Y_f is the distance from the sending end to the faulted point.

Y_t is the total length of the line

X_f is the apparent line reactance from the sending end to the faulted point

X_t is the total reactance of the line

Y_t and X_t are known values, Y_f can be determined once X_f is calculated.

2.4 Advantages of LSV and LAV Techniques.

Having introduced the curve fitting techniques to be used in this thesis, some of the advantages of these techniques are presented:

- (i) No iteration is required and hence results in less of a computational burden.
- (ii) Flexibility in choosing the sampling rate and the data window size.
- (iii) The Pseudoinverse of a matrix A can be calculated in an off line mode since the element of the matrix are known prior to the existence of the fault itself.
- (iv) No prior knowledge of source impedance at either the sending end or receiving end is required.

- (v) The freedom in choosing the number of equations of conditions which result in the presence of decaying dc component and any desired harmonic component.

CHAPTER 3

THE TRANSMISSION LINE MODEL

In this chapter two models of a power system are discussed. These two systems are set up in an off-line mode which provide transient fault data, in which both the prefault and the postfault conditions are used.

To attenuate the high frequency harmonics which are present in the postfault waveforms, a low-pass filter is required. Three different orders of a low-pass filter and their effects on the algorithm will be also discussed in this chapter.

3.1 Modelling of The Systems.

Two simple power systems are used to test the fault location techniques. The first system is a single-phase one which is represented by a series equivalent R-L model. The second one is a three-phase system which is represented by a three pi equivalent circuit [18].

3.1.1 Single-Phase Power System.

The single-phase power system is selected to represent a practical situation. The system, as shown in figure 3.1, consists of a generator feeding into a load through two transformers, and two transmission lines. The line which has been chosen to test the algorithm is a short, aluminium cable-steel reinforced (ACSR) [19] overhead transmission

line, and its length is 30 miles. All the data of the system components are given in Appendix A.

The system components are modelled using equivalent impedances. The impedances are converted to per unit base, the base voltage is 31.5 KV and the base power is 17 MVA. The prefault equivalent circuit (steady state) is shown in figure 3.2. From figure 3.2, v_{B1} and i_L , which are the initial conditions of the faulted voltage and the faulted current, can be determined easily as:

$$P_L = V_L I_L \cos \phi \quad (3.1)$$

Where,

$$\phi = \tan^{-1} Q_L / P_L \quad (3.2)$$

Thus,

$$I_L = P_L / V_L \cos \phi \quad (3.3)$$

Then,

$$V_{B1} = V_L + I_L [(R_{TL1} + R_{TL2}) + j(X_{TL1} + X_{T2} + X_{TL2})] \quad (3.4)$$

$$E_g = V_{B1} + I_L j [(X_1 + X_{T1} + X_g)] \quad (3.5)$$

Hence,

$$e = \sqrt{2} E_g \sin (\omega_o t + \rho) \quad (3.6)$$

Where,

$$I_f^o = I_L^*$$

* I_f^o is the initial condition of the faulted current.

$$V_f^o = V_{B1}^{**}$$

The pre-fault, converted to per unit base, circuit is shown in figure 3.3. Next, the post-faulted circuit is presented. As mentioned earlier, and as shown in figure 3.1, the fault was assumed to be on transmission line number one (30 miles). If the fault could occur at any point of the transmission line, the post-fault circuit will be as shown in figure 3.4.

From figure 3.4

$$e = i_f [R_y + R_f] + [L_g + L_1 + L_{T1} + L_y] \frac{\partial i_f}{\partial t} \quad (3.7)$$

Since this circuit in figure 3.4 is a simple R-L circuit, the solution of equation (3.7) [17] is:

$$i_f = I_f^o e^{-R_{total} t / L_{total}} + \frac{V_{max}}{Z} \sin (w_o t + \phi_o + \rho) \quad (3.8)$$

Where,

I_f^o = initial condition of the faulted current

$$R_{total} = R_y + R_f$$

$$L_{total} = L_g + L_1 + L_{T1} + L_y$$

$$V_{max} = \sqrt{2} E_g$$

$$Z = \sqrt{R_{total}^2 + (w_o L_{total})^2}$$

$$\rho = \text{angle of } E_g$$

$$\phi_o = \tan^{-1} \left(\frac{w_o L_{total}}{R_{total}} \right)$$

** V_f^o is the initial condition of the faulted voltage.

By differentiating equation (3.8) with respect to t , equation (3.9) is obtained.

$$\frac{\partial i_f}{\partial t} = \frac{-R_{total}}{L_{total}} I_f^o e^{-R_{total} t / L_{total}} + \omega_o \frac{V_{max}}{Z} \cos(\omega_o t + \phi - \rho) \quad (3.9)$$

From figure 3.4, v_f is given by:

$$v_f = i_f (R_y + R_f) + L_y \frac{\partial i_f}{\partial t} \quad (3.10)$$

Substituting $\frac{\partial i_f}{\partial t}$ from equation (3.7) in (3.10):

$$v_f = i_f (R_y + R_f) + L_y \left[\frac{e - i_f (R_y + R_f)}{L_{total}} \right] \quad (3.11)$$

Thus the faulted voltage and the faulted current are known.

3.1.2 Three Phase Power System.

The three phase power system is exactly the same as the single-phase system except now each element consists of three components phase A, phase B and phase C. Transmission line number one is replaced by a three phase 133.5 miles long overhead copper conductor transmission line. The three conductors are spaced 15.8 feet apart. For simplicity no mutual coupling is assumed between the three phases.

Because a symmetrical three phase fault will be discussed, the system will be assumed in a balanced three phase state. A one line diagram of this balanced system is shown in figure 3.5.

As mentioned earlier, the three phase system is represented by a three-pi sections, each section corresponds to 44.5 miles of transmission line number one. The single-phase equivalent circuit of the three-phase system is shown in figure 3.6. The various components are modelled by their equivalent impedances. Impedances are converted to per unit base, the base voltage is $\sqrt{126}/3$ KV and the base power is 100 MVA. The three phase system data are given in appendix B.

When a fault exists at a point on transmission line number one, two equivalent circuits will exist the prefault equivalent circuit and the post fault equivalent circuit (transient response). The next section will discuss both circuits in detail.

3.1.2.1 Prefault Circuit.

Figure 3.6 shows the steady state condition of the single-phase equivalent circuit of the three phase system. From figure 3.6, the prefault voltage and the prefault current, the initial conditions, can be determined as shown below:

$$E_g = V_{B1} + I_{B1} [j(X_1 + X_{T1} + X_g)] \quad (3.12)$$

$$e = \sqrt{2} E_g \sin(\omega_o t + \rho) \quad (3.13)$$

and the initial faulted current and faulted voltage are:

$$I_f^o = I_{B1}$$

$$V_f^o = V_{B1} \quad (3.14)$$

Because v_L is known and the series impedance and the shunt impedance are calcu-

lated, the initial faulted current and the initial faulted voltage can be easily determined. Appendix B shows the series impedance and the shunt impedance as well as the initial faulted voltage and the initial faulted current.

3.1.2.2 Post-Fault Circuit.

Since only a balanced three phase fault is considered, the single-phase equivalent circuit is used to study the transient response. Now consider figure 3.6; two cases are discussed, the first, when the fault occurs at A (i.e. at 44.5 miles from the sending end of the transmission line), the second, when the fault occurs at B (i.e. at 89 miles from the sending end of the transmission line).

Figure 3.7 shows the single-phase post fault equivalent circuit when the balanced three phase fault occurs at A (in figure 3.6). From figure 3.7 these equations are easily obtained:

$$e = v_f + (L_1 + L_{T1} + L_g) \frac{\partial i_f}{\partial t}$$

i.e.

$$\frac{\partial i_f}{\partial t} = (e - v_f) / (L_1 + L_{T1} + L_g) \quad (3.15)$$

and,

$$i_f = i_1 + i_2$$

$$i_f = i_1 + C_1 \frac{\partial v_f}{\partial t}$$

i.e.

$$\frac{\partial v_f}{\partial t} = \frac{i_f - i_1}{C_1} \quad (3.16)$$

and,

$$v_f = R_{TL1} i_1 + L_{TL1} \frac{\partial i_1}{\partial t}$$

i.e.

$$\frac{\partial i_1}{\partial t} = \frac{v_f - R_{TL1} i_1}{L_{TL1}} \quad (3.17)$$

Equations (3.15), (3.16) and (3.17) can be solved numerically using the Runge Kutta method. The initial conditions of the faulted voltage and the faulted current are determined using the pre-fault equivalent circuit. In this case, the fault resistance was neglected, but not in the practical case when the fault resistance (R_f) exists. So, by assuming there is no load current, the current i_1 flows into ground completely through the fault resistance. Figure 3.8 shows the equivalent post-fault circuit when the fault occurs at A and there is a fault resistance (R_f)

The following equations follow from figure 3.8

$$e = v_f + (L_1 + L_{T1} + L_g) \frac{\partial i_f}{\partial t}$$

i.e.

$$\frac{\partial i_f}{\partial t} = (e - v_f) / (L_1 + L_{T1} + L_g) \quad (3.18)$$

and,

$$i_f = i_1 + C_1 \frac{\partial v_f}{\partial t}$$

i.e.

$$\frac{\partial v_f}{\partial t} = \frac{i_f - i_1}{C_1} \quad (3.19)$$

and,

$$v_f = (R_{TL1} + R_f) i_1 + L_{TL1} \frac{\partial i_1}{\partial t}$$

i.e.

$$\frac{\partial i_1}{\partial t} = \frac{v_f - (R_{TL1} + R_f) i_1}{L_{TL1}} \quad (3.20)$$

It is obvious that equations (3.18),(3.19) and (3.20) are almost the same as equations (3.15),(3.16) and (3.17) except for the existence of the fault resistance in equation (3.20). Equations (3.18),(3.19) and (3.20) will be used to solve numerically for the faulted voltage and the faulted current using the Runge Kutta method.

The second case in which the fault occurs at B (i.e. 89 miles from the sending end of the transmission line), the single-phase post fault equivalent circuit when a balanced three phase fault occurs at B and a fault resistance exists (in figure 3.6) is shown in figure 3.9.

From figure 3.9 the following equation can be verified:

$$i_2 = 2 C_1 \frac{\partial v_c}{\partial t} + i_4$$

i.e.

$$\frac{\partial v_c}{\partial t} = \frac{(i_2 - i_4)}{2 C_1} \quad (3.21)$$

and,

$$v_c = (R_{TL1} + R_f) i_4 + L_{TL1} \frac{\partial i_4}{\partial t}$$

i.e.

$$\frac{\partial i_4}{\partial t} = - \frac{(R_{TL1} + R_f) i_4}{L_{TL1}} \quad (3.22)$$

and,

$$v_f = R_{TL1} i_2 + L_{TL1} \frac{\partial i_2}{\partial t} + v_c$$

i.e.

$$\frac{\partial i_2}{\partial t} = \frac{v_f - R_{TL1} i_2 - v_c}{L_{TL1}} \quad (3.23)$$

and,

$$i_f = C_1 \frac{\partial v_f}{\partial t} + i_2$$

i.e.

$$\frac{\partial v_f}{\partial t} = \frac{i_f - i_2}{C_1} \quad (3.24)$$

and,

$$e = v_f + (L_1 + L_{T1} + L_g) \frac{\partial i_f}{\partial t}$$

i.e.

$$\frac{\partial i_f}{\partial t} = (e - v_f) / (L_1 + L_{T1} + L_g) \quad (3.25)$$

Using the Runge-Kutta method equation (3.21) through equation (3.25) can be solved numerically, and by using the prefault data, the initial conditions, the faulted voltage and the faulted current can be solved for numerically.

The single-phase equivalent circuit can be used when a balanced three phase symmetrical fault occurs. If an unbalanced fault occurs such as single phase to ground fault or double fault to ground ... etc, this method can't be used and all three phases have to be considered in order to determine the transient response.

3.2 Design of Low-Pass Digital Filters.

As mentioned earlier, because of the high frequency harmonics which are present in the post fault waveform, a low-pass digital filter is needed to attenuate these high frequency harmonics.

There are many methods to develop a low-pass digital filter*. The method which has been chosen to design a recursive low-pass filter is the "Direct synthesis of digital filters", which has a special feature such as the Bilinear Transformation [20]. The Bilinear Transformation is a feature required to transform a transfer function from S-domain to Z-domain. The direct design method is used to find a particular function to approximate the ideal "brickwall" characteristic* [21].

* For more detail see appendix F.

* The ideal low-pass filter with cutoff frequency f_c has a "brickwall" shape. See figure 3.10

Depending on the degree of approximation, different particular functions are required in the design analysis. One such function is to simulate a low-pass digital filter corresponding to that of a Butter worth-type low-pass filter. This function has a magnitude spectrum which decreases monotonically in both passband and stopband. Also, the magnitude is decreased by 3dB at the cutoff frequency. The design procedures of the direct approach is shown below [20]:

1. Evaluate the order of the filter from the given design specifications.
2. Determine the poles positions on the Z^{-1} plane and choose those that lie outside the unit circle to ensure that a stable filter results.
3. An n^{th} order zero exists and is located at $Z^{-1} = 0$.
4. Construct the transfer function in terms of the Z^{-1} or Z-domain.

Because the low-pass digital filter has to be included in the fault location techniques, and equation (2.32) and (2.33) has a specific condition, the following specifications have to be satisfied in the design of any desired digital filter:

1. The fifth and higher harmonic components present in the post-fault transient waveforms are attenuated.
2. The sampling rate of the filter has to be at least twice the third harmonic frequency (180 HZ).

Three different order filters of the Butterworth-type have been designed. The design procedure of each filter is given in appendix C. The following paragraph will describe each filter in detail.

1. Fourth Order Low-Pass Filter.

Cutoff frequency = 203 HZ

Transition frequency= 285 HZ

Sampling frequency = 720 HZ

Attenuation at transition frequency better than 30dB

The transfer function $G(Z^{-1})$ is:

$$G(Z^{-1}) = \frac{6.078 (1 + Z^{-1})^4}{(Z^{-2} + 0.638 Z^{-1} + 2.2) (Z^{-2} + 4.212 Z^{-1} + 20.127)} \quad (3.26)$$

2. Eighth Order Low-Pass Filter.

Cutoff frequency = 200 HZ

Transition frequency = 295 HZ

Sampling frequency = 1440 HZ

Attenuation at transition frequency better than 30dB.

The transfer function $G(Z^{-1})$ is:

$$G(Z^{-1}) = \frac{0.023 (1 + Z^{-1})^8}{(Z^{-2} - 1.512 Z^{-1} + 1.351) (Z^{-2} - 2.238 Z^{-1} + 2.482)}$$

$$\frac{1}{(Z^{-2} - 3.541 Z^{-1} + 4.509)(Z^{-2} - 5.170 Z^{-1} + 7.043)} \quad (3.27)$$

3. Tenth Order Low-Pass Filter.

cutoff frequency = 218 HZ

Transition frequency = 290 HZ

Sampling frequency = 1440 HZ

Attenuation at transition frequency better than 30dB

The transfer function $G(Z^{-1})$ is:

$$G(Z^{-1}) = \frac{0.032(1+Z^{-1})^{10}}{(Z^{-2}-1.331Z^{-1}+1.292)(Z^{-2}-1.842Z^{-1}+2.173)} \cdot \frac{1}{(Z^{-2}-2.737Z^{-1}+3.713)(Z^{-2}-4.230Z^{-1}+6.283)} \cdot \frac{1}{(Z^{-2}-5.928Z^{-1}+9.209)} \quad (3.28)$$

A time delay is associated with each filter. The delay is longer for higher order filters.

This increases the time required to locate the fault. The three designed filters are used in the proposed techniques and the delay caused by each filter will be discussed in chapter

4.

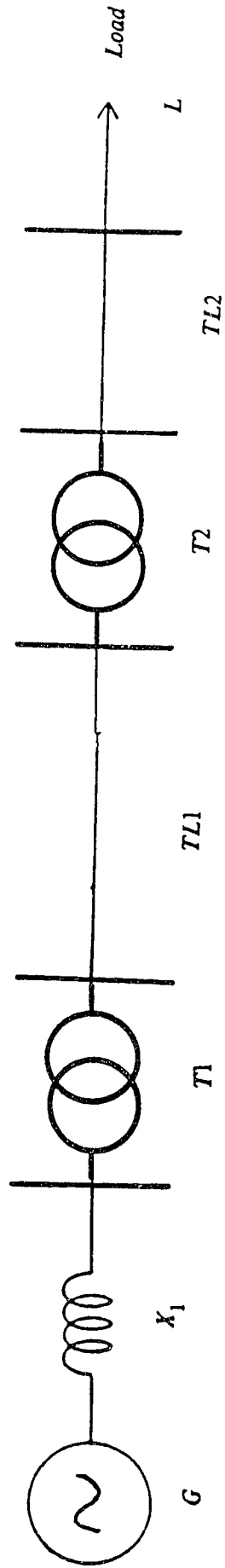


Figure 3.1: Single Phase Power System Model.

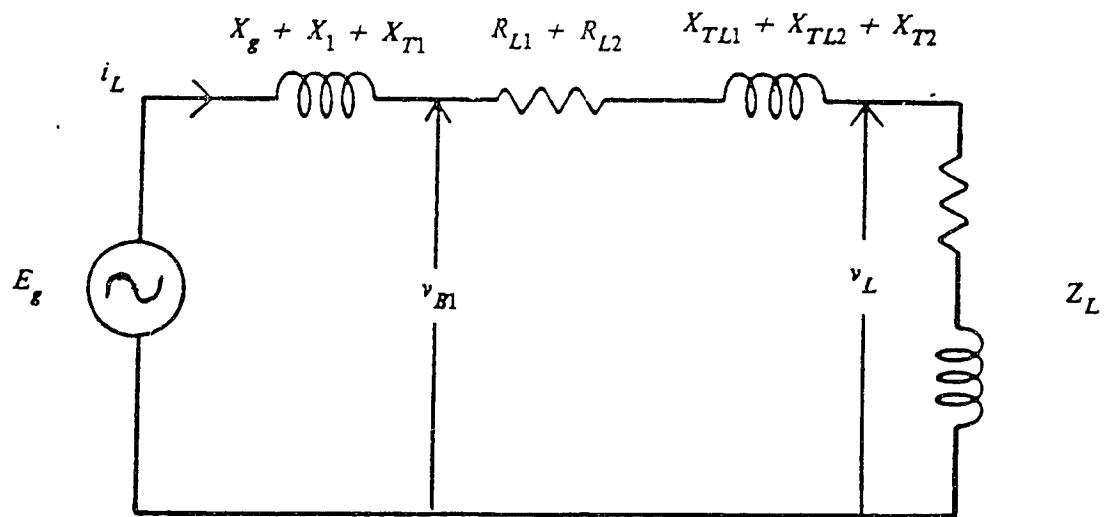
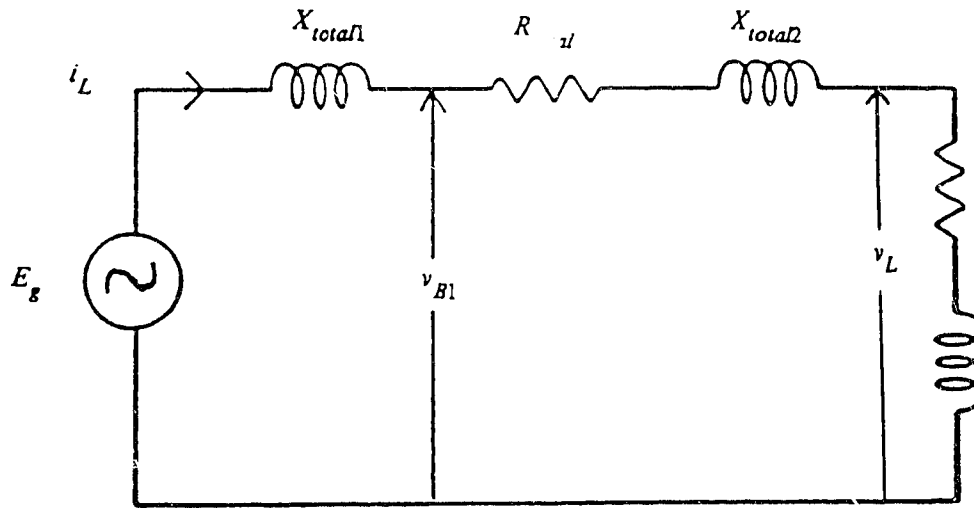


Figure 3.2: Pre-Fault Equivalent Circuit of The Single-Phase Model.



$$I_f^o = I_L = 1.0 \angle -28.07^\circ \text{ p.u.}$$

$$V_L = 1.0 \text{ p.u.}$$

$$V_f^o = V_{B1} = 1.1321 \angle 6.944^\circ \text{ p.u.}$$

$$E_g = 1.1829 \angle 10.32^\circ$$

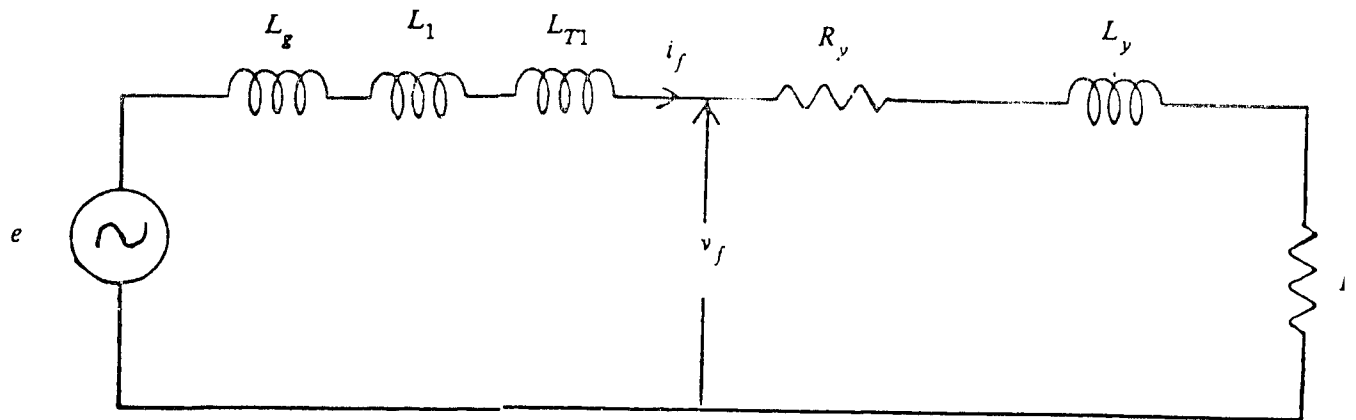
$$e = 1.6729 \sin(\omega_o t + 10.32)$$

$$\begin{aligned} X_{total1} &= X_g + X_{T1} + X_1 \\ &= 0.04099 + .032387 + 0.01161 \end{aligned}$$

$$\begin{aligned} R_{total} &= R_{TL1} + R_{TL2} \\ &= 6.39 \cdot 10^{-4} + 0.02569 \end{aligned}$$

$$\begin{aligned} X_{total2} &= X_{TL1} + X_{TL2} + X_{T2} \\ &= 6.64 \cdot 10^{-4} + .05654 + .1026 \end{aligned}$$

Figure 3.3: Pre-Fault Converted Circuit of a Single Phase Power System Model.



Where,

$v_f = \text{Faulted Voltage}$

$i_f = \text{Faulted Current}$

$L_g = \text{Generator Inductor}$

$L_1 = \text{Short Circuit Inductor}$

$L_{T1} = \text{Transformer number 1 Inductor}$

$L_y = \text{Transmission Line number 1 Inductor}^{\circ}$

$R_y = \text{Transmission Line number 1 Resistance}^{**}$

$R_f = \text{Fault Resistance}$

Figure 3.4: Post-Fault Circuit (Transient Response Circuit) of The Single-Phase Model.

[•] $L_y = \text{inductor per mile} \times \text{the distance at which the fault occurs; or, } L_y = L^*y.$

^{**} $R_y = \text{resistance per mile} \times \text{the distance at which the fault occurs; or } R_y = R^*y.$

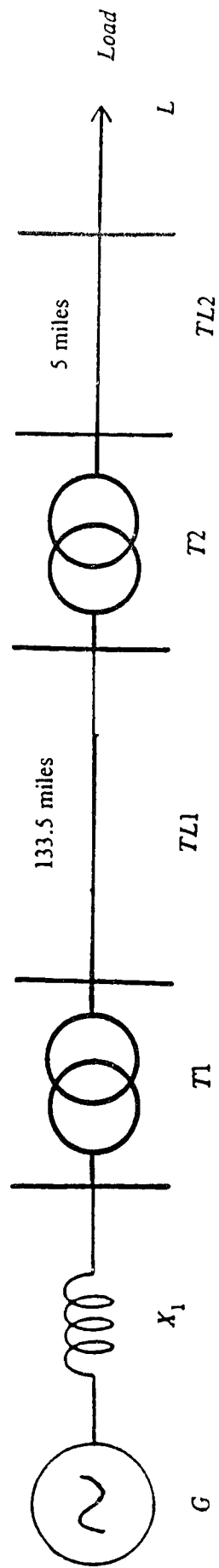


Figure 3.5: One Line Diagram of The Three Phase System.

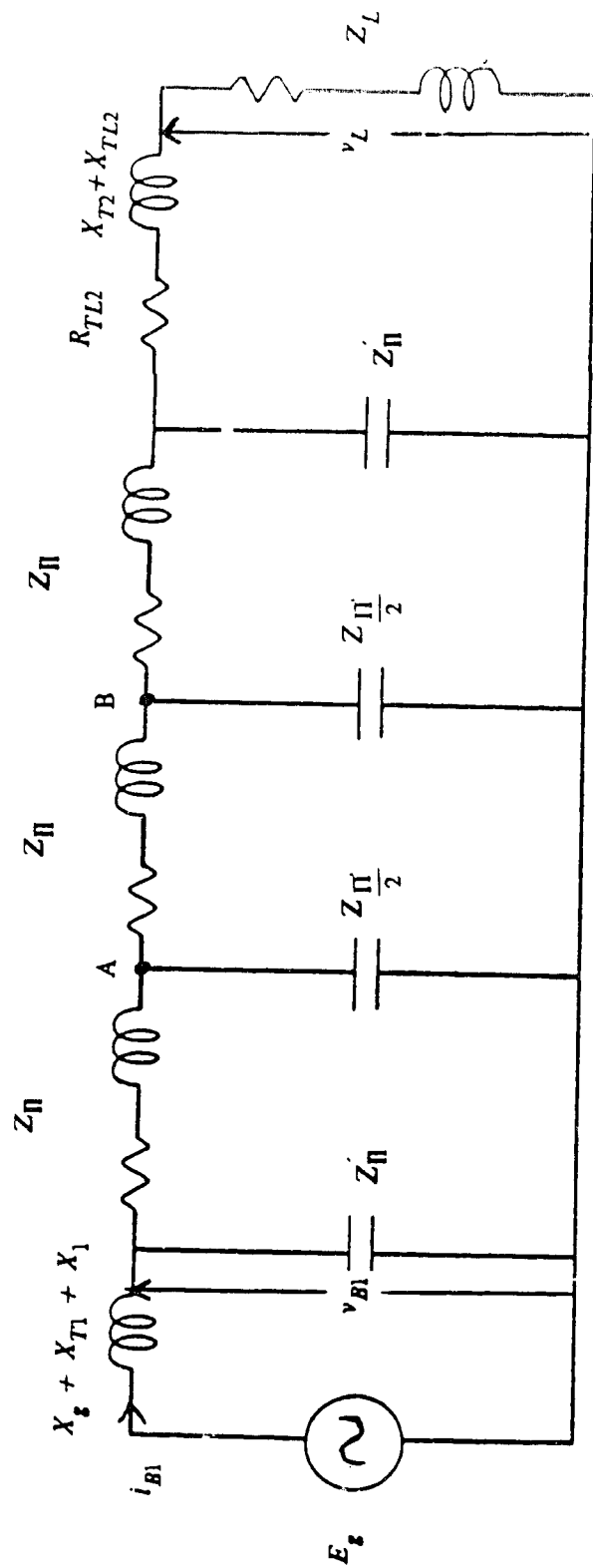


Figure 3.6: The Pre-Fault Single-Phase Equivalent Circuit of The Three Phase System.

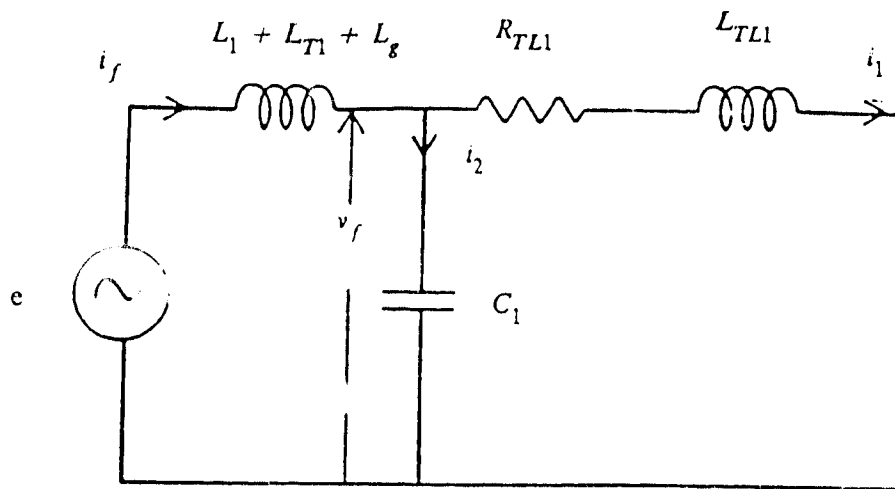


Figure 3.7: The Equivalent Post-Fault Circuit When The Fault Occurs at A (i.e. 44.5 miles from sending end), Fault Resistance Does not Exist.

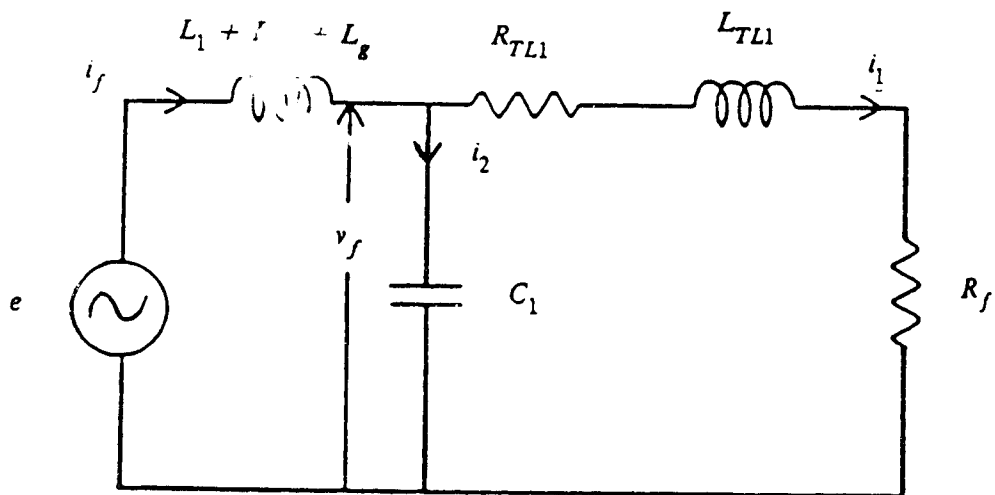


Figure 3.8: The Equivalent Post-Fault Circuit When The Fault Occurs at A (i.e. 44.5 miles from sending end), Fault Resistance Exists.

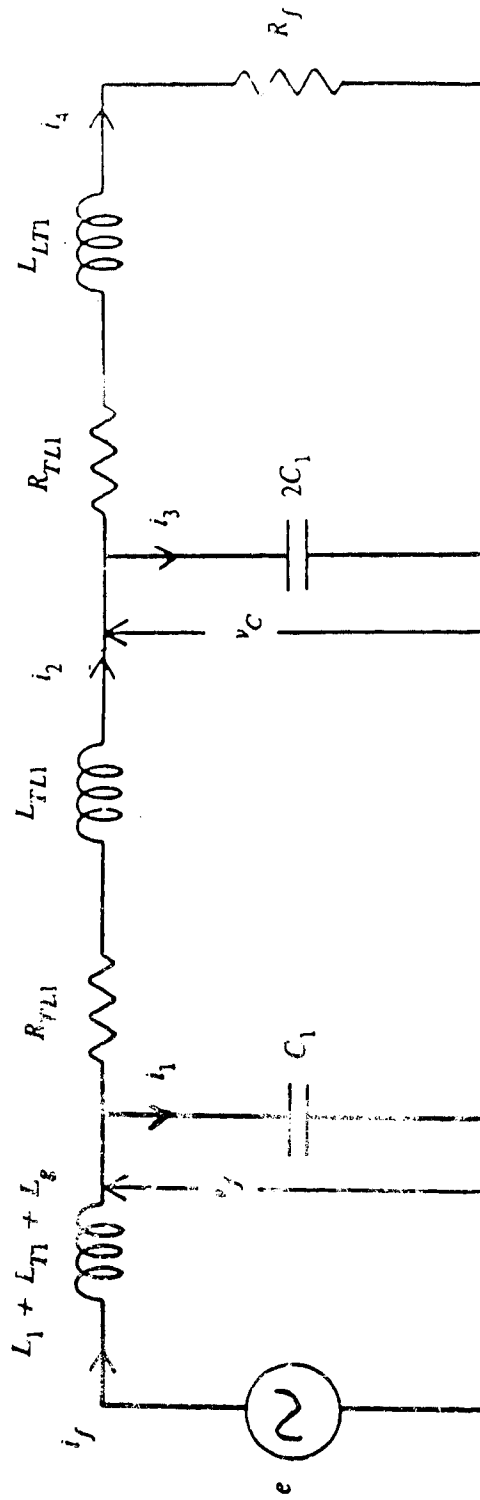


Figure 3.9: The Equivalent Post-Fault Circuit When The Fault Occurs at B (i.e. 89 miles from sending end).

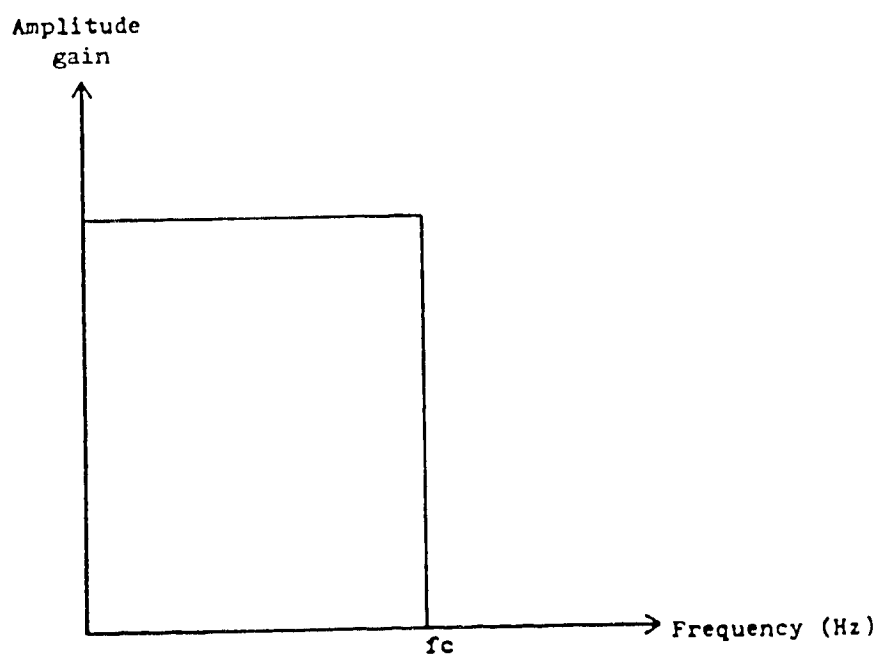


Figure 3.10: Amplitude Characteristic of an Ideal Digital Low-Pass Filter.

CHAPTER 4

NUMERICAL RESULTS FROM THE FAULT LOCATION TECHNIQUES

The previous two chapters discussed the theory of the least absolute value technique. In this chapter the numerical results and the implementation of these techniques are presented. First, the single phase system is studied. The circuit for the initial conditions (i.e. prefault circuit) and the circuit for the post fault condition were discussed in detail in chapter 3. Our study here will concern the fault location and its impedance. Different parameters are to be changed and a study of the effect of each parameter on the calculation of the fault location will be conducted. In [14], the least square error technique was used to determine the location of a fault. The fact that the impedance of the line (i.e. transmission line) is proportional to the length of the line was considered. The authors study [14] concerned the following parameters: the time reference, the number of equations and the sampling frequency. The conclusion they reached was: to get the most accurate fault estimation using the least square error technique, the parameters below have to be considered.

1. The time reference ($T=0.0$) is at the second sample.
2. The sampling frequency = 720 HZ.
3. Number of equations = 9 equations.

Numerical results of the fault location of the single phase system using the least square error technique as well as the least absolute value technique are shown. The effect of the sampling rate, the number of equations and the time reference are discussed. Also,

the effect of the arc resistance at different fault locations is studied.

Second, a three phase fault is studied. The initial condition circuit as well as the post fault circuit were discussed in chapter 3. The minimum time required to locate the fault when using a low-pass filter, the arc resistance and the change in fault location are studied.

The next section will discuss the numerical results for a fault on a single-phase power system and on a three phase power system using the least square error technique and the least absolute value technique.

4.1 Numerical Results of The Single-Phase Power System.

In this section a comparison between the LSV* and the LAV** technique is provided. The two techniques are applied to a 30 miles long overhead transmission line. A short-circuit ground fault is applied at a four different distances 0.25, 10, 15 and 20 miles from the sending end of the line. For each case, the arc resistance is varied from zero to 30 ohms. In the case where the arc resistance equals to 0.0 and there is no line shunt reactance present in the faulted model, a high degree of accuracy is expected in the fault distance measurement.

The effect of changing the sampling rate, number of equations and the time reference using those two techniques are discussed. Finally, the arc resistance and its effect on the fault location is studied.

* LSV is the least square value technique.

** LAV is the least absolute value technique.

For this special case, there is no high frequency component present in the unfiltered post-fault waveform of a single phase power system, a low-pass digital filter is not necessary for this specific model.

4.1.1 Effect of The Sampling Rate

There are two factors that have to be considered in determining the sampling rate. First, the highest frequency present in the equation of condition*** determines the lower limit of the sampling rate. Theoretically, the sampling frequency must be at least twice the largest frequency present in the signal to avoid aliasing. From equation (2.32) and (2.33), the sampling rate has to be at least 360 Hz since the equations consist of up to third harmonic components (360 Hz). In practice, a sampling rate larger than 360 Hz is desired to ensure that the aliasing effect is totally eliminated from the digitized values. The second factor to be considered is the upper limit of the sampling rate. If the sampling rate is too high, the determinant of matrix $A^T A$ becomes small and hence the inverse becomes large. A fast sampling rate is undesirable since the elements of the matrix $(A^T A)^{-1}$ have to be multiplied with the sampled values and any noise present in the signal would be amplified. Hence, the above two factors must be considered in choosing the sampling rate.

Table (4.1) shows a comparison of the LSV and LAV techniques in estimating the fault location for different sampling rates, under the following conditions:

1. The fault resistance = 0.0.

*** The equation of condition are equations (2.32), (2.33) in chapter 2.

2. Number of equations = 7
3. Fundamental frequency = 60 Hz
4. Number of unknowns = 7
5. Time reference ($T=0.0$) is at the first sample.

Referring to table (4.1), it is observed that as the sampling rate decreases the LAV technique gives more accurate results. Thus, for the LAV technique the best estimates are at sampling rate = 720 Hz. For the LSV technique the most accurate estimate of fault location is at sampling rate = 1440 Hz. The LAV technique is still more accurate than the LSV technique though. Table (4.1) clearly shows that the LAV technique gives more accurate estimation of the location of a fault than the LSV technique.

At high sampling rates, the LAV technique is not as accurate. For instance, at sampling rate = 4320 Hz the LAV technique gives strange results which are not related to the fault location at all. The reason being, as mentioned earlier, that as the sampling rate increases, the inverse of the matrix $(A^T A)^{-1}$ becomes large, and because $(A^T A)$ has to be multiplied with the sampled values, any noise present in the signal is amplified.

Table (4.2) gives the estimated fault location with the number of equations = 8. from the table, it is observed that as the sampling rate decreases, both techniques give more accurate results, Indeed, both techniques have their most accurate estimate of the fault location at sampling rate = 720 Hz. The LAV technique is still more accurate compared to the LSV technique. Also, it is observed that at sampling rate = 4320 Hz the LAV technique gives an unrelated fault estimation. The reason for this was mentioned earlier.

Similar results are observed when the number of equations is increased to 9, see table (4.3).

From the above discussion, it can be concluded that:

1. The LAV technique is more accurate than LSV technique.
2. The sampling rate that gives the most accurate estimation of the fault location using both techniques = 720 Hz.
3. If the sampling rate is too high the estimation of the fault location will be inaccurate when using both techniques.
4. As the number of equations varies, the estimation of the fault location varies in both techniques*.

The results in table (4.1) through table (4.3) were obtained under the condition that there is no fault resistance (i.e. $R_f = 0.0$). Let us now consider the case where the fault resistance exists and is equal to 30 ohms (i.e. $R_f = 30.0$). Table (4.4) shows the estimated fault location while varying the sampling rate at different location of the fault, under the following conditions:

1. Number of equations = 7
2. Number of unknowns = 7
3. Fundamental frequency = 60 Hz
4. Fault resistance = 30 ohms
5. Time reference ($T=0.0$) at the first sample

* This point will be discussed in details later on .

From table (4.4), it is observed that as the sampling rate decreases, the accuracy of the estimated fault location using LAV increases. Indeed, it is observed that the most accurate fault location using LSV technique is at sampling rate = 720 Hz. As noted earlier, the LAV technique still gives more accurate fault location estimation than the LSV technique.

By comparing table (4.1) and table (4.4), the following comments can be made:

1. The existence of R_f doesn't have a great effect on the accuracy of the estimated fault distance, which is expected due to the fact that the line length is proportional to the line reactance [6] not to the whole impedance, which makes the effect of the fault resistance small.
2. Even though the fault resistance doesn't have a great effect in estimating the fault location, it affects the LSV technique more than the LAV technique especially at a sampling rate less than 4320 Hz. As a result, the LAV technique is more accurate than LSV technique when an arc resistance exists.
3. There is an improvement in the fault location estimation, when the LAV technique is used, at sampling rate = 4320 Hz. The reason for this improvement is due to the variation on the d.c. component of the line response. Referring to equation (3.8), if R_{total} is small then $\tau R_{total}/L_{total}$ is small, which means that the d.c. component has a great effect in this case, but if R_{total} is large then $\tau R_{total}/L_{total}$ is large, which indicates that the d.c. component has little effect in this case. That is exactly what happens when the fault resistance exists, the d.c. component has

little effect which means that only the steady state value of the current is affecting the circuit. So when a fault resistance exists the location of the fault using LAV technique at sampling rate = 4320 Hz was improved.

Table (4.5) shows the estimation of the fault location under the same conditions as in table (4.4) except that the number of equations = 8.

It is obvious from table (4.5) that at sampling rate = 720 Hz both techniques gives their most accurate results, and still the LAV technique is more accurate than the LSV technique. The comments which were mentioned when comparing table (4.1) and table (4.4) are also valid when comparing table (4.2) with table (4.5), there is no need to repeat them here.

Now by increasing the number of equations by 1, and by having the same conditions as in table (4.5), table (4.6) shows the estimated fault location under these conditions. Again, the fault location estimation is more accurate at sampling rate = 720 Hz when using both techniques.

From the above discussion, a conclusion was reached. That is the existence of the fault resistance has almost no effect on the accuracy of the fault location when using a reasonable sampling rate. This indicated that the sampling rate has a great effect on estimating the fault location. The sampling rate which gives the most accurate results for this model is at 720 Hz. From now on, the sampling rate which will be used for this model is 720 Hz. It has to mentioned that the LAV technique is more accurate than LSV technique which is clear from the results discussed.

The next section will study the effect of changing the time reference ($T=0.0$) on the accuracy of estimating the fault location using the LSV technique as well as the LAV technique.

4.1.2 Effect of Time Reference.

A parameter which is yet to be discussed is the time reference. The time reference is the instant at which $T=0.0$. Thus the time reference is chosen to be at the first sample, that is $T=0.0$ at the first sample; if the time reference is chosen at the second sample that is, $T=0.0$ at the second sample and $T = -\text{window size}$ at the first sample. In our case, three time references are studied. The sampling rate is constant in these three cases and is 720 Hz. The change in the time reference is studied with the number of equations and the fault resistance varying. Of course, this study is for different assumptions of the fault location.

Table (4.7) through table (4.9) shows the fault location estimated at different assumption of fault location, using the LSV technique and the LAV technique, under the following conditions:

1. Sampling rate = 720 Hz
2. Number of unknowns = 7
3. Fundamental frequency = 60 Hz
4. Fault resistance = 0.0

The only parameter which varies among these tables is the number of equations. That is the number of equations = 7 in table (4.7), the number of equation = 8 in table (4.8),

and the number of equations = 9 in table (4.9).

It is observed from table (4.7) through Table (4.9) that the most accurate fault location estimation using LAV technique is at the first sample, while the most accurate fault location estimation using LSV technique is at time reference = the second sample. Even when the time reference is at the first sample for LAV technique and the time reference is at the second sample for LSV technique, the LAV technique still is more accurate than the LSV technique.

It has to mentioned, referring to table (4.7) through table (4.9), while the number of equations changes, the accuracy of both techniques changes, this point will be discussed in details in the next section.

Tables (4.10) through (4.12) show results under the same conditions as that in tables (4.7) through (4.9), except for the fault resistance which exists in this case and is 30 ohms. now the study will be on the effect of this fault resistance on both techniques.

It is observed from table (4.10) through table (4.12) that the LAV technique gives its most accurate results when the time reference is at the first sample, while the LSV technique gives its most accurate results when the time reference is at the second sample for table (4.10) and table (4.11), but for table (4.12) the LSV technique has its most accurate results at the first sample.

When comparing tables (4.7) with (4.10), (4.8) with (4.11), and (4.9) with (4.12), it could be concluded that the fault resistance has almost no effect on the accuracy of both techniques, which is expected.

From the above discussion, it is seen that the time reference at the first sample is the most accurate for LAV technique and the time reference at the second sample is the most accurate for the LSV technique. Because the LAV technique had the more accurate results than the LSV technique, the time reference at the first sample will be used for the rest of the thesis.

The next section will study the effect of the number of equations on the accuracy of both techniques.

4.1.3 Effect of Varying The Number of Equations.

One of the parameters that affects the techniques accuracy is the number of equation. In equation (2.34) and (2.36) the number of equations is a variable. Here, the number of equations will be varied. The goal of this section is to study the effect of the number of equations on the LAV and the LSV techniques.

As mentioned earlier, the sampling rate chosen is 720 Hz and the time reference ($T=0.0$) is at the first sample. Since the LSV technique has its most accurate results at the second sample, a special run was made to insure that our results are still more accurate.

Tables (4.13) and (4.14) show the error* of the estimated fault location at different assumptions of the fault location using both techniques, LSV and LAV. The conditions under which the runs on table (4.13) and (4.14) were made are: sampling rate = 720 Hz, fundamental frequency = 60 Hz, number of unknowns = 7 and there is no fault resistance. The only condition that is different in the results in table (4.13) from the results in table

* The error of the estimated fault location = the assumed fault location - the estimated fault location.

(4.14) is that in table (4.13) the time reference is at the first sample while in table (4.14) the time reference is at the second sample.

By observing table (4.13), it is noticed that the most accurate results for the LAV technique is when number of equations = 8, while the most accurate results for the LSV technique is when number of equation = 9. Of course, the fewer equations, the less the computation time is, which decreases the time required to locate the fault. Another observation which has to be mentioned is that the LAV technique is more accurate than the LSV technique, when using number of equations = 8 for LAV technique and number of equation = 9 for LSV technique. Thus, the LAV technique provides more accurate results with less computation time.

Now, taking the time reference at the second sample as shown in table (4.14). It is obvious that the LSV technique has its most accurate results at number of equations = 8 and the LAV technique has its most accurate results at number of equations = 9. When comparing the results of the LAV technique when number of equations = 9 with the results of the LSV technique when number of equations = 8, the LAV technique gives more accurate results than the LSV technique.

From the above discussion, it could be concluded that the number of equation which was chosen for the rest of the thesis is 8 (i.e. number of equations = 8), when the time reference is at the first sample and the sampling rate = 720 Hz. This procedure was made for the case where the fault resistance does not exists. The same procedure was used when the fault resistance exists and the same conclusion was reached.

As a result of these studies, it can be concluded that the parameters producing the most accurate results (and this will be used for this model) are:

1. The sampling rate = 720 Hz.
2. The time reference is at the first sample.
3. Number of equations = 8.

Now after confirming these parameters our next study will concern the estimated impedance of the line, in other words the resistance and the reactance of the line. The estimation of the impedance of the line has a great effect on estimating the fault location, due to the fact that the impedance of line is proportional to its length [14].

Results are shown for different assumptions of fault location and two values of fault resistance (0.0 and 30.0 ohms). Because the samples of three cycles are stored on every estimation of the fault location, these samples were used to estimate the fault location. The program was adjusted to get the estimated fault location from 8 samples, then to skip these 8 samples and use the following 8 samples till the three cycles are finished.

Figure 4.1 through figure 4.4 shows the estimated resistance versus the estimated reactance using LSV technique, under the condition that there is no fault resistance. Each figure is for a different fault location. It is observed from these figures that the resistance versus the reactance are scattered on the figure. For the LAV technique, the resistance and the reactance does not change at all, which means that there is only one point on the figure. From this observation, it could be concluded that the LAV technique is more accurate than LSV technique in estimating the impedance.

Figure 4.5 through figure 4.8 show the estimated resistance versus the reactance estimated using the LSV technique, under the condition that the fault resistance exists. Each figure has its own fault location assumption. It is also observed that the impedances are scattered on the R-X plane. When the same procedure was made using LAV technique, the resistance and the reactance do not change and they is only one point on the figure.

Thus it seems the LSV technique change its estimation depending on the time the samples are taken. On the other hand, the LAV technique was not affected by these changes.

From the above discussion the following comments are in order:

1. The LAV technique gives an accurate estimation of the resistance and the reactance regardless of the point the samples were taken at as long as it is within the first three cycles. This indicates that the fault location estimated is also accurate and it does not depend on the point the samples were taken from.
2. The LSV technique gives an estimation of the resistance and the reactance near the actual value, but these are scattered round the actual value, which is not as accurate as the LAV technique.
3. The LAV technique is more accurate than the LSV technique.
4. The fault resistance does not have a great effect on the accuracy of the estimated impedance for both techniques.

The last parameter which was studied is the effect of the fault resistance on estimating the fault location. It was concluded earlier that the fault resistance has no great effect on the accuracy of the fault location. But our study was concerned with two cases only, the case where there is no fault resistance, and the case where the fault resistance exists. The next paragraph will discuss the effect of changing the fault resistance from 0.0 to 30 ohms gradually (i.e. 5 ohms at a time) on the estimated fault location.

Figures 4.9 through figure 4.11 shows the fault resistance versus the error of the estimated fault location at different assumptions of fault location, using the LSV technique and the LAV technique. Because the fault resistance has no great effect on estimating the fault location, i.e. the error is small, it is changed to meters rather than miles to make it clear to the reader. From the figures, it is shown that with respect to LSV technique, as the fault resistance increases the error of the estimated fault decreases and as the assumed distance of the fault location increases, the error of the fault location increases, so the range of the error for LSV for all the curves together is from 90m to above 330m; but for the LAV technique the error does not increase when increasing the assumed fault location and the range of error is small (0.0 to 30m) compared to LSV technique. Also the increases in the error that occur when the fault resistance increases are relatively small. Then it could be concluded that the fault resistance does not relatively affect the LAV technique as it does relatively affect the LSV technique.

From the results of the single phase model it can be concluded that:

1. The LAV technique is more accurate than the LSV technique in estimating the fault location.
2. The three parameters which provide the most accurate results are:
 - A. sampling rate = 720 Hz.
 - B. Number of equations = 8 .
 - C. Time reference at the first sample.
3. The fault resistance does not have a great effect on the accuracy of the fault location using both techniques.

Next, the results of the three-phase system are presented.

4.2 Numerical Results of The Three Phase System .

From the study of previous section, it is reasonable to choose the following parameters, sampling rate is 720 Hz, number of equations are equal to 8 and the time reference is at the first sample.

Because our study is only concerned with the symmetrical three phase fault, the three- phase system considered does not differ from single phase system in the previous section except that the transmission line number 1* is now 133.5 miles long. This transmission line is divided into three pi sections, each section represents 44.5 miles.

The single phase system did not require the use of a low-pass filter, but the three phase system requires a low-pass filter**. The three filters used were designed in chapter

* See chapter 3 for more details.

3. The effect of these filters on the location of the fault will be studied, as well as the effect of the shunt capacitance. Then the effects of the fault resistance on the fault location will also be studied.

4.2.1 Effect of The Low-Pass Filter.

It is known that as the order of the filter increases, its effect in attenuating high frequency harmonics increases. Thus, the effect of increasing the order of the filter on the accuracy of the fault location techniques will be studied as well as the estimated impedance. Then the time delay that is caused by the filter will be discussed. Finally, a comparison between the LAV technique and the LSV technique is made.

4.2.1.1 Effect of The Order of The Filter.

Three different order filters were designed, the 4th order filter, the 8th order filter and the 10th order filter. Figures 4.12 through figure 4.14 shows the estimated fault location versus the time delay at 44.5 miles (i.e. one pi section) from the sending end, using the LAV technique and the LSV technique.

It is obvious that, as the order of the filter increases, the accuracy of the estimated fault location increases.

Figure 4.18 through 4.23 show the corresponding impedances using LSV technique and LAV technique. The true impedance for the first pi section is $0.061+j0.236$ p.u., if this true impedance is compared with calculated ones, it is concluded that as the order of

** The low-pass filter is used to attenuate the high frequency harmonics.

the filter increases the impedance converges to its true value. Thus, the 10th order filter gives the highest accuracy in calculating the impedance of the line and thus locating the fault.

4.2.1.2 Effect of Time Delay.

It is known that the presence of a filter introduces a time delay. This time delay differs as the order of the filter changes. By looking at figures 4.12, 4.13 and 4.14, it is noticed that the 4th order filter has the shortest time delay compared to the other filters. The time delay for the 4th order filter is 0.0125 second, before this period both techniques give unrelated fault location results. As the order of the filter increases, the time delay increases. This delay has to be minimized in order to increase the availability of power transfer. But, as discussed earlier, as the order of the filter increases the accuracy of the techniques increases. As a result, there is a trade off between speed and accuracy.

4.2.1.3 A Comparison Between The LAV and LSV Techniques.

In comparing the LAV technique and LSV technique, it was found that:

1. The LAV technique is more accurate than the LSV technique, this can be seen from the results shown in figure 4.12, 4.13, and 4.14.
2. By comparing the figures of the impedances for the LAV technique and LSV technique, it can be concluded that the LAV technique gives more accurate results than the LSV technique does.

3. The time delay that is caused by the use of filter is less when the LAV technique is used.

4.2.2 Effect of Line Shunt Capacitance.

In the previous section, the assumed fault location was at 44.5 miles from the sending end, which is the length of one pi section*. To be able to see the effect of the line capacitance, another location of the fault is introduced. Let the fault be at 89 miles from the sending end (i.e. 2 pi sections*), a comparison was made in the accuracy of the fault location, between the fault that occurs at 44.5 mile and the fault that occurs at 89 miles. A comparison between their impedances was also discussed.

When comparing figure 4.12 with 4.15, figure 4.13 with 4.16 and figure 4.14 with 4.17, it is found that both techniques converges to the true fault location when the fault is at 44.5 miles from the sending end. However, the results of both techniques when the fault occurs at 89 miles from the sending end is not as accurate, but still within a reasonable range. This is due to the line shunt capacitance. However, it should be noted that the effect of the line shunt capacitance has relatively small effect on estimating the fault location.

Now when comparing figure 4.18 with 4.24, figure 4.19 with 4.25, figure 4.20 with 4.26, figure 4.21 with 4.27, figure 4.22 with 4.28 and figure 4.23 with 4.29, it is obvious that the impedances converges to its true value in the case where the fault is at 44.5 miles

* Which is only one shunt capacitance.

* Which is two shunt capacitances.

from the sending end, specially for the case of the fourth order filter, it converges to its true value when the fault occurs at 44.5 miles from sending end and it is scattered on the figure when the fault occurs at 89 miles from the sending end. This is because of the effect of the line shunt capacitance.

4.2.3 Effect of Fault Resistance.

The results in the above section all were computed with no fault resistance (i.e. $R_f=0.0$). In this section, the effect of the fault resistance is studied. Three different fault resistances were studied with the fault at 44.5 miles from the sending end and the 8th order filter used, the fault resistance was changed from 10 ohms to 20 ohms to 30 ohms. The estimated fault location (for the three fault resistance) versus the time delay is shown in figure 4.30 and figure 4.31 using LSV technique and LAV technique respectively. It was observed that the effect of the fault resistance is relatively small. However, when the fault resistance is small the accuracy of the estimated fault increases. By comparing figure 4.30 with figure 4.31, it is observed that the LAV technique is more accurate than the LSV technique.

From the above results, it is concluded that:

1. As the order of the filter increases, the accuracy of both algorithms increases and the time delay increases. As a result, the choice of the filter is a trade off between speed and accuracy.

2. The line shunt capacitance does not have a great effect on the accuracy of both techniques specially when using a high order filter.
3. The fault resistance does not have a great effect on the accuracy of the LAV technique and LSV technique. However, when the fault resistance does not exist the results are relatively more accurate.
4. The LAV technique gives more accurate results than the LSV technique.

| Estimated Fault Location (in miles) | | | | | | | | |
|-------------------------------------|---------|--------|--------|--------|--------|--------|--------|---------|
| Sampling rate (Hz) | Y = .25 | | Y = 10 | | Y = 15 | | Y = 20 | |
| | LSV | LAV | LSV | LAV | LSV | LAV | LSV | LAV |
| 4320 | .25710 | 29.433 | 23.929 | 4.166 | 19.622 | 60.694 | 26.944 | 156.189 |
| 2160 | .21919 | .32295 | 11.144 | 10.15 | 14.24 | 15.54 | 19.423 | 20.543 |
| 1440 | .22710 | .26613 | 9.711 | 10.099 | 15.015 | 15.051 | 20.596 | 20.143 |
| 720 | .28508 | .24999 | 11.590 | 10.000 | 17.500 | 15.000 | 23.465 | 20.000 |

Table 4.1: The Estimates of Fault Location at Different Values of Sampling Rate.

Fault Resistance = 0.0

No. of Equations = 7

Fundamental frequency = 60 Hz.

No. of Unknowns = 7

Time Reference (T=0.0) at The First Sample.

| Sampling rate (Hz) | Estimated Fault Location (in miles) | | | | | | | |
|-----------------------|-------------------------------------|--------|---------|--------|---------|--------|--------|--------|
| | Y = .25 | | Y = 10 | | Y = 15 | | Y = 20 | |
| | LSV | LAV | LSV | LAV | LSV | LAV | LSV | LAV |
| 4320 | .29909 | 8.737 | 18.190 | 4.166 | -0.0415 | 56.345 | 27.364 | 46.599 |
| 2160 | .33391 | .32958 | 11.5441 | 10.151 | 18.818 | 15.414 | 24.559 | 20.665 |
| 1440 | 1.939 | .24123 | 48.463 | 9.947 | 58.845 | 14.970 | 65.101 | 20.004 |
| 720 | .25205 | .24999 | 10.054 | 10.000 | 15.148 | 15.000 | 20.206 | 19.999 |

Table 4.2: The Estimates of Fault Location at Different Values of Sampling Rate.

Fault Resistance = 0.0

No. of Equations = 8

Fundamental frequency = 60 Hz.

No. of Unknowns = 7

Time Reference ($T=0.0$) at The First Sample.

| Sampling rate (Hz) | Estimated Fault Location (in miles) | | | | | | | |
|-----------------------|-------------------------------------|--------|--------|--------|--------|--------|--------|---------|
| | Y = .25 | | Y = 10 | | Y = 15 | | Y = 20 | |
| | LSV | LAV | LSV | LAV | LSV | LAV | LSV | LAV |
| 4320 | .20423 | 29.433 | 12.96 | 6.617 | 13.008 | 60.694 | 17.652 | 156.189 |
| 2160 | .25403 | .26413 | 11.163 | 10.336 | 16.765 | 15.189 | 22.987 | 20.541 |
| 1440 | .156 | .25627 | 6.497 | 10.019 | 9.932 | 15.017 | 13.491 | 20.181 |
| 720 | .25018 | .25000 | 10.008 | 10.001 | 15.012 | 15.001 | 20.017 | 20.002 |

Table 4.3: The Estimates of Fault Location at Different Values of Sampling Rate.

Fault Resistance = 0.0

No. of Equations = 9

Fundamental frequency = 60 Hz.

No. of Unknowns = 7

Time Reference (T=0.0) at The First Sample.

| Estimated Fault Location (in miles) | | | | | | | | |
|-------------------------------------|---------|--------|--------|--------|--------|--------|--------|--------|
| Sampling rate (Hz) | Y = .25 | | Y = 10 | | Y = 15 | | Y = 20 | |
| | LSV | LAV | LSV | LAV | LSV | LAV | LSV | LAV |
| 4320 | .25165 | .30083 | 12.316 | 8.483 | 19.904 | 24.129 | 28.233 | 36.673 |
| 2160 | .25067 | .25034 | 10.895 | 10.044 | 16.837 | 15.164 | 23.003 | 20.262 |
| 1440 | .25100 | .25010 | 11.344 | 10.011 | 17.803 | 15.015 | 24.647 | 20.027 |
| 720 | .25022 | .25000 | 10.329 | 10.006 | 15.703 | 15.009 | 21.177 | 20.020 |

Table 4.4: Estimates of Fault Location at Different Values of Sampling Rate.

Fault Resistance = 30.0 ohms

No. of Equations = 7

Fundamental frequency = 60 Hz.

No. of Unknowns = 7

Time Reference ($T=0.0$) at The First Sample.

| Estimated Fault Location (in miles) | | | | | | | | |
|-------------------------------------|---------|--------|--------|--------|--------|--------|--------|--------|
| Sampling rate | Y = .25 | | Y = 10 | | Y = 15 | | Y = 20 | |
| (Hz) | LSV | LAV | LSV | LAV | LSV | LAV | LSV | LAV |
| 4320 | .25191 | .38008 | 12.689 | 8.973 | 20.712 | 15.575 | 29.631 | 13.095 |
| 2160 | .24844 | .24943 | 9.303 | 9.995 | 13.595 | 15.129 | 17.747 | 20.228 |
| 1440 | .24766 | .25017 | 6.949 | 10.011 | 8.812 | 15.020 | 10.039 | 20.046 |
| 720 | .25002 | .25001 | 10.025 | 9.993 | 15.055 | 14.992 | 20.094 | 19.993 |

Table 4.5: Estimates of Fault Location at Different Values of Sampling Rate.

Fault Resistance = 30.0 ohms

No. of Equations = 8

Fundamental frequency = 60 Hz.

No. of Unknowns = 7

Time Reference (T=0.0) at The First Sample.

| | | Estimated Fault Location (in miles) | | | | | | | |
|---------------|--|-------------------------------------|--------|--------|---------|--------|--------|--------|--------|
| Sampling rate | | Y = .25 | | Y = 10 | | Y = 15 | | Y = 20 | |
| (Hz) | | LSV | LAV | LSV | LAV | LSV | LAV | LSV | LAV |
| 4320 | | .25035 | .30083 | 11.735 | 10.0435 | 15.908 | 24.189 | 21.466 | 36.673 |
| 2160 | | .25127 | .25034 | 10.017 | 10.010 | 18.625 | 15.164 | 26.022 | 20.262 |
| 1440 | | .25005 | .24987 | 10.017 | 10.010 | 15.007 | 15.015 | 19.079 | 20.028 |
| 720 | | .25000 | .25022 | 10.005 | 10.013 | 15.011 | 14.996 | 20.019 | 19.998 |

Table 4.6: Estimates of Fault Location at Different Values of Sampling Rate.

Fault Resistance = 30.0 ohms

No. of Equations = 9

Fundamental frequency = 60 Hz.

No. of Unknowns = 7

Time Reference (T=0.0) at The First Sample.

| Estimated Fault Location (in miles) | | | | | | | | |
|-------------------------------------|---------|--------|--------|--------|--------|--------|--------|--------|
| Time Reference ($T=0$) | Y = .25 | | Y = 10 | | Y = 15 | | Y = 20 | |
| | LSV | LAV | LSV | LAV | LSV | LAV | LSV | LAV |
| First sample | .28508 | .24999 | 11.590 | 10.000 | 17.500 | 15.000 | 23.465 | 20.000 |
| Second sample | .25266 | .25000 | 10.079 | 9.999 | 15.099 | 14.998 | 20.111 | 19.998 |
| Third sample | .23528 | .24999 | 9.380 | 9.999 | 14.056 | 15.001 | 18.729 | 20.003 |

Table 4.7: Estimates of Fault Location at Different Values of Time Reference.

Fault Resistance = 0.0

No. of Equations = 7

Fundamental Frequency = 60 Hz.

No. of Unknowns = 7

Sampling Frequency = 720 Hz.

| Time Reference | Estimated Fault Location (in miles) | | | | | | | |
|----------------|-------------------------------------|--------|--------|--------|--------|--------|--------|--------|
| | Y = .25 | | Y = 10 | | Y = 15 | | Y = 20 | |
| | LSV | LAV | LSV | LAV | LSV | LAV | LSV | LAV |
| (T=0.0) | | | | | | | | |
| First sample | .25205 | .24999 | 10.094 | 10.000 | 15.148 | 15.000 | 20.206 | 19.999 |
| Second sample | .25007 | .24995 | 10.001 | 9.999 | 15.001 | 14.998 | 19.999 | 19.998 |
| Third sample | .24959 | .24996 | 9.982 | 10.000 | 14.972 | 14.999 | 19.963 | 20.002 |

Table 4.8: Estimates of Fault Location at Different Values of Time Reference.

Fault Resistance = 0.0

No. of Equations = 8

Fundamental Frequency = 60 Hz.

No. of Unknowns = 7

Sampling Frequency = 720 Hz.

| Estimated Fault Location (in miles) | | | | | | | | |
|-------------------------------------|---------|--------|--------|--------|--------|--------|--------|--------|
| Time Reference (T=0.0) | Y = .25 | | Y = 10 | | Y = 15 | | Y = 20 | |
| | LSV | LAV | LSV | LAV | LSV | LAV | LSV | LAV |
| First sample | .25018 | .25000 | 10.008 | 10.000 | 15.012 | 15.001 | 20.017 | 20.002 |
| Second sample | .25010 | .25002 | 10.005 | 9.999 | 15.008 | 14.999 | 20.011 | 20.000 |
| Third sample | .24992 | .25001 | 9.997 | 10.000 | 14.995 | 14.999 | 19.994 | 20.000 |

Table 4.9: Estimates of Fault Location at Different Values of Time Reference.

Fault Resistance = 0.0

No. of Equations = 9

Fundamental Frequency = 60 Hz.

No. of Unknowns = 7

Sampling Frequency = 720 Hz.

| Estimated Fault Location (in miles) | | | | | | | | |
|-------------------------------------|---------|--------|--------|--------|--------|--------|--------|--------|
| Time Reference (T=0.0) | Y = .25 | | Y = 10 | | Y = 15 | | Y = 20 | |
| | LSV | LAV | LSV | LAV | LSV | LAV | LSV | LAV |
| First sample | .25022 | .25000 | 10.329 | 10.007 | 15.703 | 15.015 | 21.177 | 20.028 |
| Second sample | .24997 | .25001 | 9.970 | 10.009 | 14.945 | 15.022 | 19.918 | 20.042 |
| Third sample | .24996 | .25002 | 9.940 | 10.010 | 14.879 | 15.023 | 19.789 | 20.046 |

Table 4.10: Estimates of Fault Location at Different Values of Time Reference.

Fault Resistance = 30.0 ohms

No. of Equations = 7

Fundamental Frequency = 60 Hz.

No. of Unknowns = 7

Sampling Frequency = 720 Hz.

| Estimated Fault Location (in miles) | | | | | | | | |
|-------------------------------------|---------|--------|--------|--------|--------|--------|--------|--------|
| Time Reference (T=0.0) | Y = .25 | | Y = 10 | | Y = 15 | | Y = 20 | |
| | LSV | LAV | LSV | LAV | LSV | LAV | LSV | LAV |
| First sample | .25002 | .25001 | 10.025 | 9.993 | 15.055 | 14.992 | 20.094 | 19.993 |
| Second sample | .25000 | .25001 | 10.006 | 10.009 | 15.014 | 15.022 | 20.026 | 20.042 |
| Third sample | .25000 | .25000 | 10.007 | 10.009 | 15.015 | 15.023 | 20.037 | 20.056 |

Table 4.11: Estimates of Fault Location at Different Values of Time Reference.

Fault Resistance = 30.0 ohms

No. of Equations = 8

Fundamental Frequency = 60 Hz.

No. of Unknowns = 7

Sampling Frequency = 720 Hz.

| Estimated Fault Location (in miles) | | | | | | | | |
|-------------------------------------|---------|--------|--------|--------|--------|--------|--------|--------|
| Time Reference (T=0.0) | Y = .25 | | Y = 10 | | Y = 15 | | Y = 20 | |
| | LSV | LAV | LSV | LAV | LSV | LAV | LSV | LAV |
| First sample | .25000 | .25001 | 10.005 | 10.009 | 15.011 | 14.996 | 20.019 | 19.998 |
| Second sample | .25000 | .25001 | 10.008 | 10.013 | 15.019 | 15.021 | 20.034 | 20.041 |
| Third sample | .25000 | .25001 | 10.009 | 10.026 | 15.022 | 15.030 | 20.042 | 20.091 |

Table 4.12: Estimates of Fault Location at Different Values of Time Reference.

Fault Resistance = 30.0 ohms

No. of Equations = 9

Fundamental Frequency = 60 Hz.

No. of Unknowns = 7

Sampling Frequency = 720 Hz.

| The Error of Estimated Fault Location (in miles) | | | | | | | | |
|--|---------|--------|--------|--------|--------|--------|--------|--------|
| No. Of Equations (T=0.0) | Y = .25 | | Y = 10 | | Y = 15 | | Y = 20 | |
| | LSV | LAV | LSV | LAV | LSV | LAV | LSV | LAV |
| 7 | .03508 | .00001 | 1.590 | .00028 | 2.500 | .00067 | 3.465 | .00090 |
| 8 | .00205 | .00001 | .09409 | .00028 | .148 | .00067 | .2063 | .00037 |
| 9 | .00018 | 0.0 | .00788 | .0007 | .01223 | .00121 | .01662 | .00203 |

Table 4.13: The Error of The Estimated Fault Location at Different Number of Equations.

Fault Resistance = 0.0

Time Reference (T=0.0) At The First Sample.

Fundamental Frequency = 60 Hz.

No. of Unknowns = 7

Sampling Frequency = 720 Hz.

| The Error of Estimated Fault Location (in miles) | | | | | | | | |
|--|---------|--------|--------|--------|--------|--------|--------|--------|
| No. Of Equations (T=0.0) | Y = .25 | | Y = 10 | | Y = 15 | | Y = 20 | |
| | LSV | LAV | LSV | LAV | LSV | LAV | LSV | LAV |
| 7 | .00266 | 0.0 | .0786 | .00092 | .0994 | .00177 | .11131 | .00211 |
| 8 | .00007 | .00005 | .00123 | .0011 | .00061 | .00216 | .00041 | .00185 |
| 9 | .0001 | .00002 | .00475 | .00039 | .00773 | .00031 | .01106 | .00015 |

Table 4.14: The Error of The Estimated Fault Location at Different Number of Equations.

Fault Resistance = 0.0

Time Reference (T=0.0) At The Second Sample.

Fundamental Frequency = 60 Hz.

No. of Unknowns = 7

Sampling Frequency = 720 Hz.

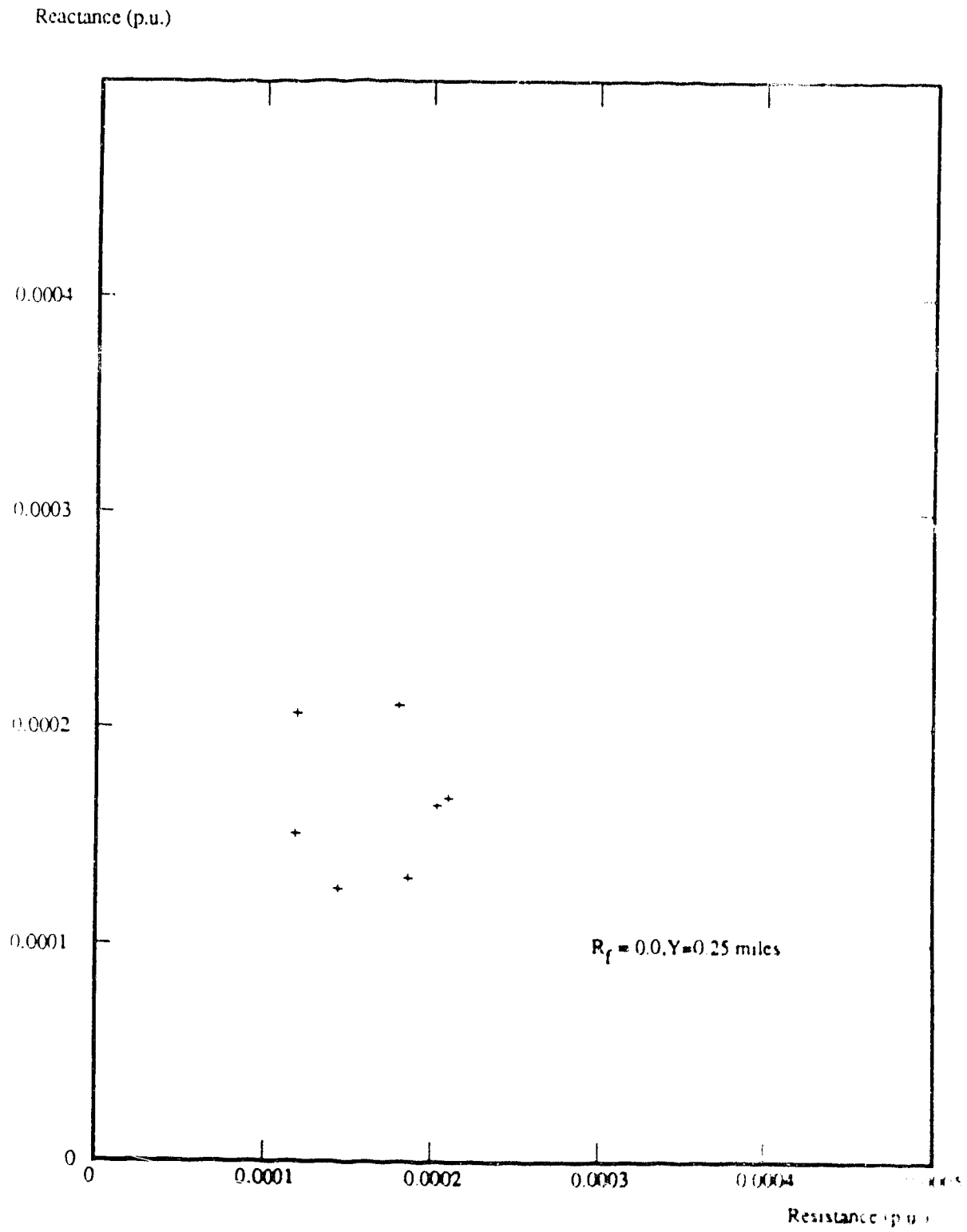


Figure (4.1): Impedance of a single phase system

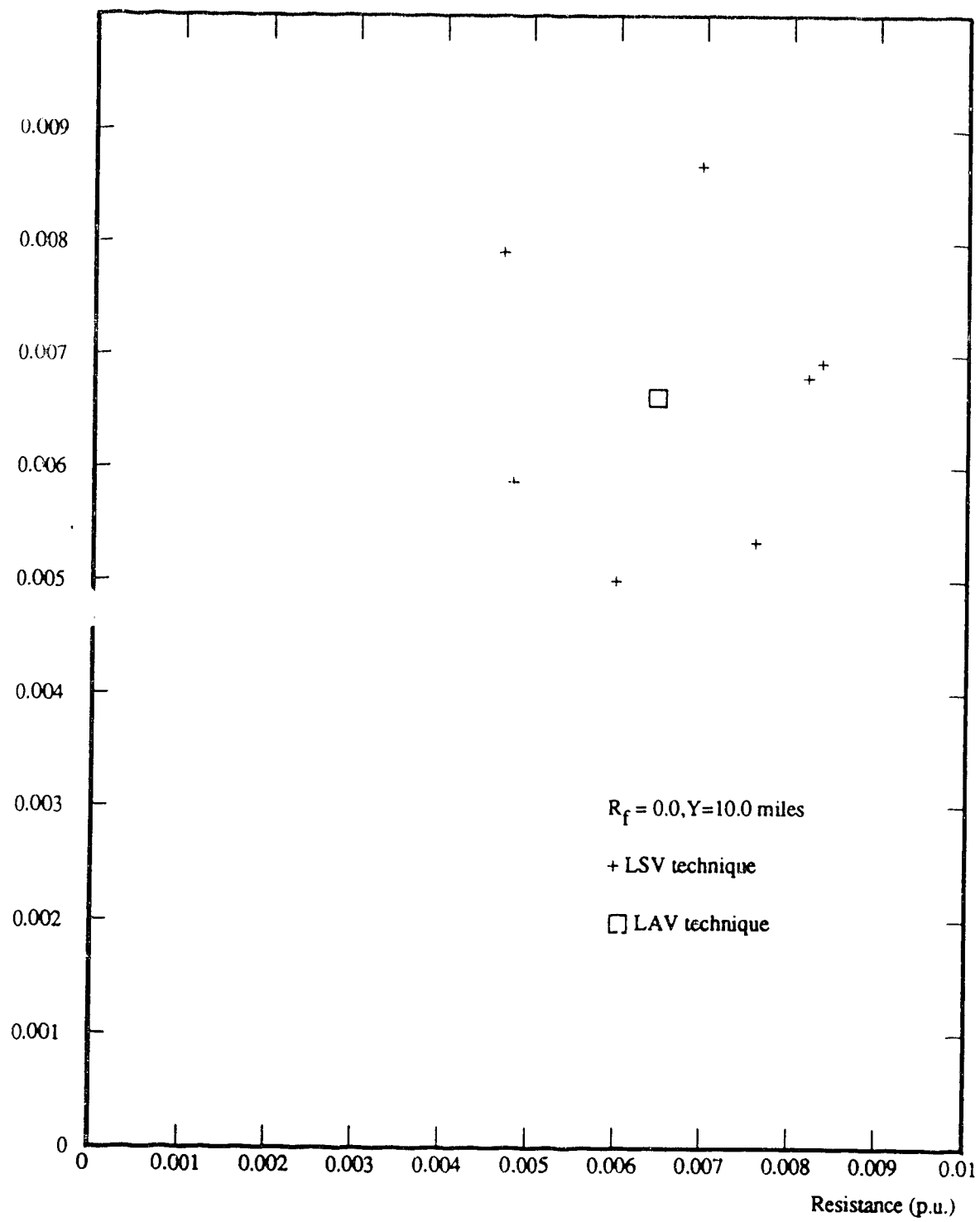


Figure (4.2): Impedance of the single phase system using LSV.

Reactance (p.u.)

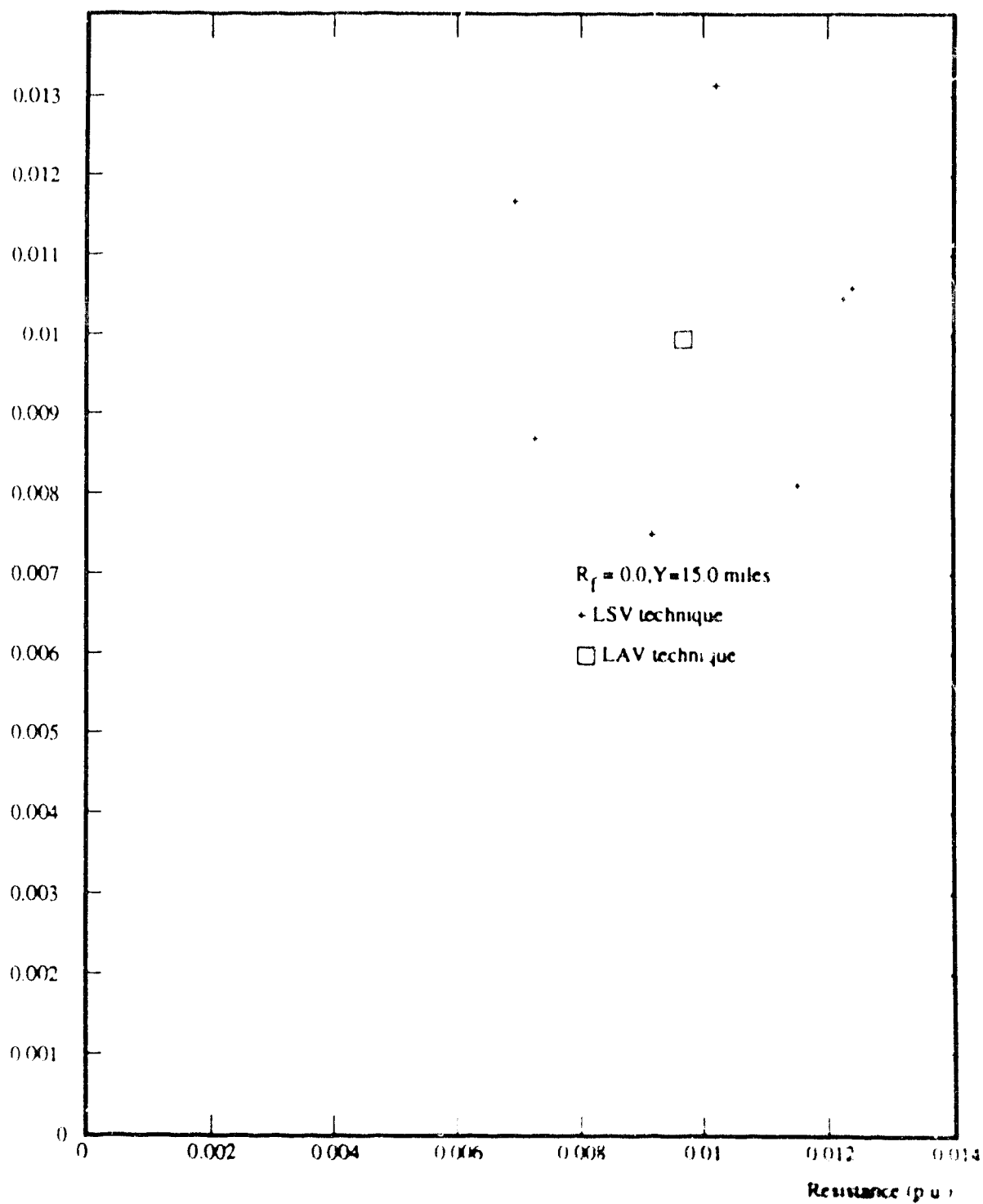


Figure (4.9): Impedance of the single phase system using LSV

Reactance (p.u.)

9()

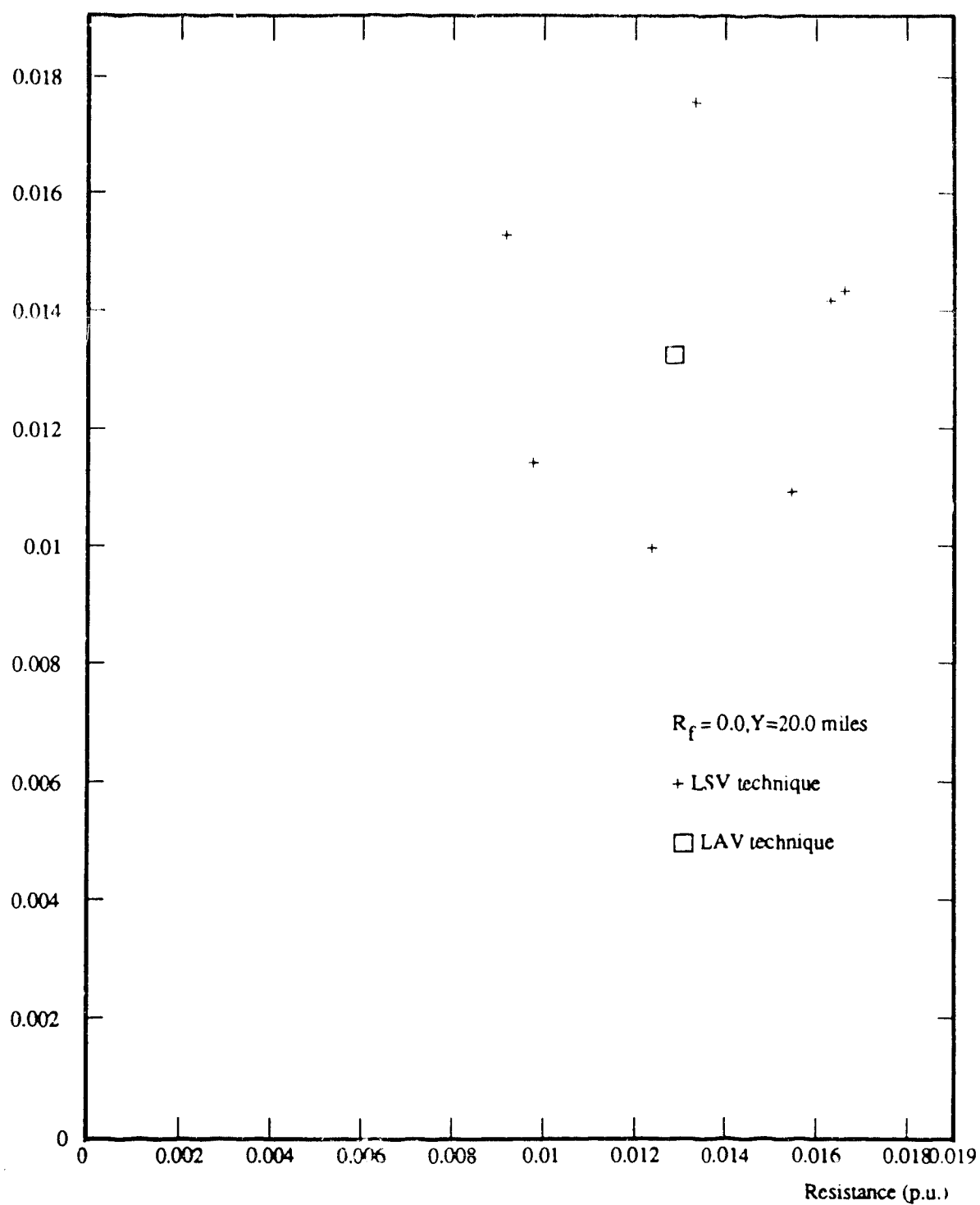


Figure (4.4): Impedance of the single phase system using LSV.

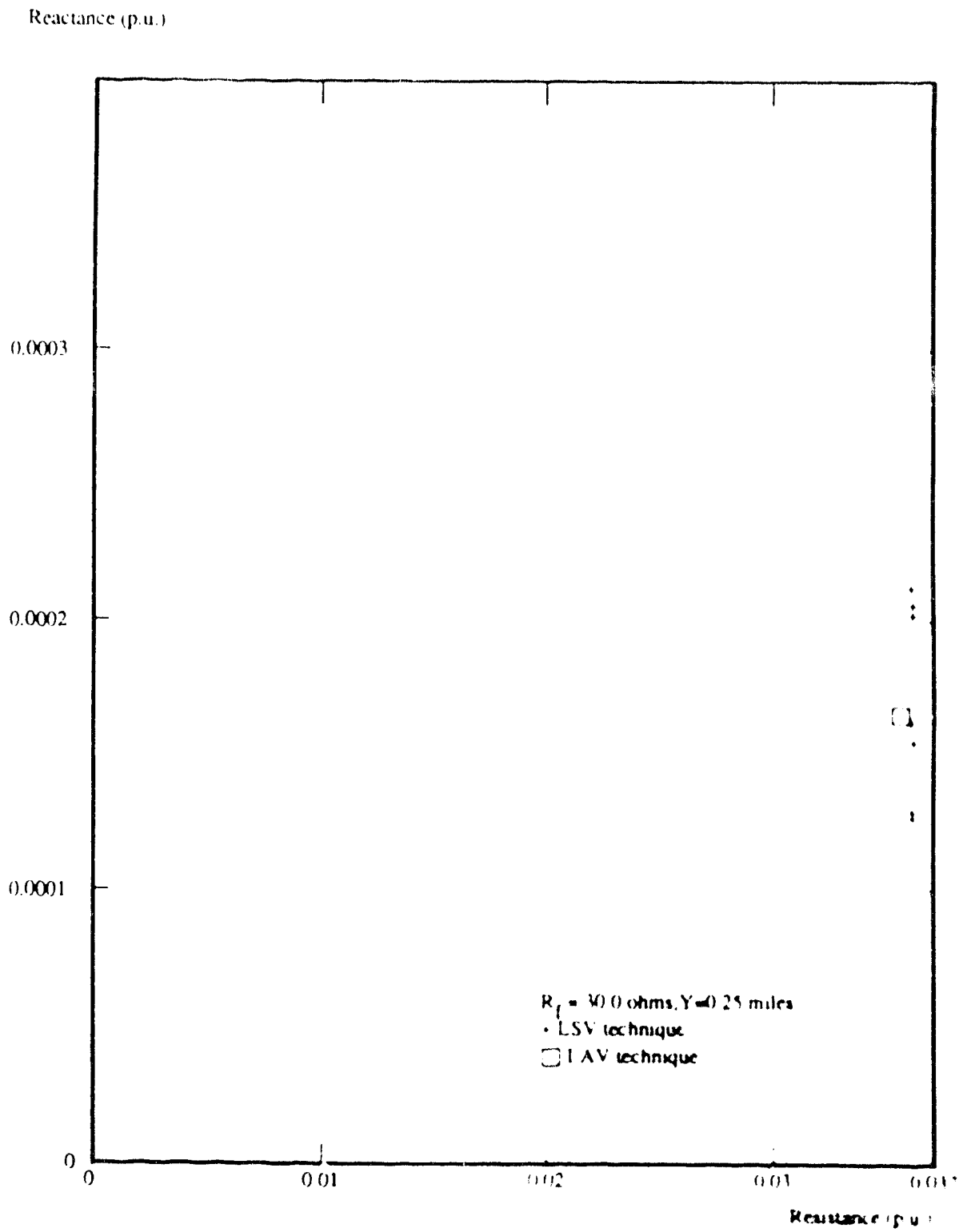
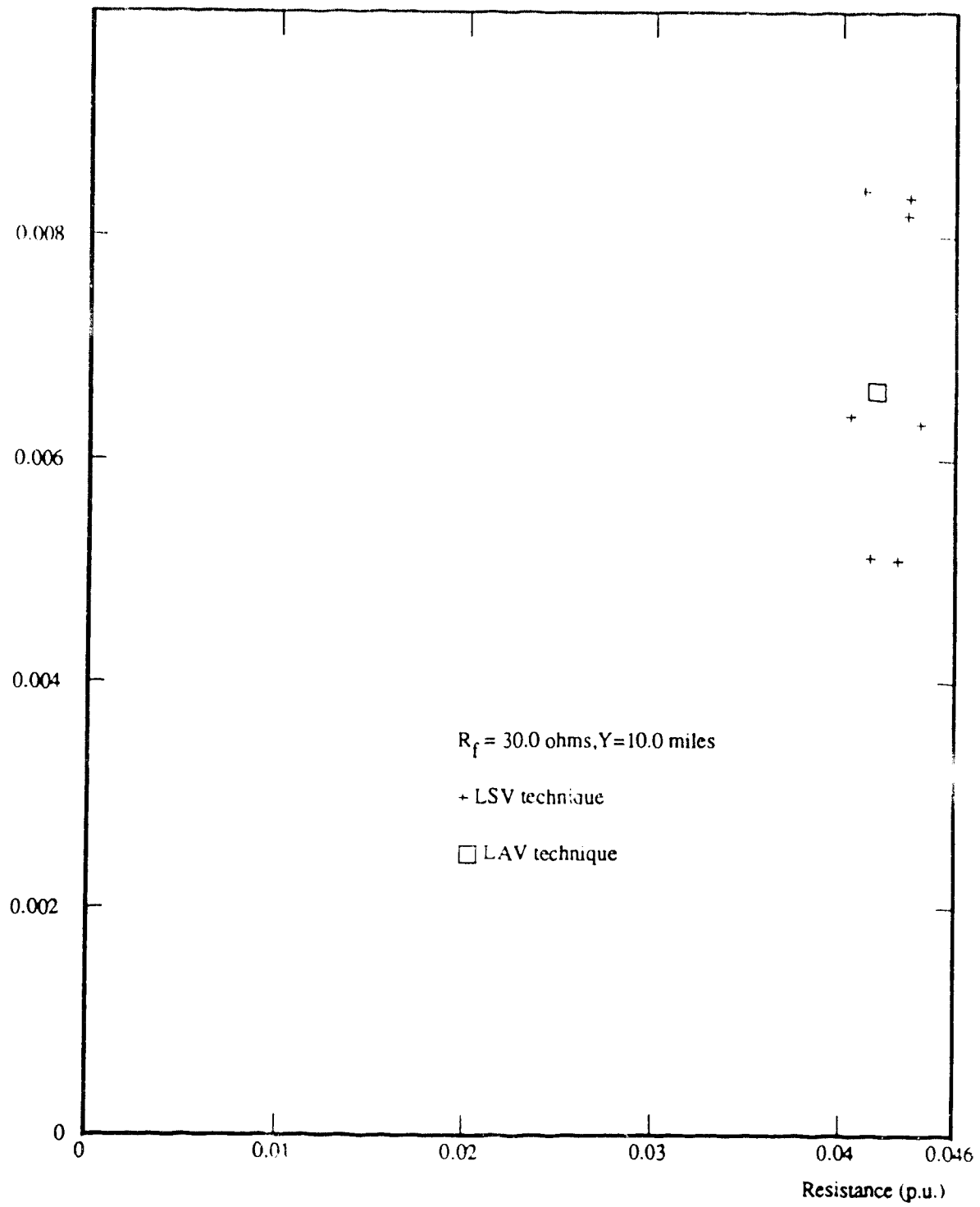


Fig. 4.5: Impedance of the single phase system using LSV

Reactance (p.u.)

**Figure (4.6):** Impedance of the single phase system using LSV.

Reactance (p.u.)

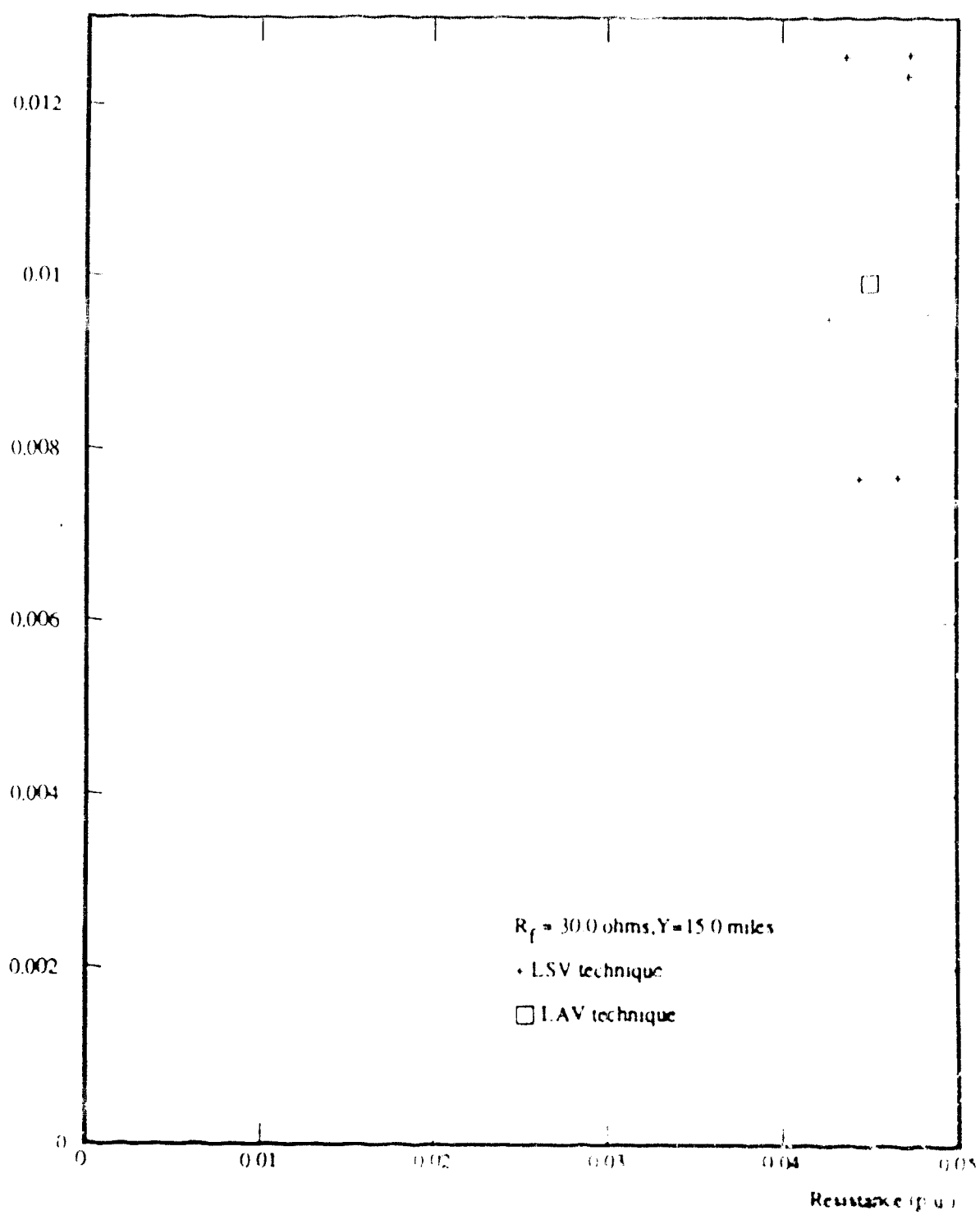
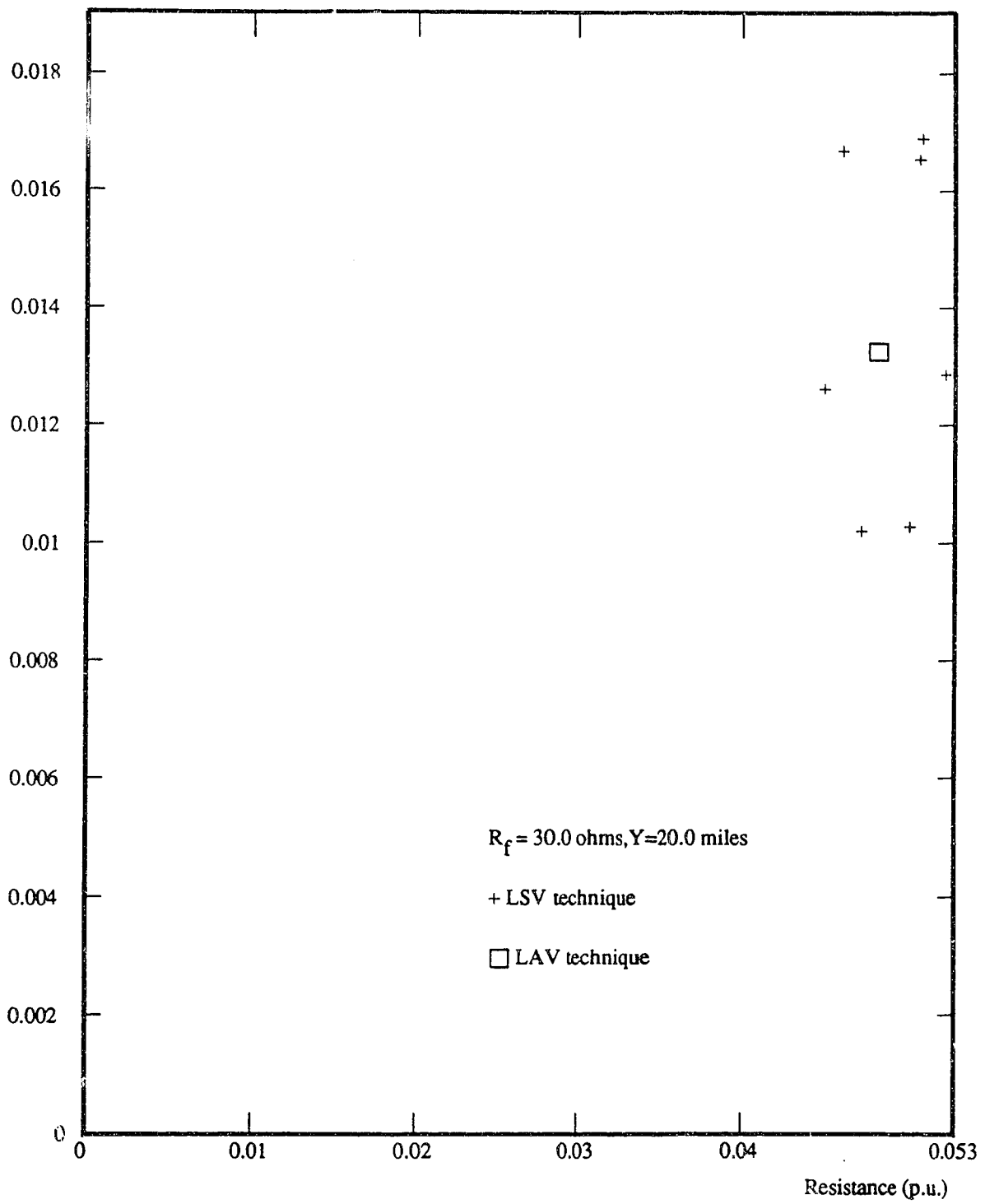


Figure (4.7): Impedance of the single phase system using LSV

Reactance (p.u.)

**Figure (4.8):** Impedance of the single phase system using LSV.

Error of estimates distance (m)

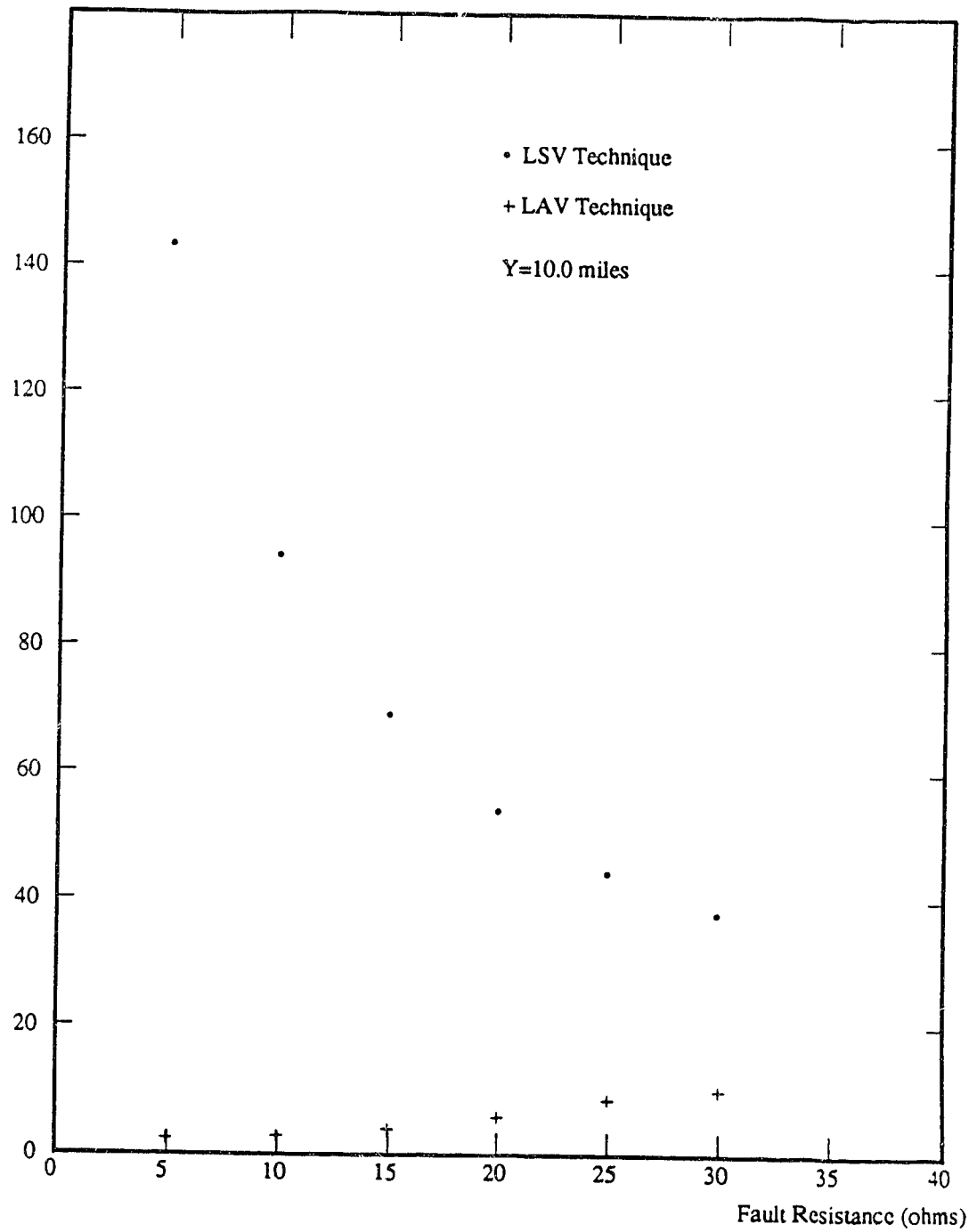


Figure (4.9): The fault resistance versus the error of distance.

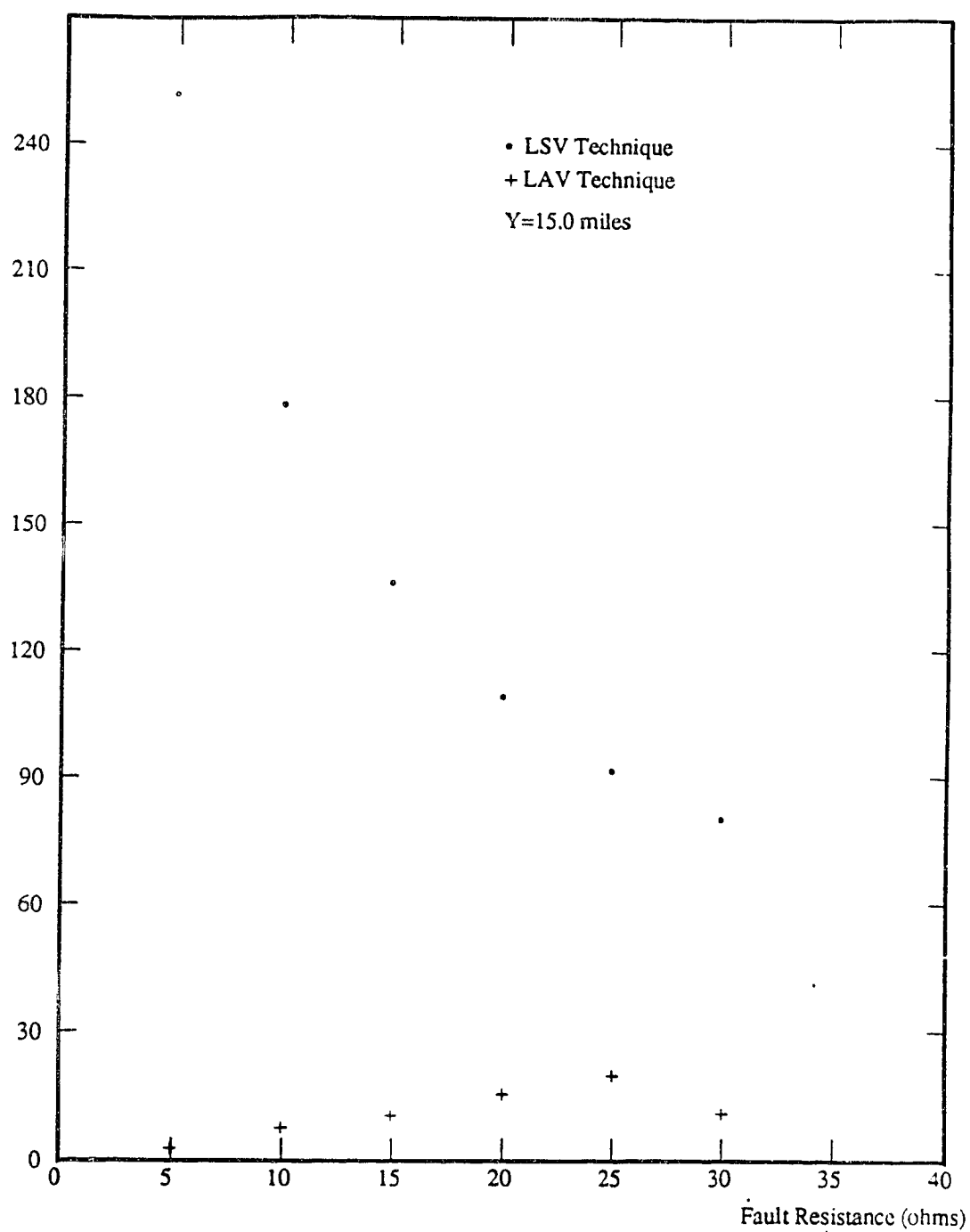


Figure (4.10): The fault resistance versus the error of distance.

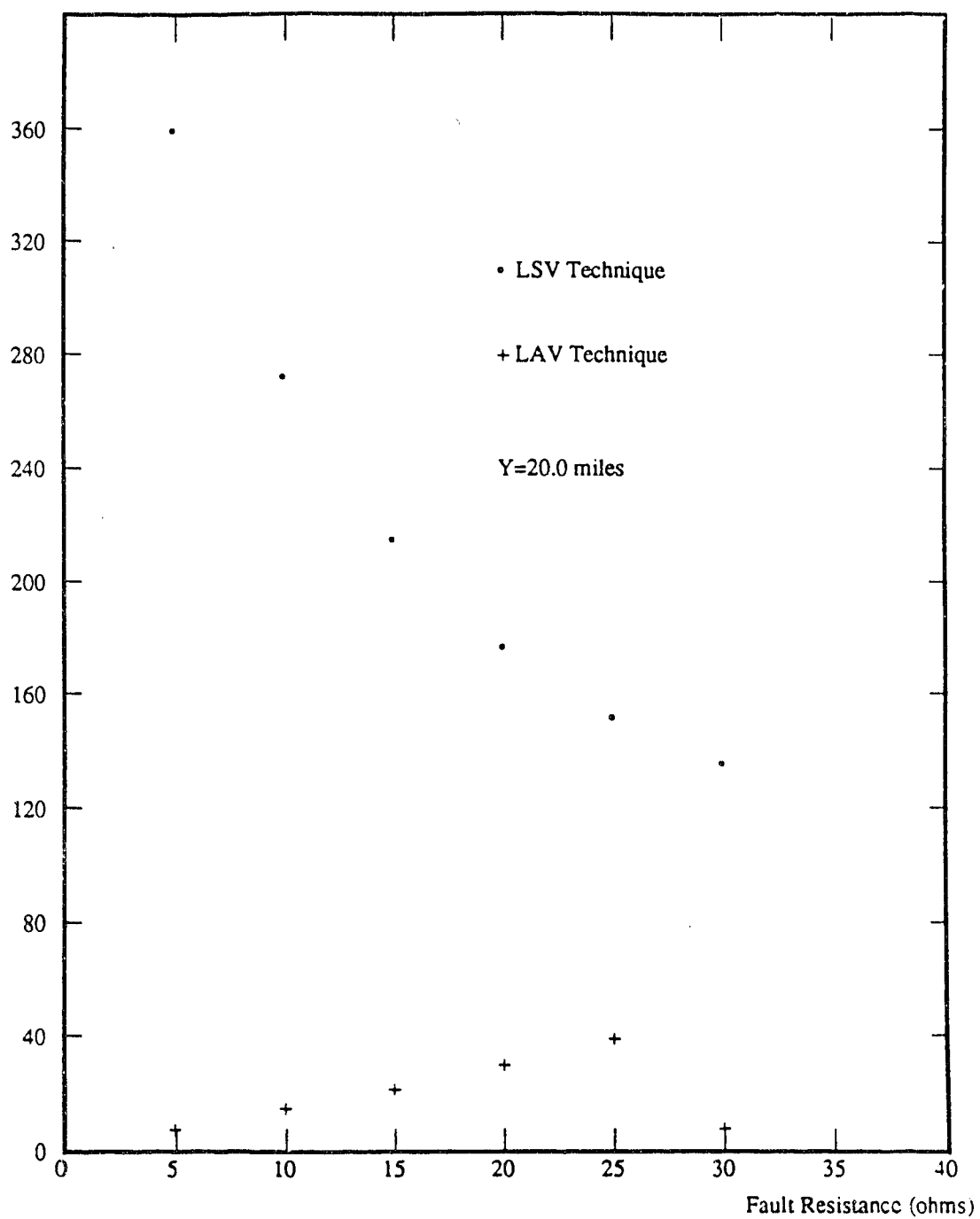


Figure (4.11): The fault resistance versus the error of distance.

The estimated distance (miles)

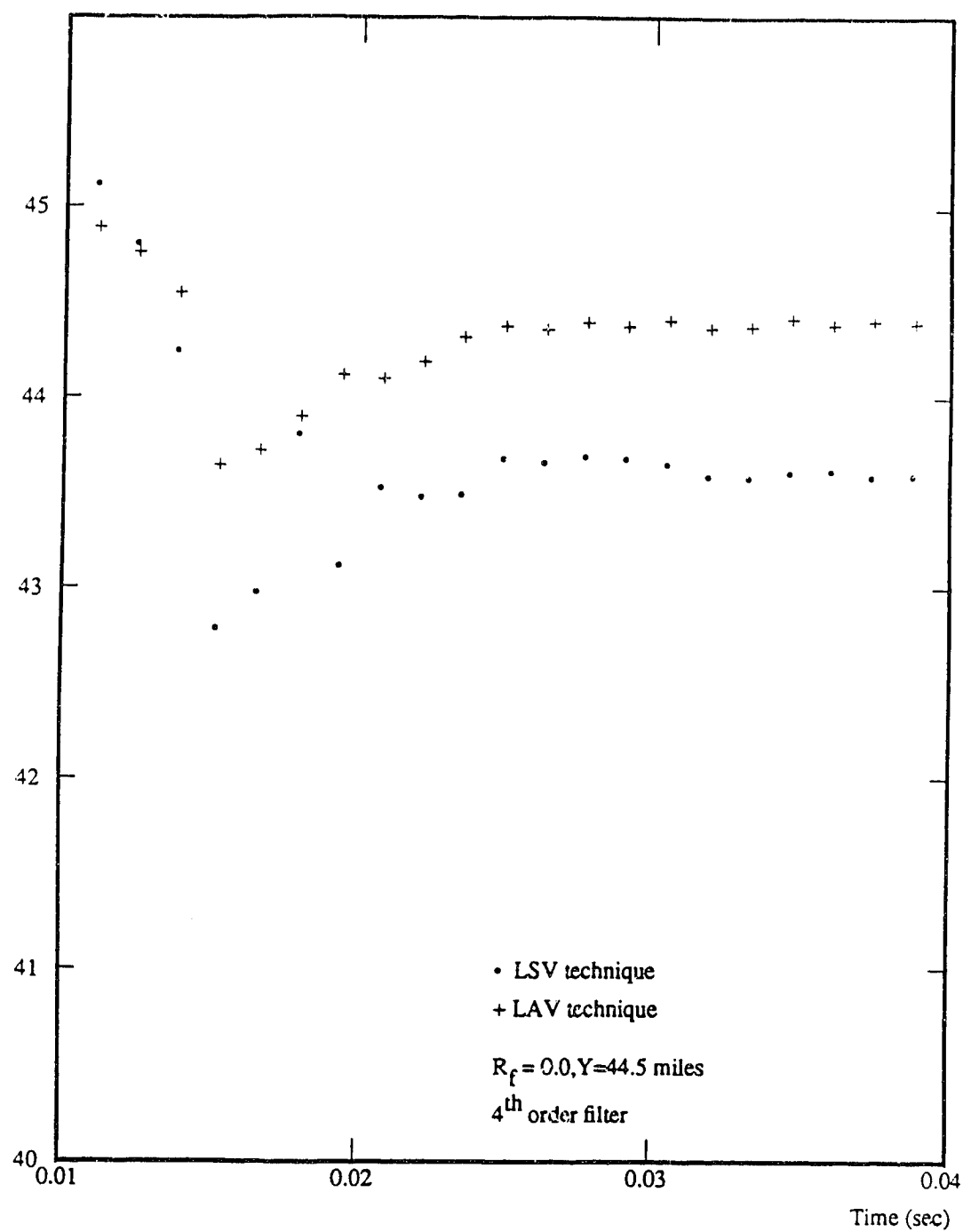


Figure (4.12): Estimated distance versus time delay

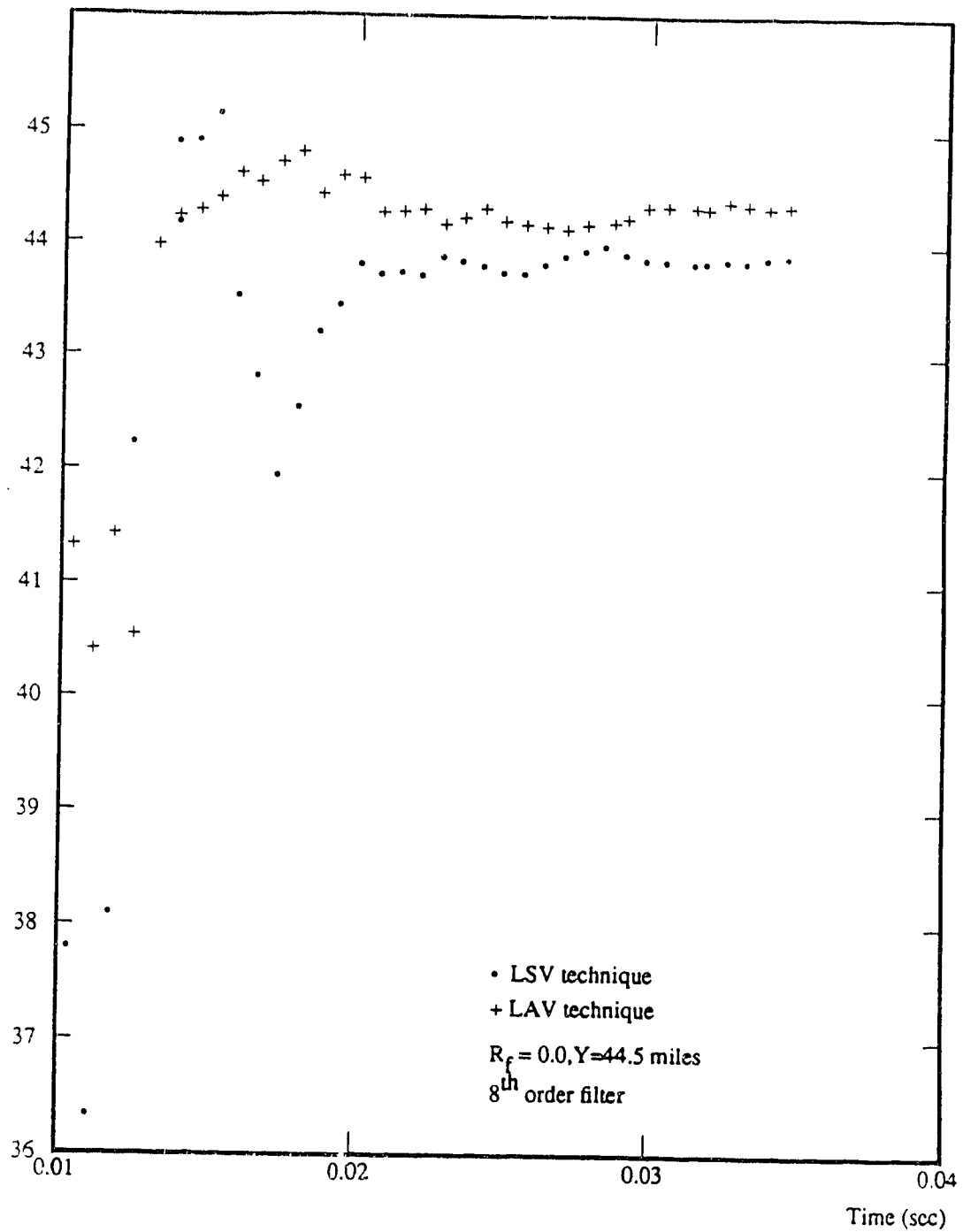


Figure (4.13): Estimated distance versus time delay

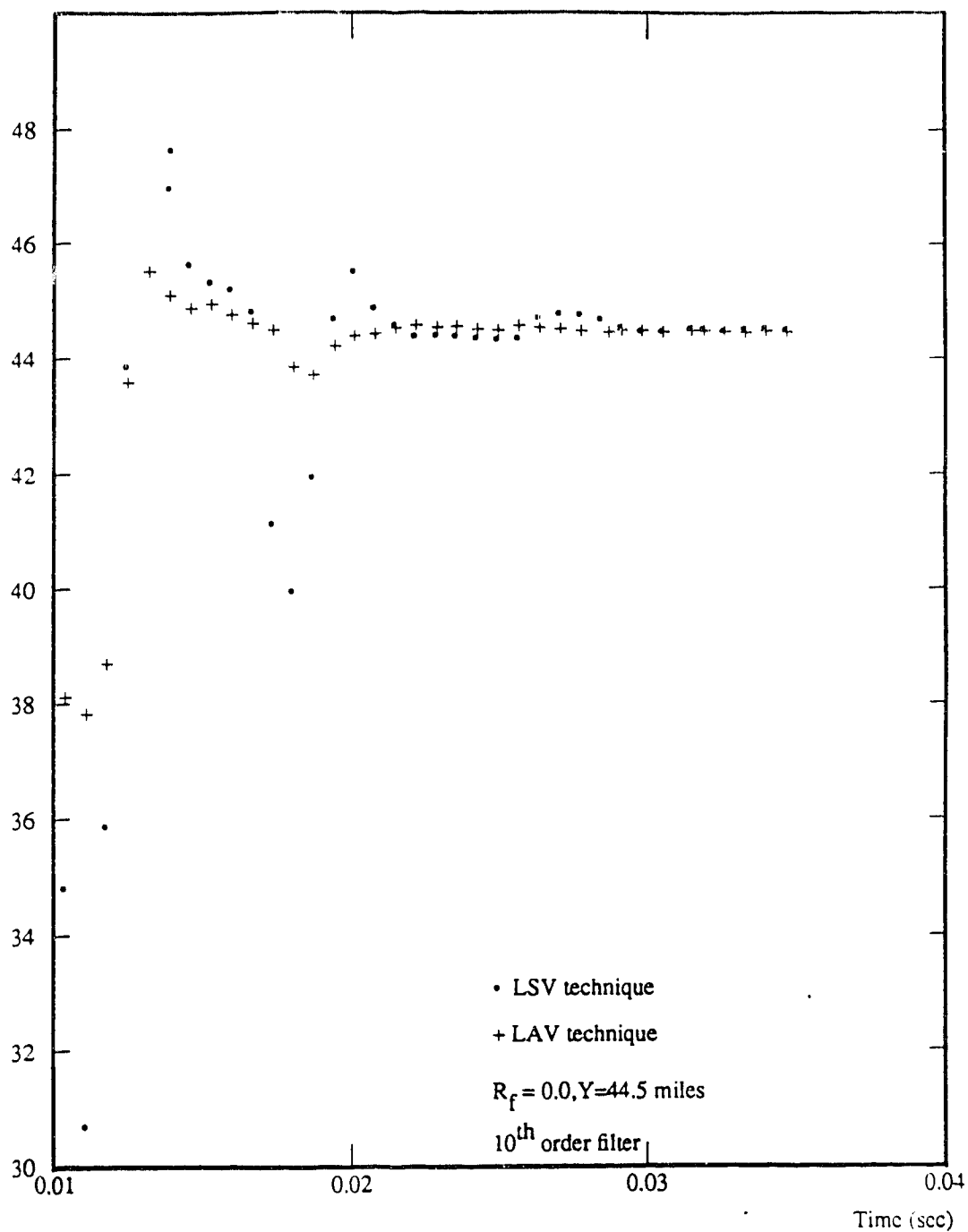


Figure (4.14): Estimated distance versus time delay

The estimated distance (miles)

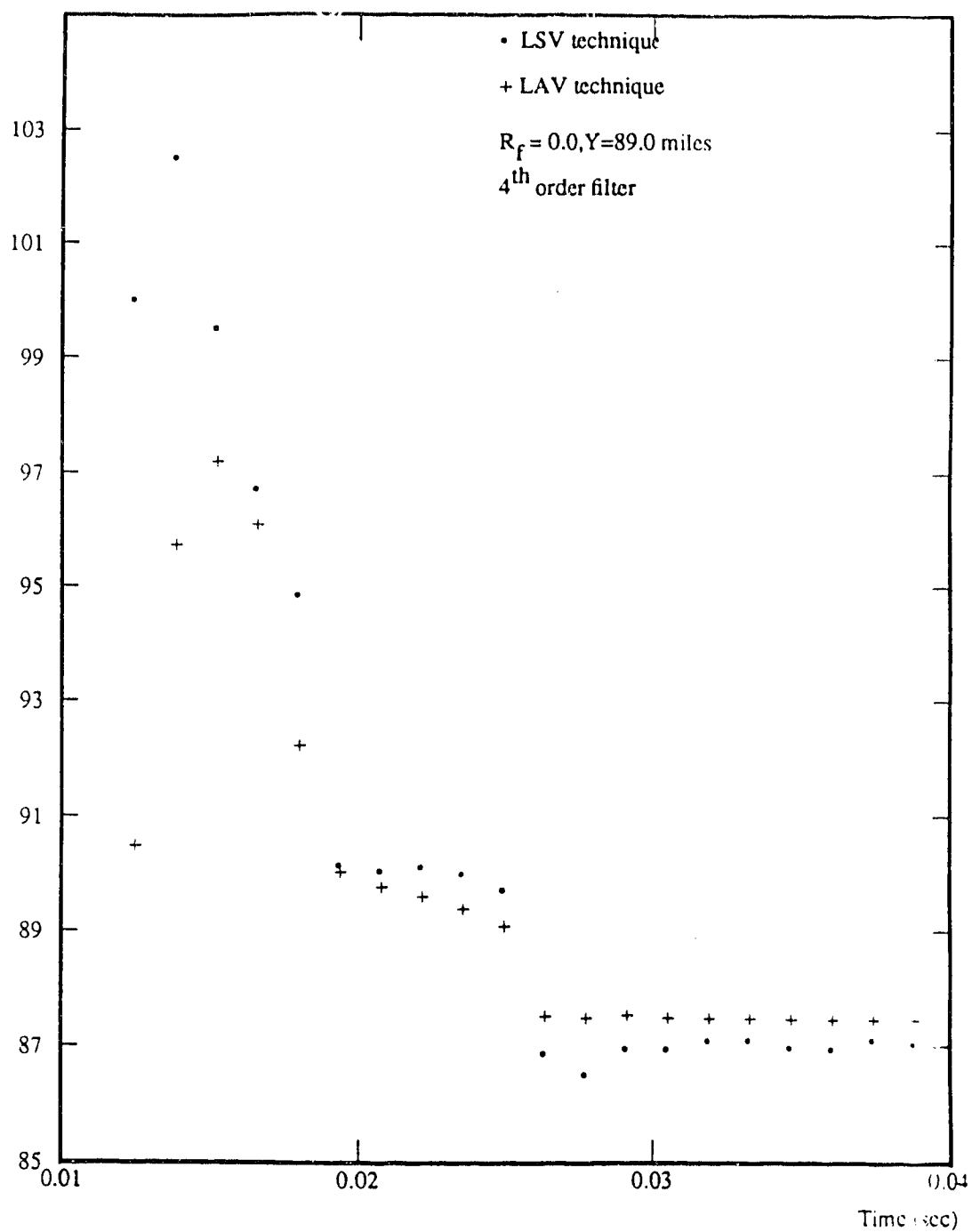


Figure (4.15): Estimated distance versus time delay

The estimated distance (miles)

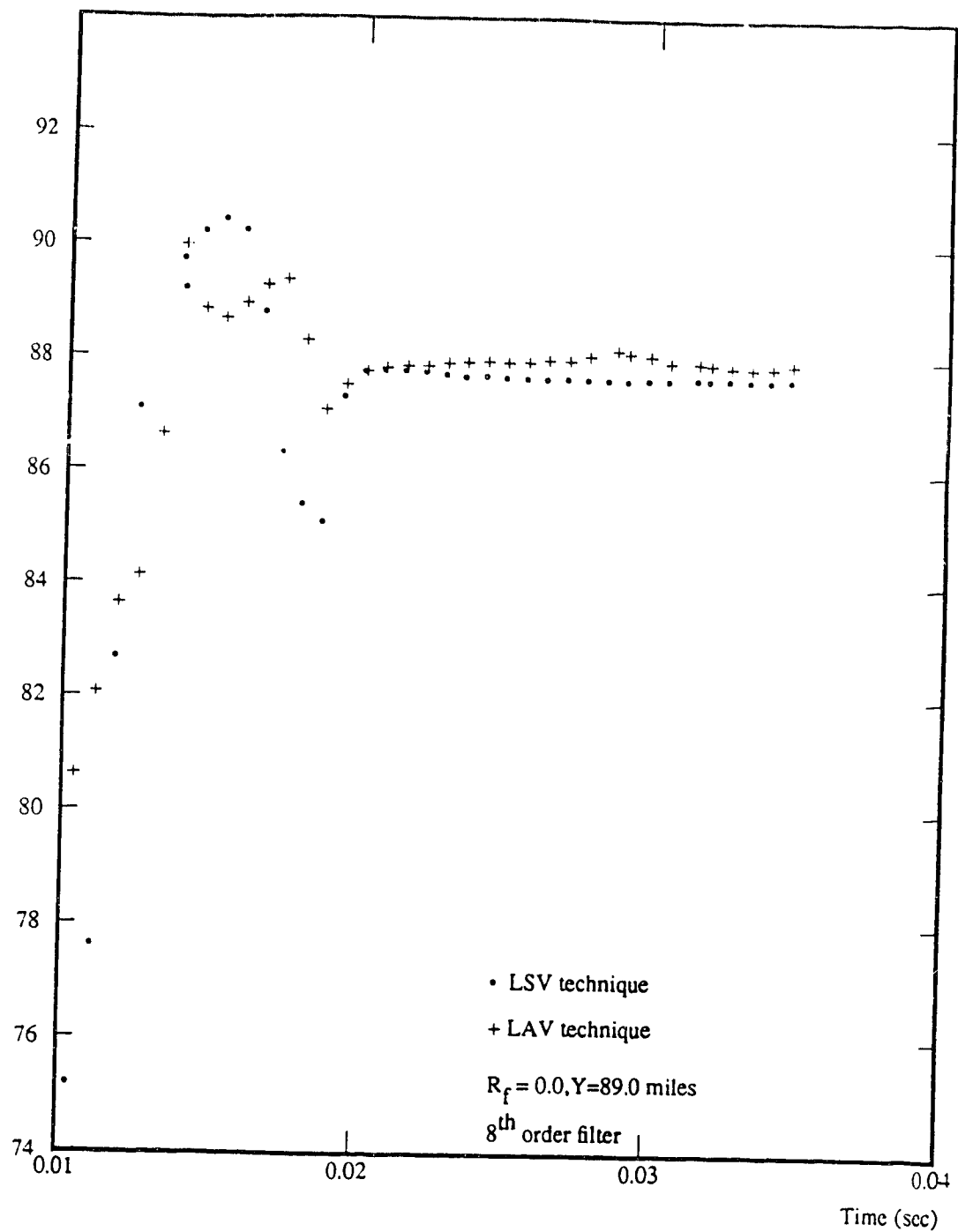


Figure (4.16): Estimated distance versus time delay

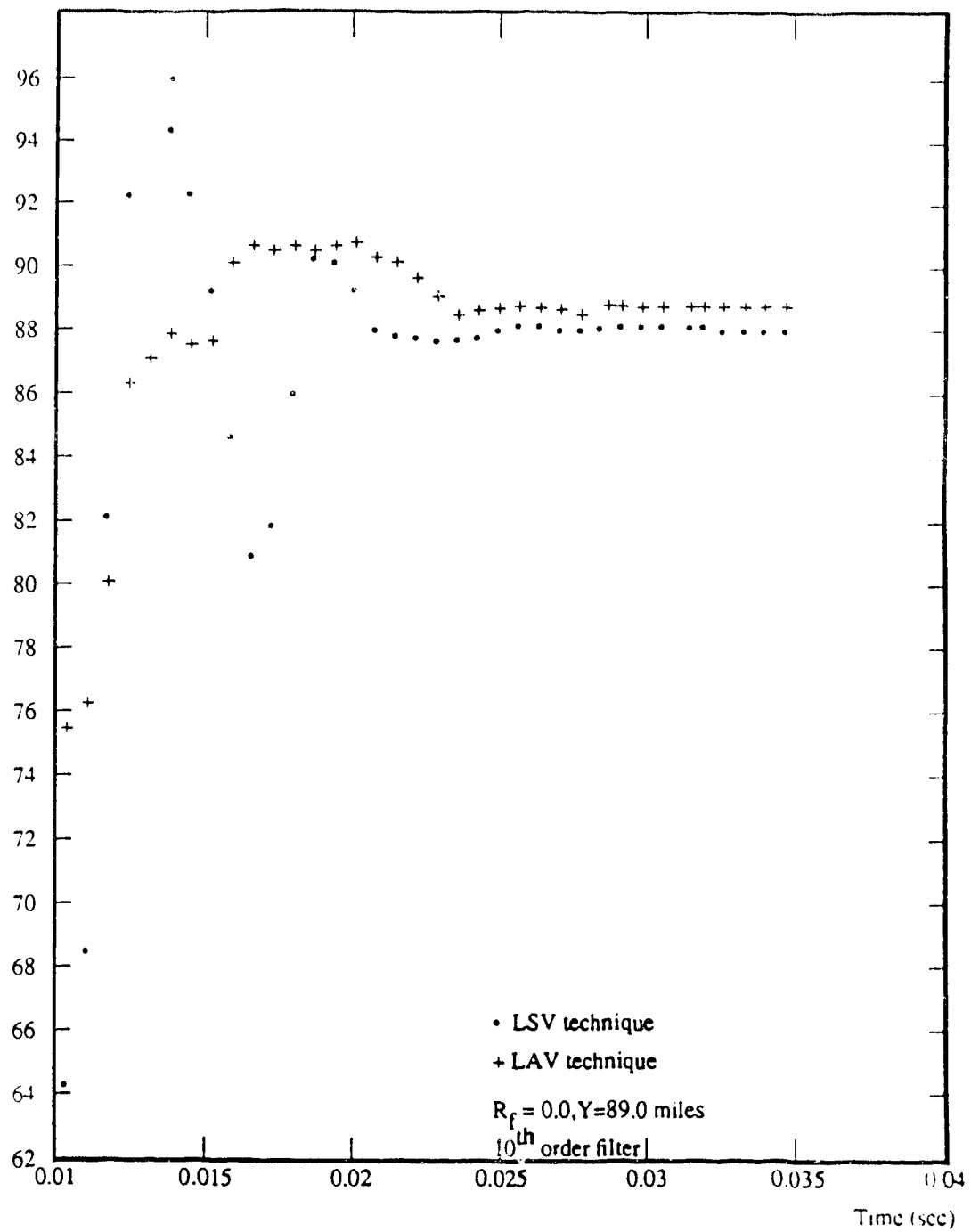
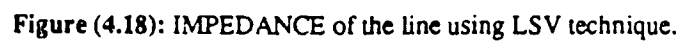


Figure (4.17): Estimated distance versus time delay



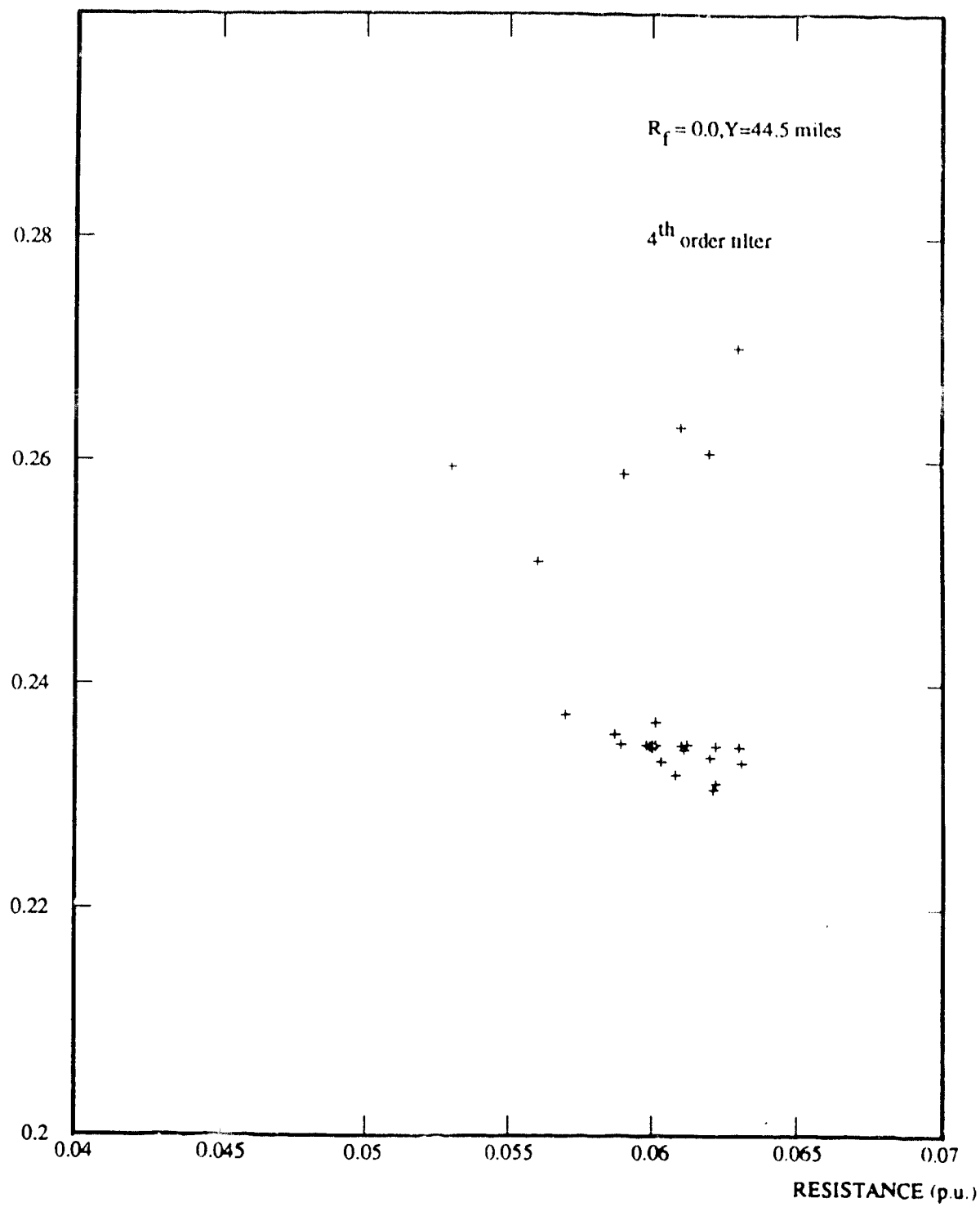


Figure (4.19): IMPEDANCE of the line using LAV technique.

REACTANCE (p.u.)

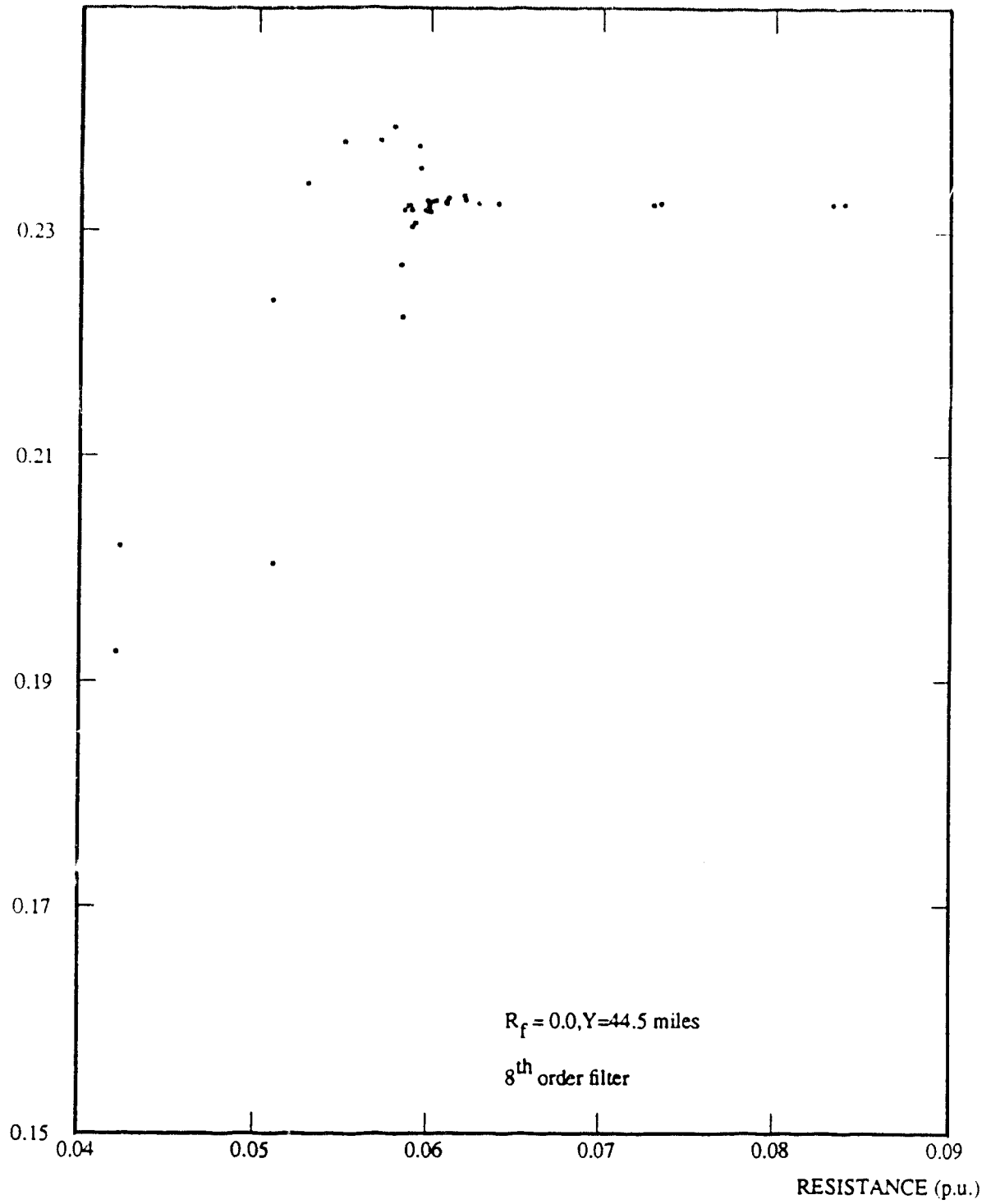


Figure (4.20): IMPEDANCE of the line using LSV technique.

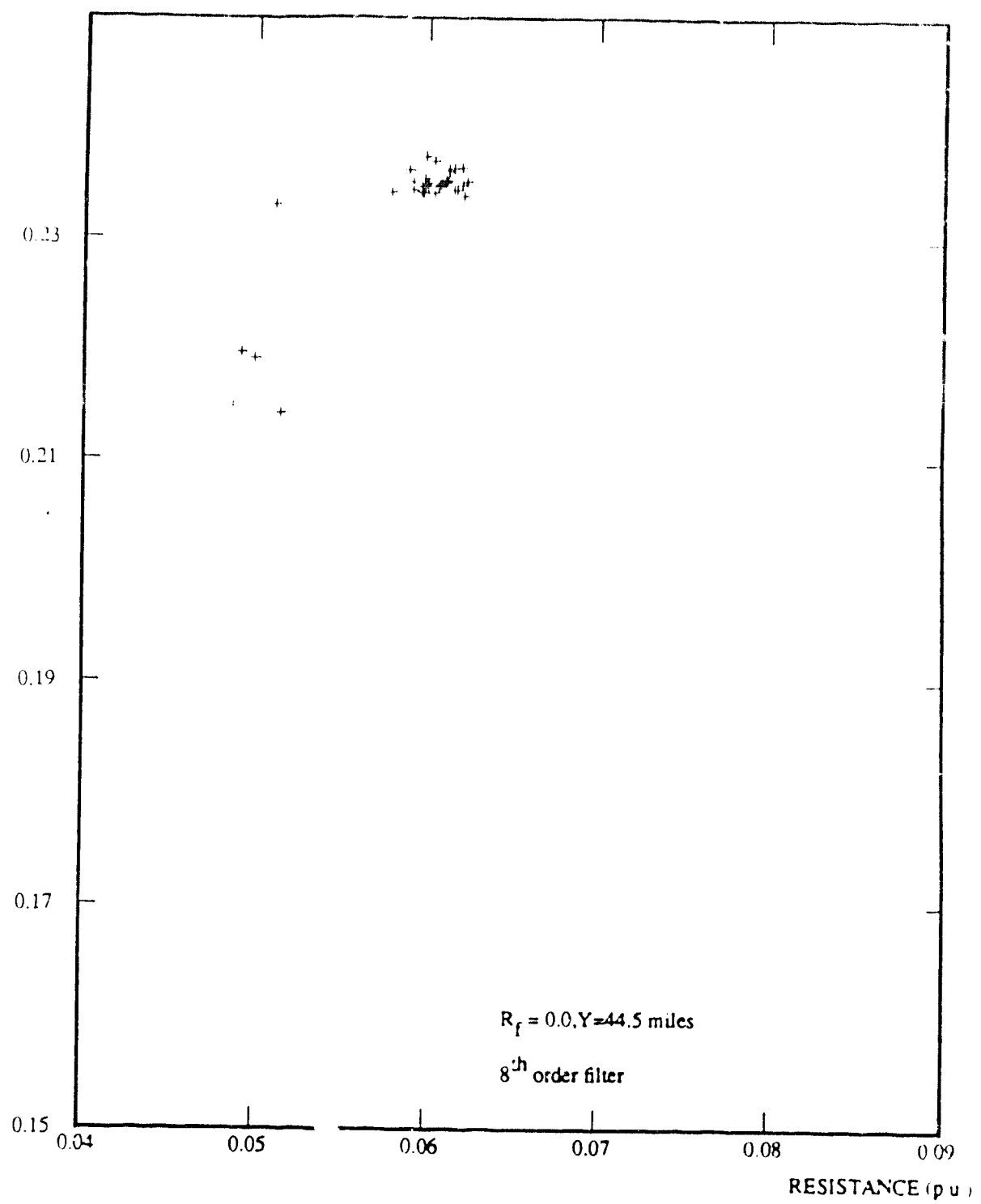


Figure (4.21): IMPEDANCE of the line using LAV technique.

REACTANCE (p.u.)

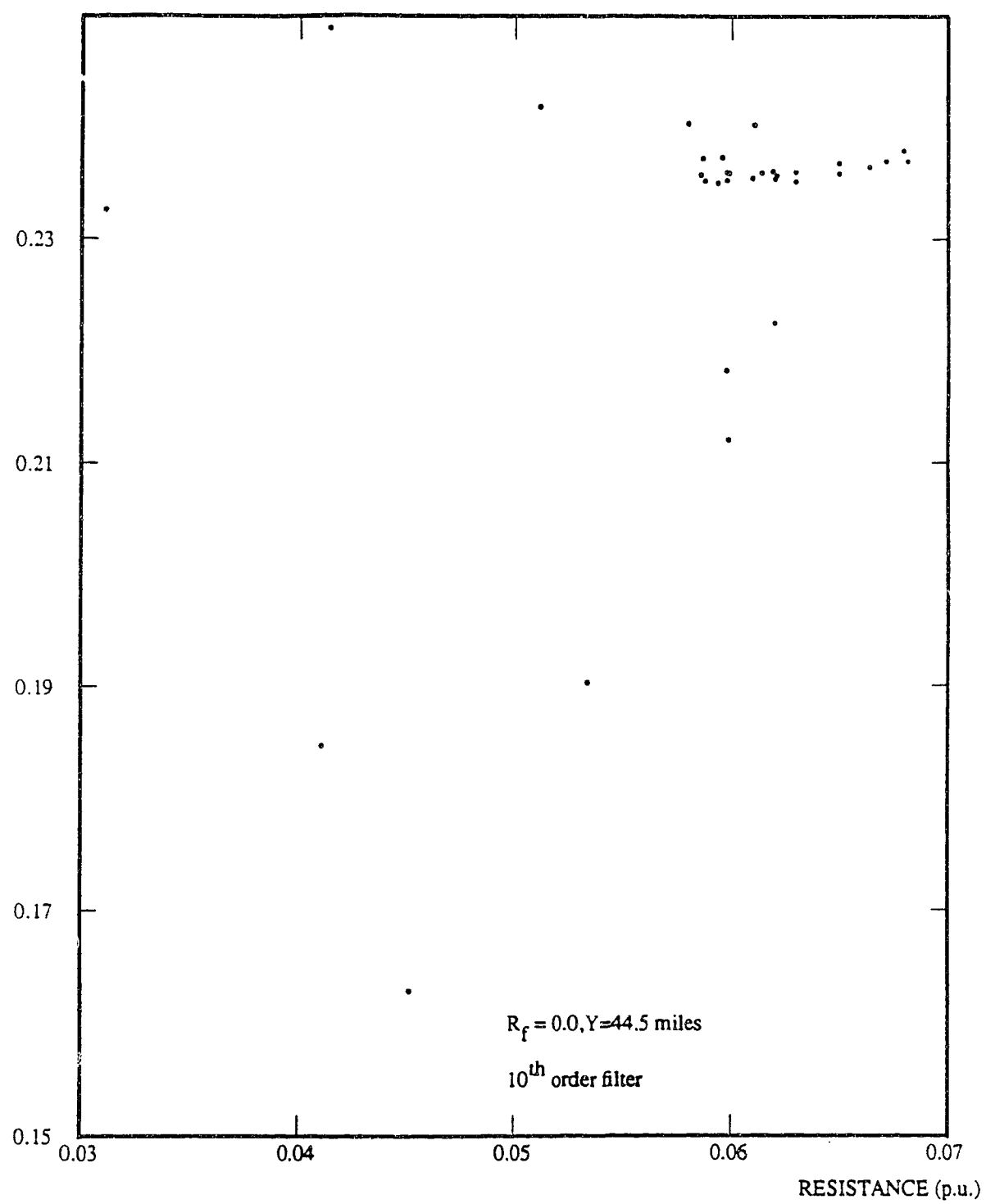
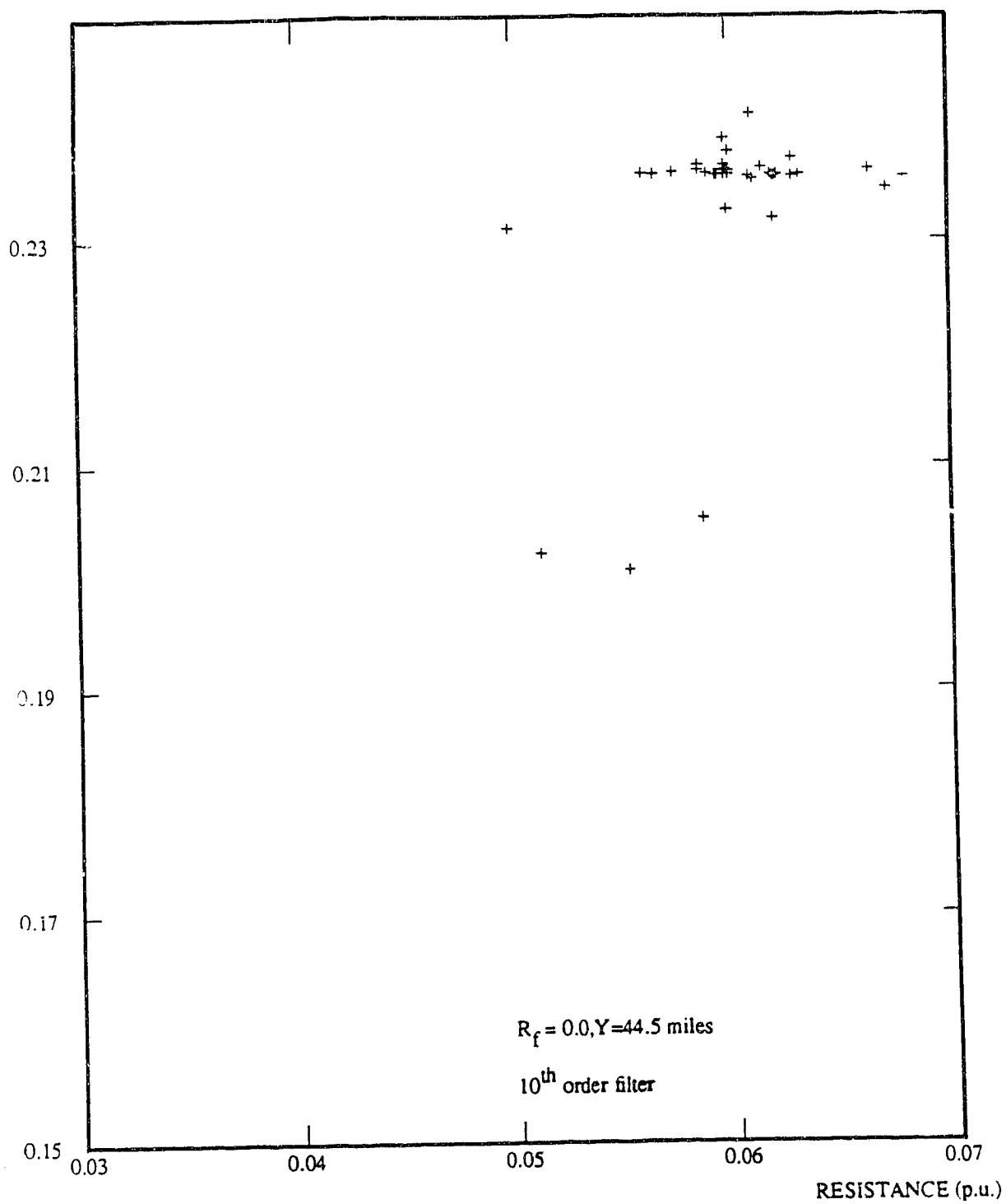


Figure (4.22): IMPEDANCE of the line using LSV technique.

REACTANCE (p.u.)

**Figure (4.23):** IMPEDANCE of the line using LAV technique.

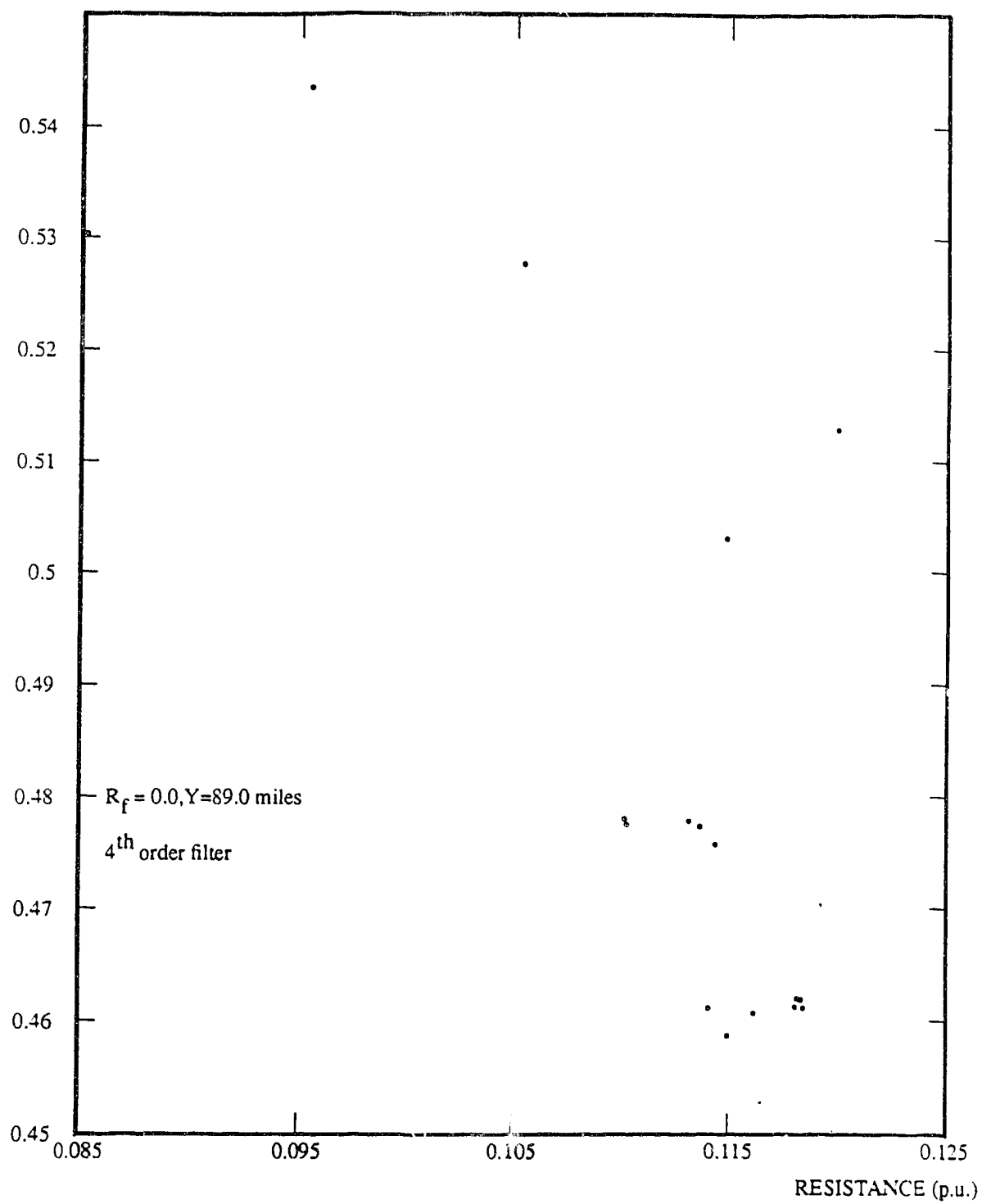


Figure (4.24): IMPEDANCE of the line using LSV technique.

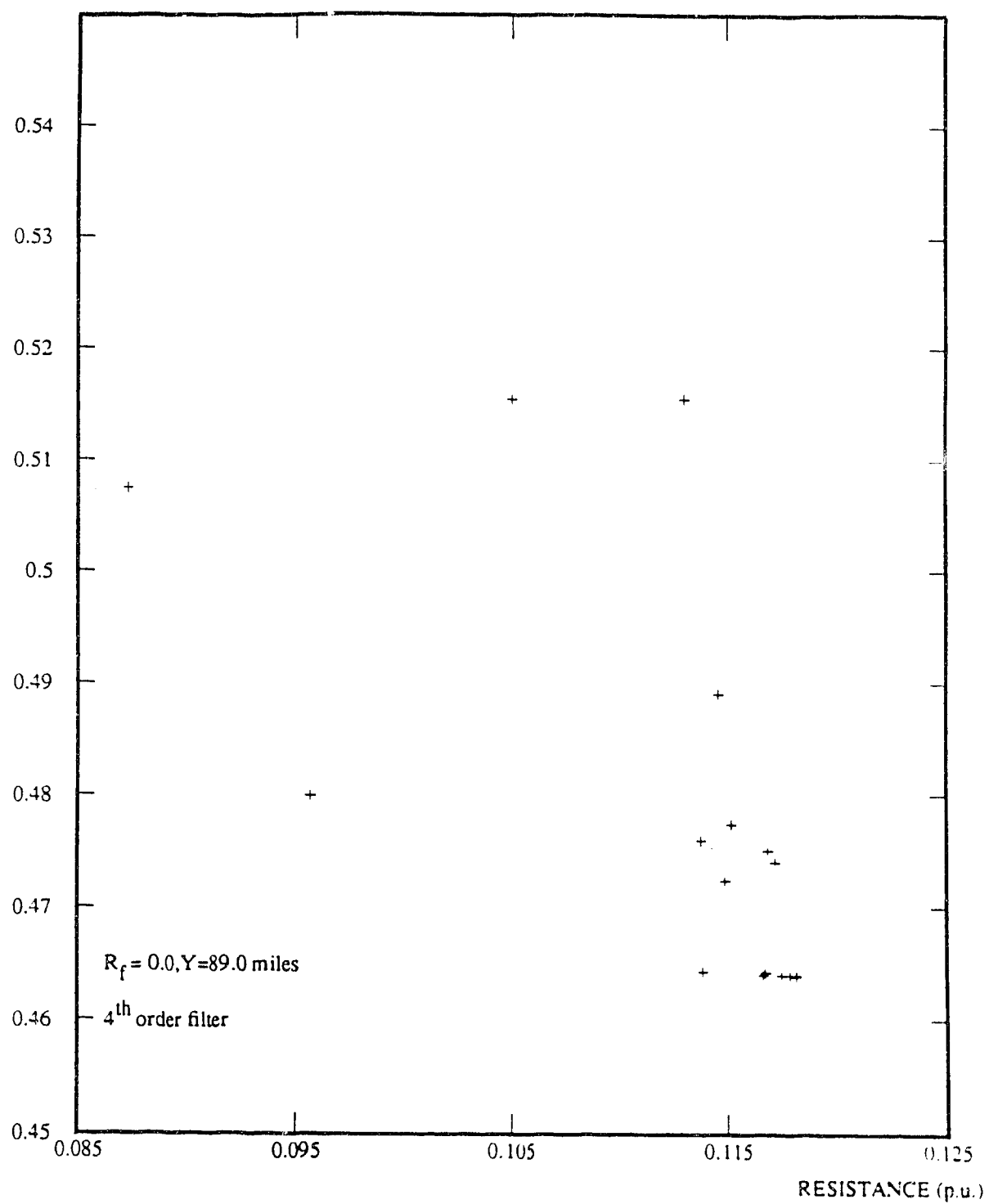
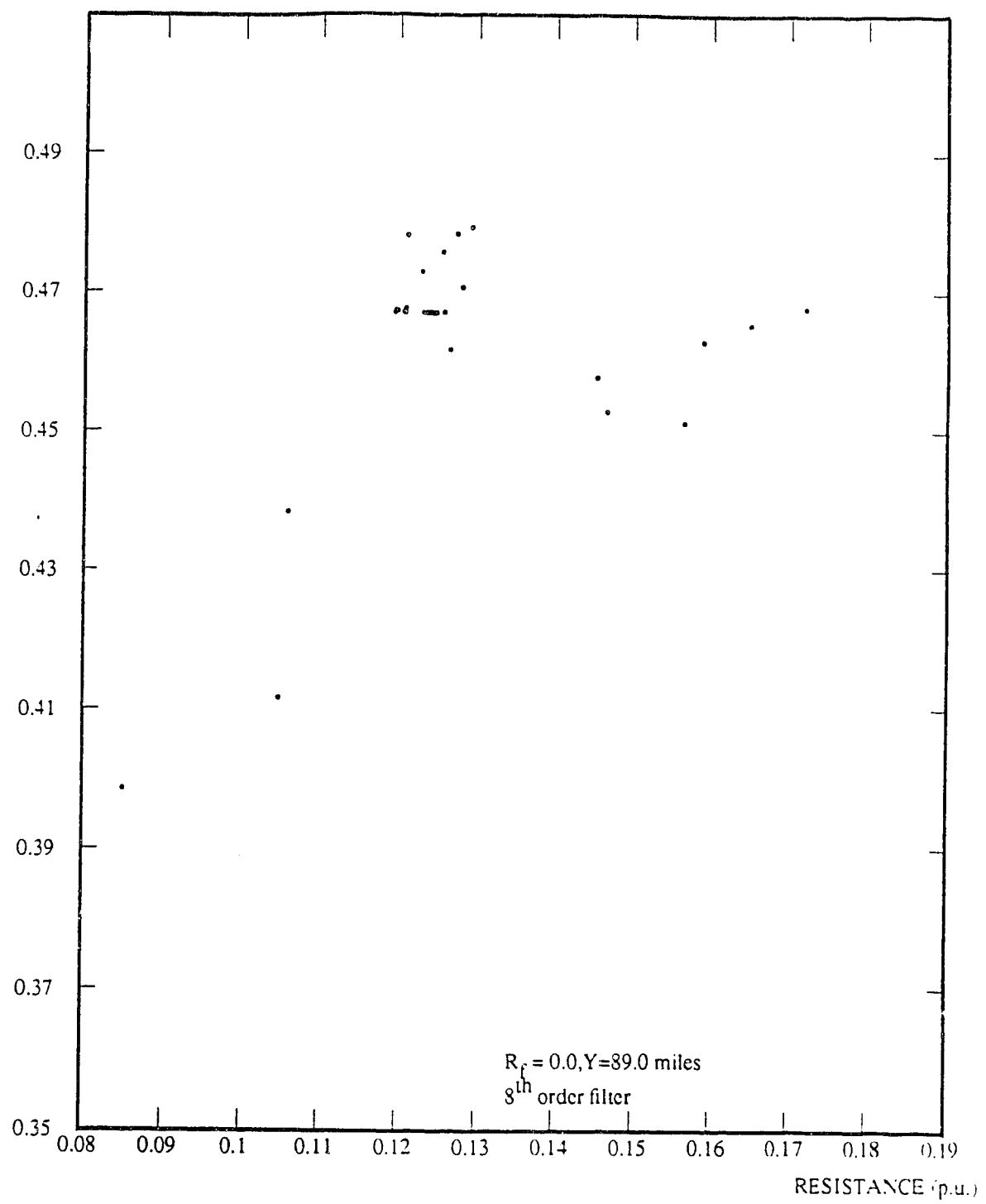


Figure (4.25): IMPEDANCE of the line using LAV technique

REACTANCE (p.u.)

**Figure (4.26):** IMPEDANCE of the line using LSV technique

REACTANCE (p.u.)

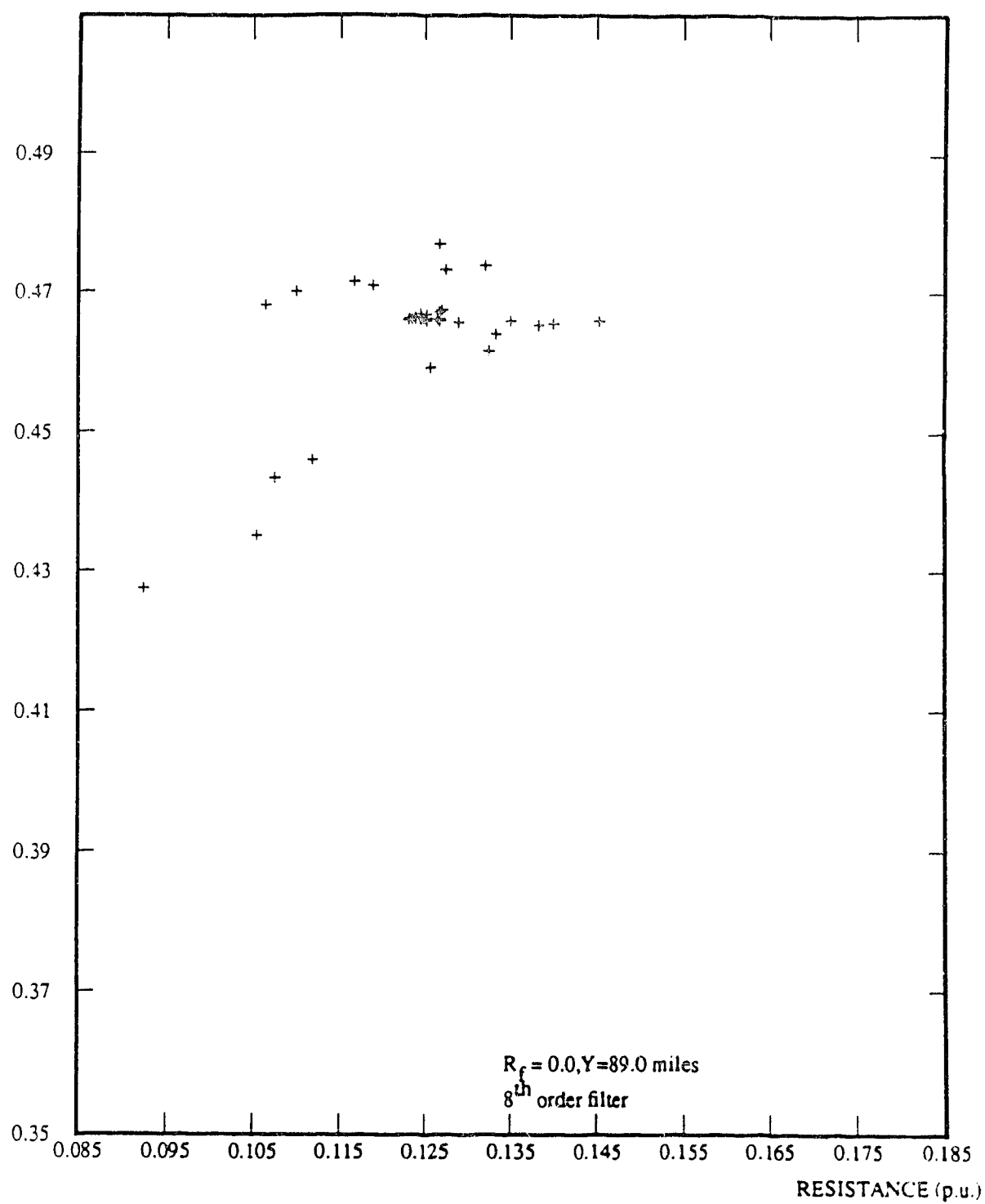


Figure (4.27): IMPEDANCE of the line using LAV technique.

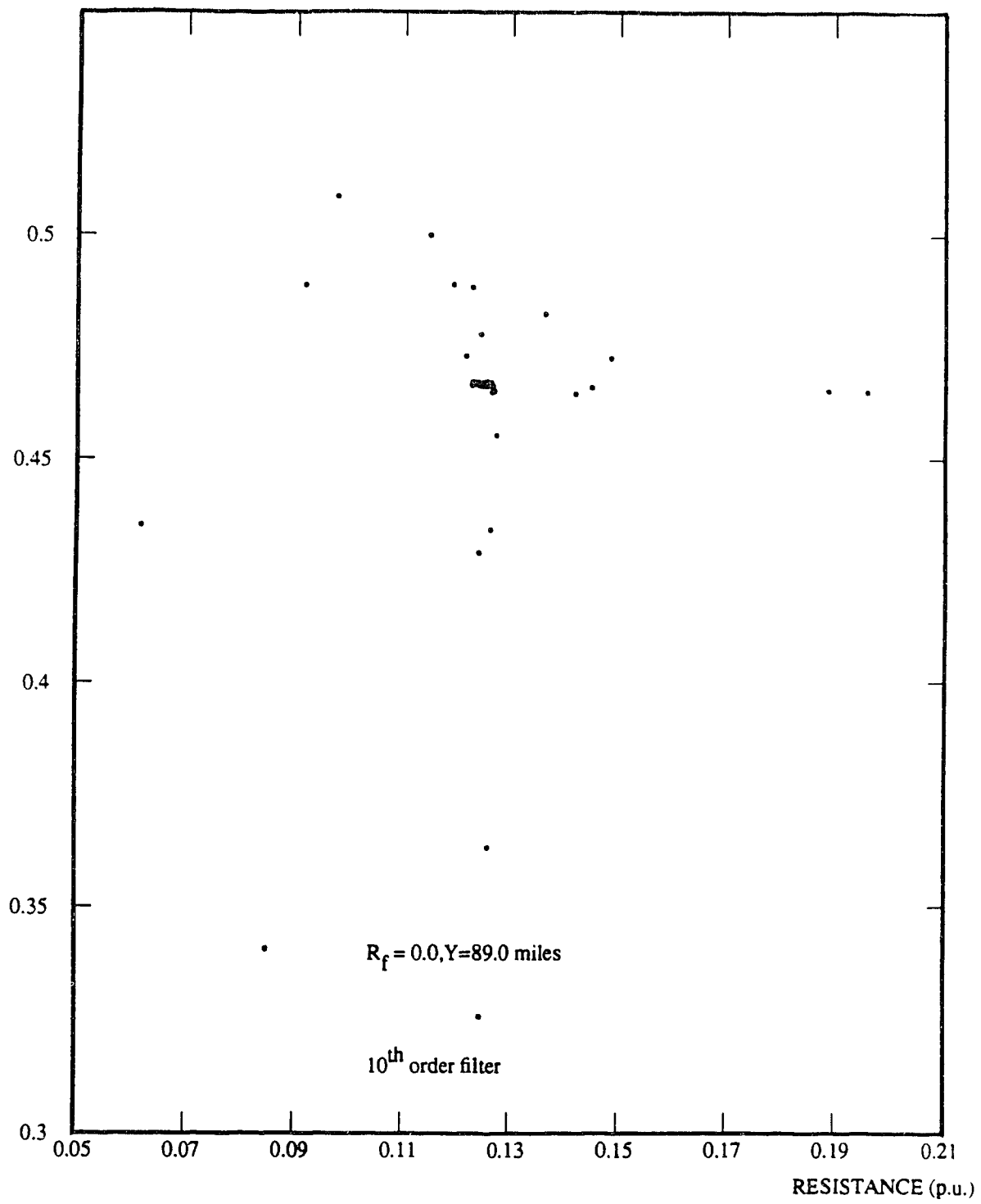
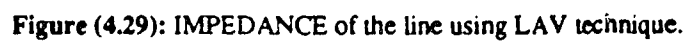


Figure (4.28): IMPEDANCE of the line using LSV technique.



The estimated distance (miles)

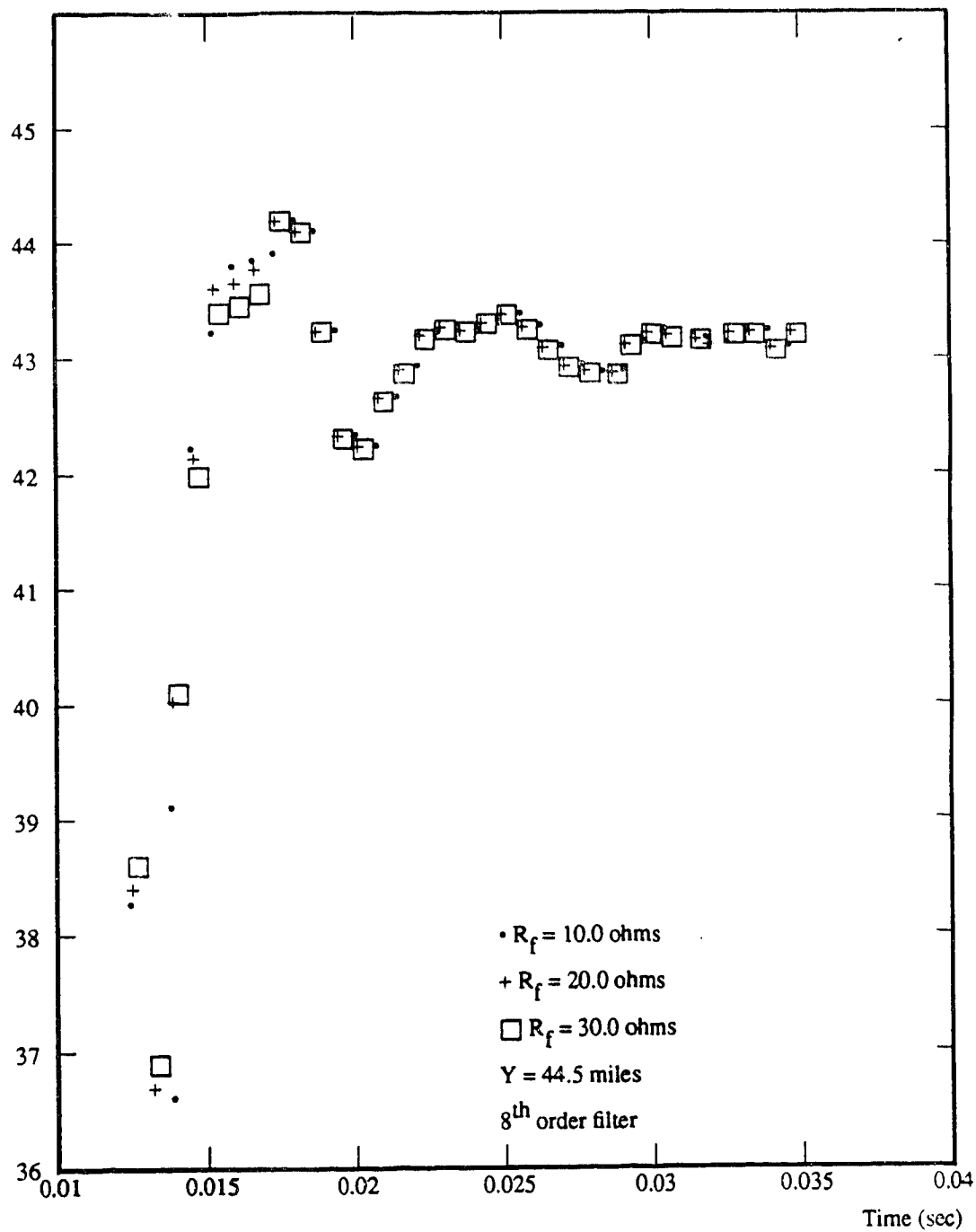


Figure (4.30): Estimated distance versus time delay using LSV technique

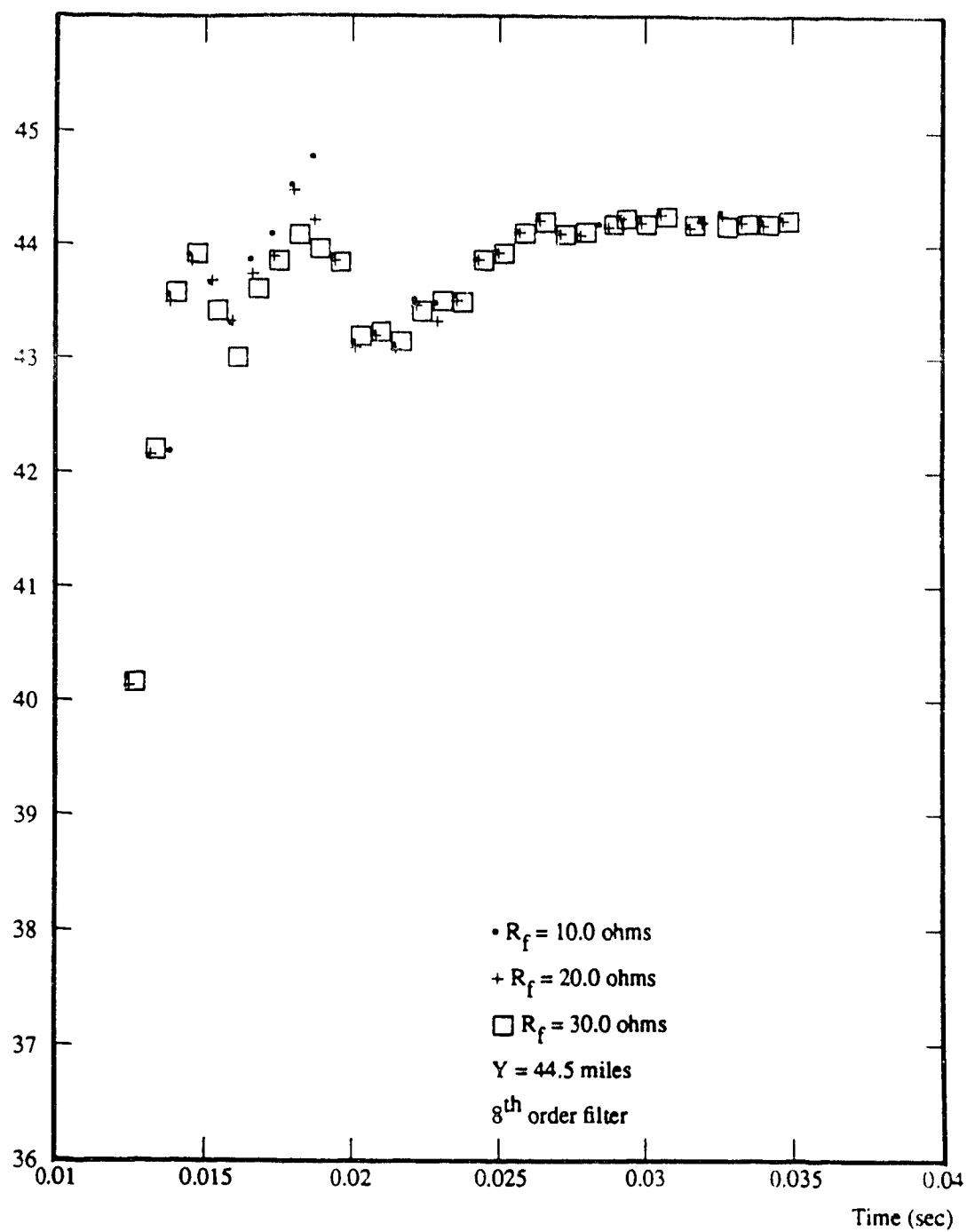


Figure (4.31): Estimated distance versus time delay using LAV technique.

CHAPTER 5

CONCLUSION

5.1 Summary

Two methods involving curve fitting techniques for locating transmission line faults were studied and tested. The first method is the least square error technique proposed by Sachdev and Baribeau [14], the second one is the least absolute value technique proposed by Soliman and Christensen [17]. The fault location is determined by making use of the fact that the line reactance is proportional to the length between the measuring point and the fault location [14].

Two models of the power system were presented. The single-phase model and the three phase model. The three phase model was limited to the symmetrical three phase fault.

Simulation results show that the LAV technique is more accurate than the LSV technique. The results also show that the fault resistance and the shunt capacitance do not greatly affect the estimation of the fault location.

5.2 Future Work

In this thesis, the voltage and current were determined in an off-line mode. A worthwhile extension is to use an on-line approach, since it would allow at least some connectivity of the power system while repair is undergoing.

Recall that the three-phase model was limited to the symmetrical direction for future work is to consider the applicability of the LAV technique in estimating fault locations for all types of fault (i.e. symmetrical fault and unsymmetrical fault). This model will make the LAV technique more practical, since the fault location could be estimated for any type of fault.

Finally, a fault detection routine must be associated with the fault locating technique described in this thesis. To detect the occurrence of a fault, a fault detection routine must exist. In practice, fault detection is important, since the occurrence of a fault will not be known without this detector.

5.3 Concluding Remarks

The work in this thesis shows that:

1. The LAV technique is more accurate than the LSV technique.
2. The fault resistance does not have a great effect on the accuracy of either technique.
3. The line shunt capacitance does not affect the accuracy of either technique.

Indeed, if a high order filter is used the results provided by both techniques are almost perfect.

4. The order of the filter affects the accuracy of both techniques, as well as the time delay that is caused by using a filter.
5. The three parameters that give the most accurate results when using LAV technique are:

- A. Sampling rate = 720 Hz.
- B. No. of equations = 8 .
- C. Time reference ($T=0.0$) at the first sample.

References

- [1] C.A.GROSS. *Power System Analysis*, John Wiley & Sons, New York, 1979.
- [2] M.Vitins, "A correlation Method For Transmission Line Protection", *IEEE Trans. Power Apparatus and Sys.*, Vol. Pas-97, No. 5, Sept/Oct. 1973, pp 1607-1615.
- [3] J. Kohlas, "Estimation of fault locations on power lines", *Proc. third IFAC Symp., the Hague/Delft, the Netherlands*, June 1973, pp. 393-402
- [4] W.D. Stevenson, Jr., "Elements of Power System Analysis", Fourth Edition, *McGraw-Hill Book Company*, Newyork, 1982.
- [5] T.Takagi, Y.Yamakoshi, J.Baba, K.Vemura and T.Sakaguchi, "A New Algorithm of an Accurste Fault Location For EHV/UHV Transmission Lines: Part I - Fourier Transformation Method", *IEEE Trans. Power Apparatus and Sys.*, Vol. PAS-100, No. 3, Mar. 1981, pp. 1316-1322.
- [6] S.E.Westlin and J.A.Bubenko, "Newton-Raphson Technique Applied to the Fault Location", Paper No.A 76 334-3, *IEEE PES Summer Meeting*, Portland, 18-23 July 1976.
- [7] G.G.Richards and O.T.Tan, "An Accurate Fault Location Estimator for Transmission Lines", *IEEE Transactions on Power Apparatus and Systems*, Vol.Pas-101, No.4, April 1982, pp.945-949.
- [8] G.G.Richards and O.T.Tan, "Fault Location for Transmission Lines with Current-Transformer Saturation", *IEE proc.*, Vol.130, Pt.C, No.1, January 1983, pp.22-27.
- [9] E. Born, J. Jager, "Fault Locators for High-Voltage Overhead Lines", *Siemens Review*, Vol.33, pp.487-91, Oct. 1966.
- [10] B.J.Mann and I.F.Morrison, "Digital Calculation of Impedance for Transmission Line Protection", *IEEE Transactions on Power Apparatus and Systems*, Vol.

Pas-90, No.1, Jan./Feb. 1971, pp.270-276.

- [11] G.B.Gilcrest, G.D.Rockefeller and E.A.Urden, "High-Speed Distance Relaying Using a Digital Computer: 1-System Description and 2-Test Results", *IEEE Transactions on Power Apparatus and Systems*, Vol.PAS-91, No.3, May/June 1972, pp.1235-1252.
- [12] W.D.Breingan, M.M.Chen and T.F.Gallen, "The Laboratory Investigation of a Digital System for the Protection of Transmission Lines", *IEEE Transactions on Power Apparatus and Systems*, Vol.PAS-98, No.2, March/April 1979, pp.350-358.
- [13] A. W. Brooks, "Distance Relaying using Least-Squares Estimates of Voltage, Current and Impedance", *IEEE Conf. Proc. Power Ind. Compt. Appl. Conf. PICA '77*, 10th Toronto, Ont., pp. 394-402, May 24-27, 1977.
- [14] M.S.Sachdev and M.A.Baribeau, "A New Algorithm for Digital Impedance Relays", *IEEE Transactions on Power Apparatus and Systems*, Vol.PAS-98, No.6, Nov./dec. 1979, pp.2232-2238.
- [15] G.Ziegler, "Fault Location in H.V. Power Systems", *IFAC Symposium on Automatic Control in Powe Generation, Distribution and Protection*, 15-19 Sep. 1980, pp.121-129.
- [16] M.T.Sant and Y.G.Paithankar, "Online Digital Fault Locator for Overhead Transmission Line", *IEE*, Vol.126, No.11, Nov. 1979, pp.1181-1185.
- [17] S.A.Soliman, G.S.Christensen and A.Rouhi, "A New Technique For Curve Fitting Based on Minimum Absolute Deviations", *Computational Statistics & Data Analysis*, North-Holland, June 1988, pp.341-351. 1987.
- [18] J.Zaborszky and J.W.Rittenhouse, "Electric Power Transmission", *The Ronald Press Company*, NewYork, 1954.
- [19] D.Beeman, "Industrial Power Systems Handbook", McGraw-Hill Book Company, NewYork, 1955.
- [20] R.E.Bogner and A.G.Constantinides, "Introduction to Digital Filtering", John Wiley and Sons, London, 1975.

- [21] E.A.Robinson and M.T.Silvia, "Digital Signal Processing and Time Series Analysis", *Holden-Day, Inc.*, San Francisco, 1980.
- [22] D. M. Etter, "Structured Fortran 77 for Engineers and Scientists", Second Edition, The Benjamin/Cummings Publishing Company, Inc., 1987.
- [23] T.W.Stringfield, D.J.Marihart and R.F.Stevens, "Fault Location Methods For Overhead Lines", *AIEE trans.*, Vol.76, Aug. 1957, pp. 518-529.
- [24] A.S.Dief, *Advanced Matrix Theory For Scientists and Engineers*, Abacus Press, Kent, 1982.
- [25] A.Antoniou, "Digital Filters: Analysis and Design", McGraw-Hill Book Company, NewYork, 1979.

APPENDIX A

Data for the single phase system (i.e. is given in figure 3.1) is outlined in this appendix. This data is taken from reference [18]:

[1] Generator G_1 :

105 MW capacity at 0.9 p.f. rated at 22 KV.

18.1 percent reactance on 105/0.9 MVA.

[2] Short-circuit limiting reactor:

$X_1 = 0.237$ ohms.

[3] Transformer T_1 :

Transformer ratio 142/22

Load carrying capacity of 60 MVA.

8.2 percent reactance on 60 MVA base at 142 KV tap setting.

[4] Transmission line Li_1 :

30 miles-long overhead aluminium-cable-steel reinforced conductor.

Series resistance of 0.5438 ohms/mile.

Series reactance of 0.5650 ohms/mile.

[5] Transformer T_2 :

Transformation ratio 126/33

Load carrying capacity of 20 MVA.

11 percent reactance on 20 MVA base at 126 KV tap setting.

[6] Transmission Line Li_2 :

5 miles-long over head copper conductor line.

Total series resistance of 1.5 ohms.

Total series reactance of 3.3 ohms.

[7] Load L_1 :

Real power of 15 MW.

Reactive power of 8 MVA.

Terminal Voltage of 31.5 KV.

APPENDIX B

The data for the three phase system is the same as the single phase system except for transmission line number 1 which is 133.5 miles-long, and is divided into three pi sections which is represented in figure 3.6. The data for figure 3.6 are:

Series impedance $Z_{\Pi} = 9.54 + j37.4$ ohms.

Shunt impedance $Z_{\Pi'} = -j8860$ ohms.

Initial pre-faulted voltage (V_{B1}) = $V_A + I_1 Z_{\Pi}$

Initial pre-faulted current (I_{B1}) = $I_1 + I_2$

$$= I_1 + V_{B1}/Z_{\Pi}$$

APPENDIX C

C.1 Fourth Order Filter.

Cutoff frequency $f_c = 203$ Hz.

Transition frequency $f_1 = 285$ Hz.

Sampling frequency $f_s = 720$ Hz.

Hence, the sampling interval is given by:

$$T = 1 / f_s$$

$$T = 1 / 720 \text{ sec.}$$

and,

$$\tan (w_1 T / 2) = \tan \left(\frac{285 \times 2 \pi}{2 \times 720} \right) = 2.945905.$$

and,

$$\tan (w_c T / 2) = 1.223939$$

By considering the amplitude characteristic and at the transition frequency the following equation is obtained.

$$\log \left[1 + \left(\frac{\tan (w_1 T / 2)}{\tan (w_c T / 2)} \right)^{2n} \right] = 30$$

i.e.

$$2n = \frac{2.999565}{\log (2.999565/1.223939)}$$

$$n = 3.9317 = 4$$

Where n is the order of the required filter.

From the value of $\tan(\omega_c T/2)$, it can be shown that the poles, which lie on the Z^{-1} plane, have the following X and Y coordinates.

| X | Y |
|-----------|----------------|
| -.104637 | $\pm .196817$ |
| -.144995 | $\pm .658432$ |
| -.318989 | ± 1.448533 |
| -2.105975 | ± 3.961229 |

Note that four poles lie inside the unit circle of the Z^{-1} plane and the other four lie outside the unit circle. Therefore, the four poles which yield a stable function are:

$$-.318989 \pm j1.448533$$

$$-2.105975 \pm j3.961229$$

The corresponding polynomial due to the stable poles given by:

$$\begin{aligned}
 A(Z^{-1}) &= (Z^{-1} + .31899 + j1.44853)(Z^{-1} + .31899 - j1.44853) \\
 &\times (Z^{-1} + 2.10598 + j3.96123)(Z^{-1} + 2.10598 - j3.96123) \\
 &= (Z^{-2} + .6380 Z^{-1} + 2.20)(Z^{-2} + 4.2120 Z^{-1} + 20.1265)
 \end{aligned}$$

Thus, the required transfer function is:

$$G(Z^{-1}) = K \frac{(1+Z^{-1})^4}{A(Z^{-1})}$$

Where, K is a gain constant and is given by:

$$1 = K \frac{2^4}{(3.83798)(2 \times 3.33842)}$$

i.e.

$$K = 6.07802$$

C.2 Eighth Order Filter.

Cutoff frequency $f_c = 200$ Hz.

Transition frequency $f_1 = 295$ Hz.

Sampling frequency $f_s = 1440$ Hz.

Hence, the sampling interval is given by:

$$T = 1/f_s$$

$$T = 1/1440 \text{ sec.}$$

and,

$$\tan\left(\frac{\omega_1 T}{2}\right) = \tan\left(\frac{295 \pi}{1440}\right) = .75014$$

and,

$$\tan\left(\frac{\omega_c T}{2}\right) = \tan\left(\frac{200 \pi}{1440}\right) = .46631$$

n is obtained from,

$$2n = \frac{2.999565}{\log\left(\frac{.75014}{.46631}\right)}$$

$$n = 7.26 = 8$$

From the calculated values of $\tan\left(\frac{\omega_c T}{2}\right)$, it can be shown that the X and Y coordinates of the poles which lie on the Z^{-1} plane are:

| X | Y |
|----------|----------------|
| .367027 | $\pm .085336$ |
| .392673 | $\pm .259994$ |
| .450890 | $\pm .446794$ |
| .559212 | $\pm .653643$ |
| .755727 | $\pm .883342$ |
| 1.119040 | ± 1.108873 |
| 1.770487 | ± 1.172254 |
| 2.58465 | $\pm .600985$ |

The eight poles which yield a stable function are:

$$0.755727 \pm j0.883342$$

$$1.119040 \pm j1.108873$$

$$1.770487 \pm j1.172254$$

$$2.58465 \pm j0.600985$$

Therefore, the polynomial in terms of Z^{-1} which corresponds to the stable poles is:

$$A(Z^{-1}) = (Z^{-2} - 1.5115Z^{-1} + 1.354)(Z^{-2} - 2.2381Z^{-1} + 2.4819) \\ * (Z^{-2} - 3.5410Z^{-1} + 4.5088)(Z^{-2} - 5.1697Z^{-1} + 7.0427)$$

Hence, the required transfer function is given by:

$$G(Z^{-1}) = K \frac{(1+Z^{-1})^8}{A(Z^{-1})}$$

Where K is a gain constant and is given by:

$$1 = K \frac{2^8}{(0.83996)(1.24377)(1.96783)(2.87298)}$$

i.e.

$$K = 0.02307$$

C.3 Tenth Order Filter.

Cutoff frequency $f_c = 218$ Hz.

Transition frequency $f_1 = 290$ Hz.

Sampling frequency $f_s = 1440$ Hz.

Hence, the sampling interval is given by:

$$T = 1 / f_s$$

$$T = 1 / 1440 \text{ sec.}$$

And,

$$\tan (\omega_1 T/2) = \tan \left(\frac{290 \pi}{1440} \right) = .73323$$

And,

$$\tan (\omega T/2) = \tan \left(\frac{218 \pi}{1440} \right) = .51503$$

Hence, n is calculated from:

$$2n = \frac{2.999565}{\log\left(\frac{.73323}{.51503}\right)}$$

i.e.

$$n = 9.78 = 10$$

Using the calculated value of $\tan(\omega_c T/2)$, X and Y coordinates of the poles are shown to be:

| X | Y |
|----------|----------------|
| .321884 | $\pm .070592$ |
| .336568 | $\pm .214214$ |
| .368548 | $\pm .365347$ |
| .423998 | $\pm .529629$ |
| .515107 | $\pm .713253$ |
| .665457 | $\pm .921438$ |
| .921173 | ± 1.150664 |
| 1.368509 | ± 1.356622 |
| 2.114579 | ± 1.345853 |
| 2.964173 | $\pm .650062$ |

The ten poles which yield a stable transfer function are:

$$0.665457 \pm j.921432$$

$$0.921173 \pm j1.150664$$

$$1.368509 \pm j1.356622$$

$$2.114579 \pm j1.345853$$

$$2.964173 \pm j.650062$$

Therefore, the corresponding polynomial due to the stable poles is given by:

$$A(Z^{-1}) = (Z^{-2} - 1.3309Z^{-1} + 1.2919)(Z^{-2} - 1.8423Z^{-1} + 2.1726)$$

$$\begin{aligned}
 & * (Z^{-2} - 2.7370Z^{-1} + 3.7132)(Z^{-2} - 4.2292Z^{-1} + 6.2828) \\
 & * (Z^{-2} - 5.9283Z^{-1} + 9.2087)
 \end{aligned}$$

Hence, the required transfer function is given by:

$$G(Z^{-1}) = K \frac{(1+Z^{-1})^{10}}{A(Z^{-1})}$$

Where K is given by:

$$1 = K \frac{2^{10}}{(0.96097)(1.33024)(1.97622)(3.0536)(4.28042)}$$

i.e.

$$K = .032246$$

APPENDIX D

COMPUTER IMPLEMENTATION

In this appendix the fault location algorithm program will be discussed. This program is divided into three separated segments. The block diagram shown in figure D.1 shows that these three segments are linked together. The first program finds the pseudoinverse of a matrix A (see chapter 2), and this pseudoinverse matrix will be an input to the main program. The second program finds the initial conditions of the faulted voltage and the faulted current, then from these initial conditions finds the unfiltered voltage and the unfiltered current, then from these and by using the low-pass filters the filtered faulted voltage and the filtered faulted current are found. (see the block diagram in figure D.2). The output of this program will be an input to the main program. The main program finds the impedance of the line and the fault location for a specific input from program 1 and program 2.

These programs were implemented on the MTS system. These programs are written in a high level language Fortran 77 [22]. The IMSL library was also used for ease of the development of these programs.

The next section describes the details of each program and its flow chart as well as the efficiency of dividing the program into three separated programs.

D.1 Pseudoinverse Program: (Program 1)

This program calculates the pseudoinverse of a matrix A in chapter 2. the rational behind having the computation of the matrix A as a separate program is that, the pseudoinverse of the matrix A need only be calculated once, thus it is inefficient to calculate it in every run of the main program. The flow chart of this program is shown in figure D.3.

D.2 Filtered Faulted Voltage And Filtered Faulted Current Program: (Program 2)

This program is used to simulate the simple transmission line system under both pre-fault and post-fault conditions. The test model is either a single- phase or three-phase system. In both cases, a single-phase equivalent circuit is used to obtain the transient response of the faulted system as discussed in chapter 3.

This program contains two subroutines. The model simulation (i.e. the initial condition and the unfiltered voltage and the unfiltered current subroutine) and the low-pass digital filter (i.e. the filtered voltage and the filtered current subroutine). The flow chart of the model simulation of the initial condition and the unfiltered voltage and current is shown in figure D.4.

D.2.1 Model Simulation Routine:

The routine is straight forward, starting by setting the dimensions and the sampling rate, then the prefault voltage and current phases (which are obtained from the prefault steady state model), required to calculate the instantaneous current and voltage prior to the occurrence of a fault. The fault location is also an input to the program and can be

varied according to the user choice. According to the location of the fault, the differential equations of the faulted system are formulated. The equations which find the prefaulted voltage and current are solved using Runge-Kutta method. Then these quantities are stored and then used as an input to determine the filtered voltage and current.

D.2.2 Low-Pass Digital Filter Routine:

The low-pass digital filter is required to attenuate the high frequency harmonics which are present in the post-fault waveforms. A flow chart of the low-pass digital filter subroutine is shown in figure D.5. Difference equations of the three developed filters are formulated from their corresponding transfer functions. From these difference equations the filtered response is obtained. These filtered responses are stored to be used as an input to the main program in order to determine the fault location.

D.3 Main Program: (Program 3)

This program is used to locate the fault of the faulted model which is simulated in program 2. This program contains two subroutines, the impedance calculation subroutine and the fault location subroutine. The flow chart of the main program is shown in figure D.6. The inputs to this program are the total line length, entire line impedance, the order of the filter, the pseudoinverse matrix and the total number of the post-fault samples along with the respective current and voltage values. Equations (2.73) and (2.74) are used to calculate the impedance seen between the sending end of the line to the faulted point. The location of the fault is then determined from the computed reactance ratio using equation (2.75). This program continuously locates the fault till the last set of samples is

reached.

D.4 Summary

This appendix discusses the fault location techniques program briefly. A flow chart for each segment of the program is provided. As well an explanation of the details of each program is discussed. These programs were implemented on the AMDAHL/MTS system using FORTRAN as the programming language. Finally, the objective of the programs was to study the performance of the LAV and the LSV techniques in estimating fault locations in transmission lines.

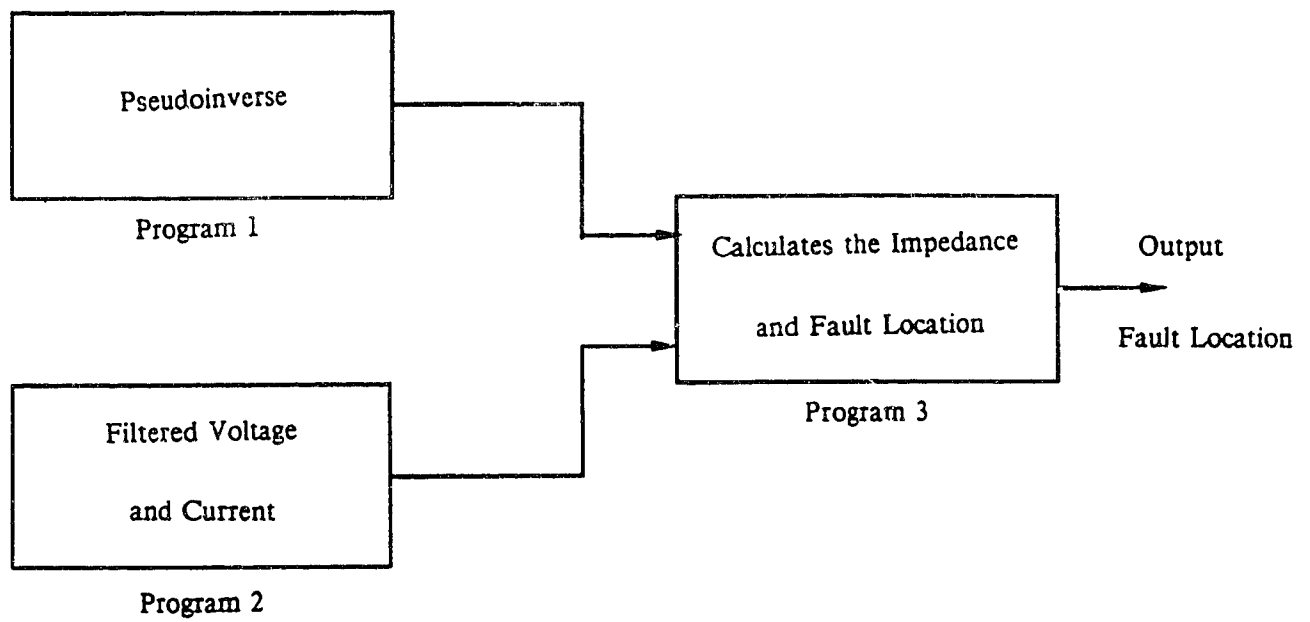


Figure D.1: A block diagram shows how the three programs are linked together.

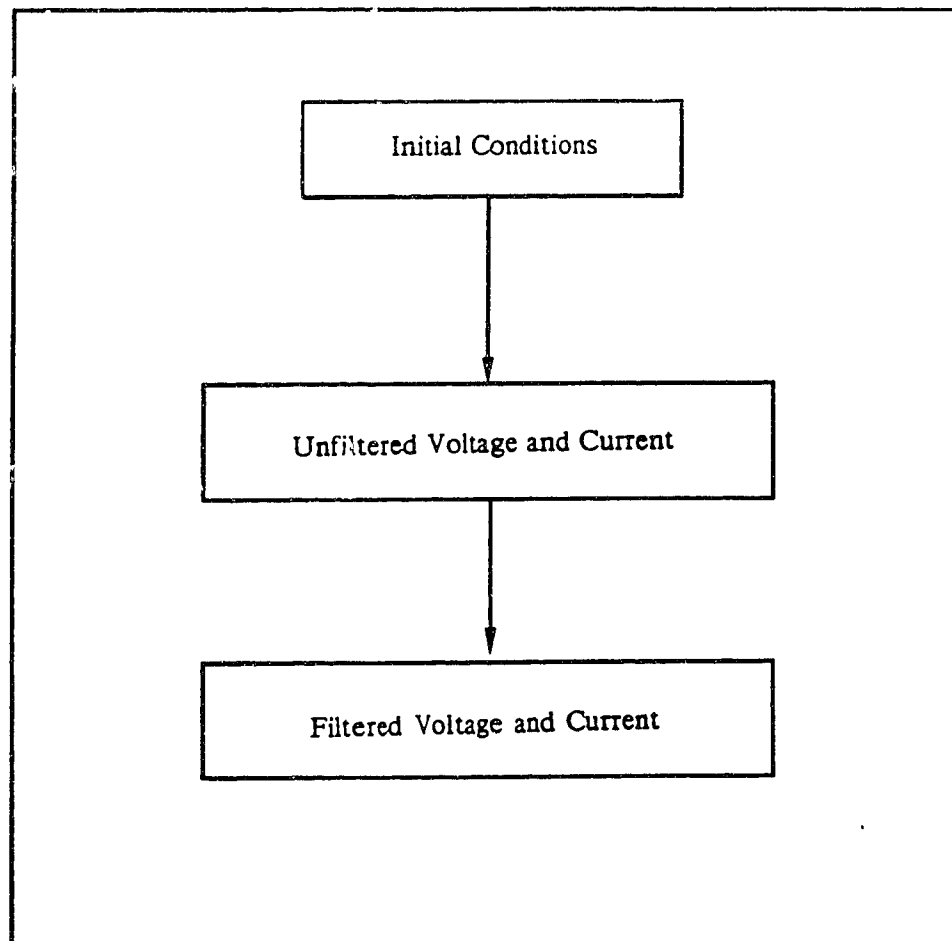


Figure D.2: A block diagram for program 2.

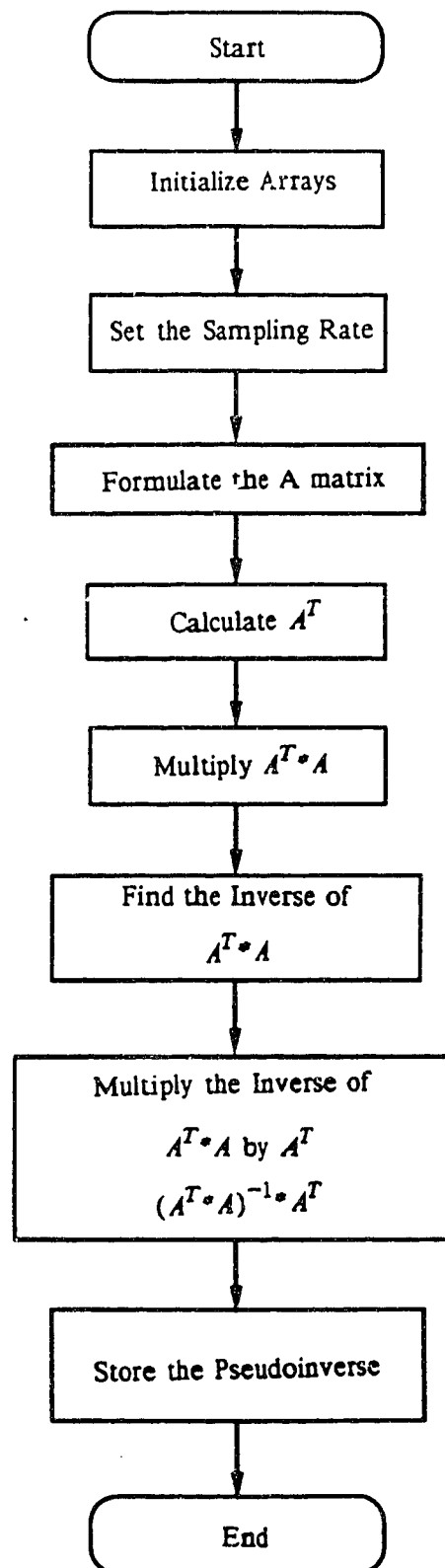


Figure D.3: Program 1, the flow chart of the pseudoinverse program.

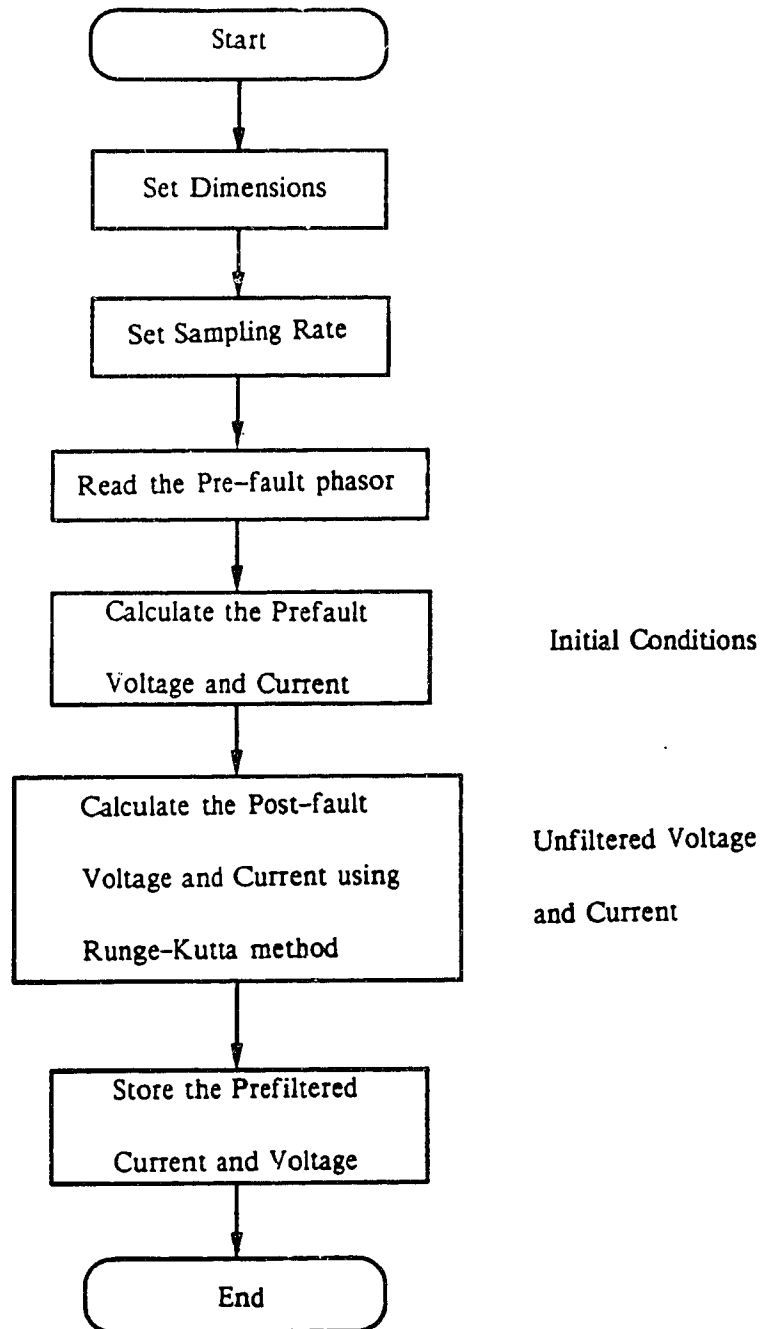


Figure D.4: Flow chart to determine and store the initial conditions and the unfiltered voltage and current.

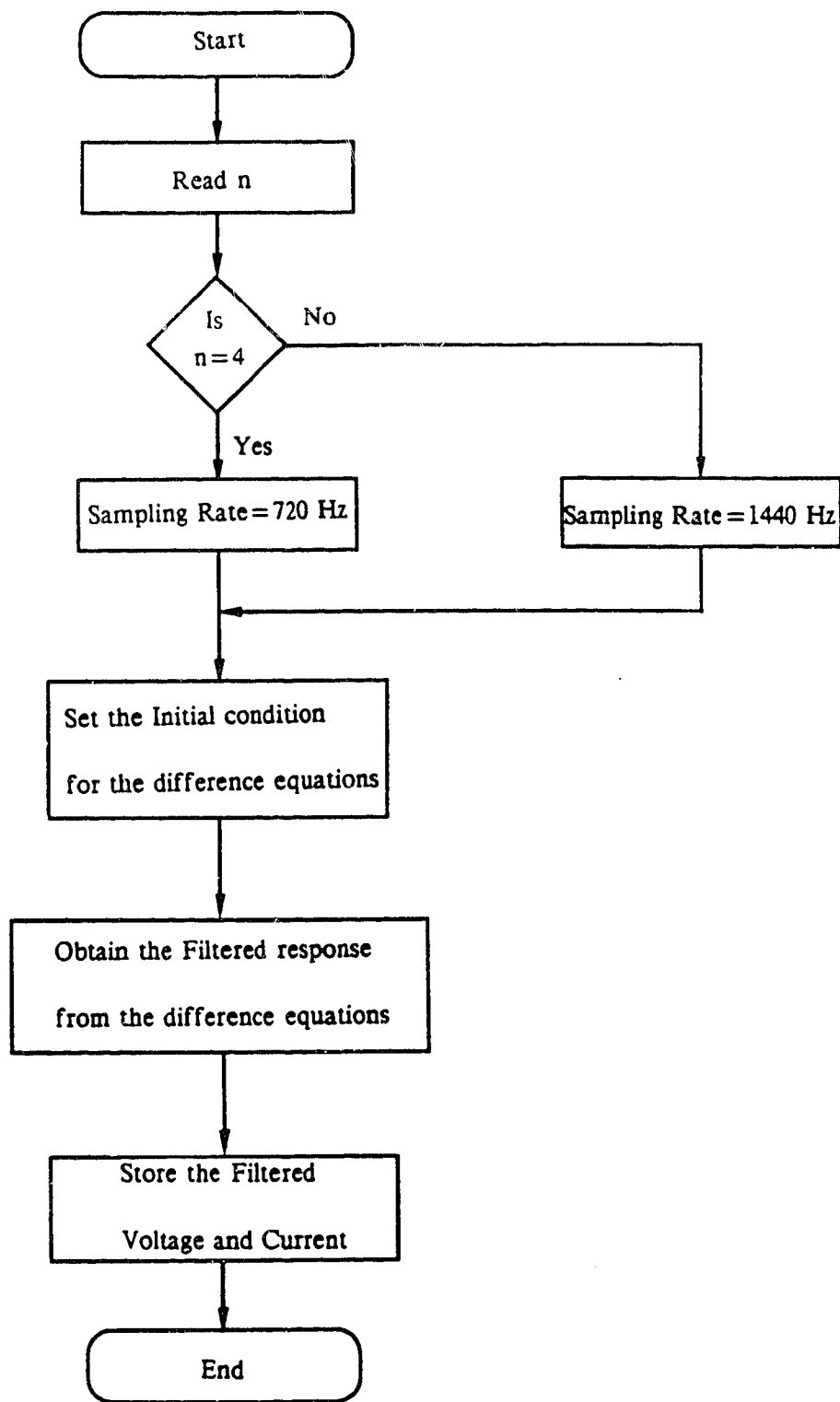


Figure D.5: Flow chart of low-pass digital filter routine.

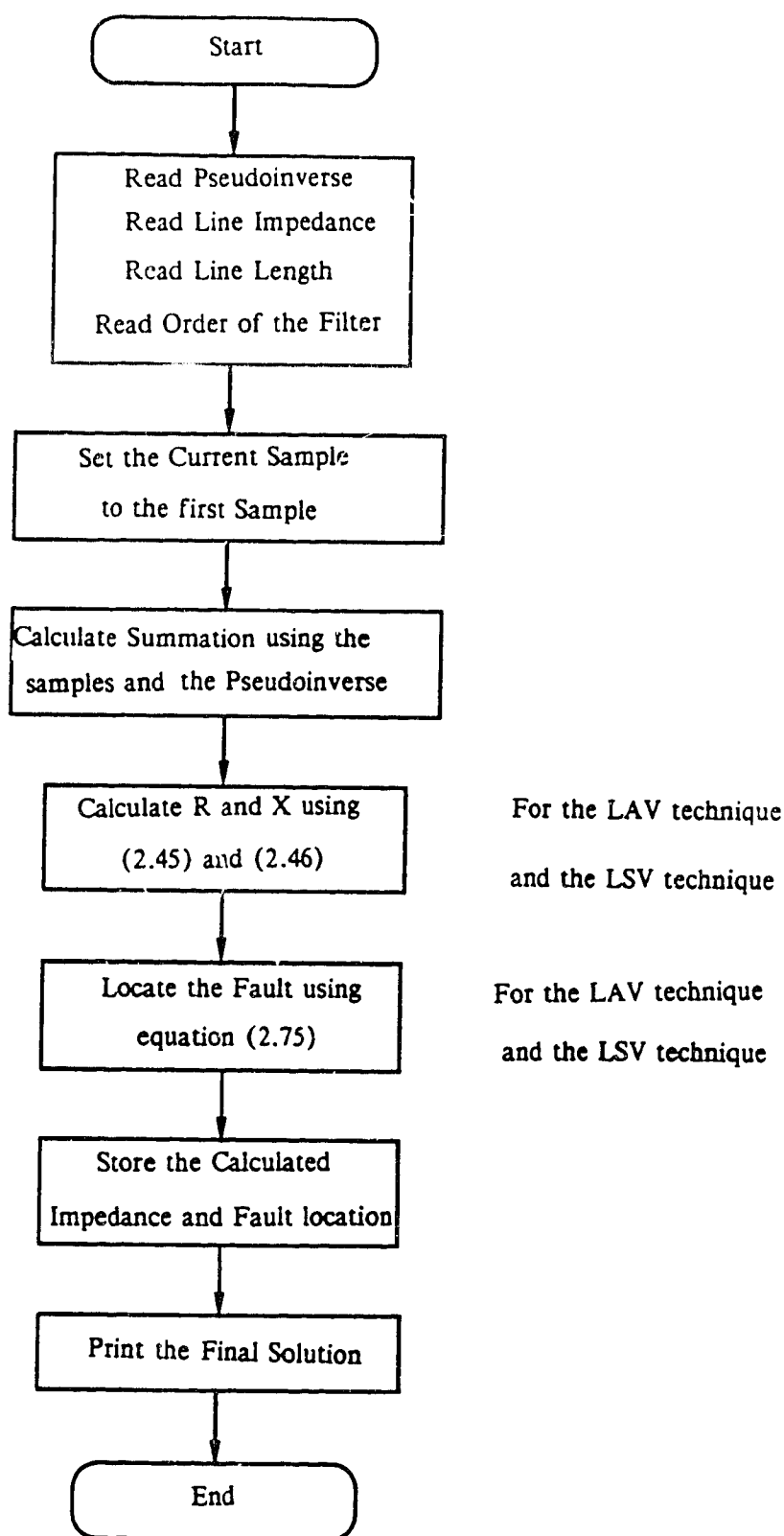


Figure D.6: Flow chart for the main program.

APPENDIX E

PSEUDOINVERSE

If a matrix is square, its inverse exists if it is a full rank matrix. For example, if we have the system below:

$$\underline{Y} = \underline{A} \underline{X} \quad (\text{E.1})$$

Where,

\underline{Y} is a known vector

\underline{A} is an rxn known matrix

\underline{X} is an unknown vector

If $r=n$ and \underline{A} is a full rank matrix, then the inverse of \underline{A} exists and we can solve for \underline{X} .

But if r is not equal to n , then \underline{A} is a rectangular matrix and the pseudoinverse solution must be used.

For instance, if $r > n$, the system is called an overdetermined system and the left pseudo inverse is used. On the other hand, if $r < n$, the system is called an underdetermined system and the right pseudoinverse is used.

Thus if $r > n$ in equation E.1, the left pseudoinverse is used.

Multiply equation E.1 by \underline{A}^T

$$\underline{A}^T \underline{Y} = \underline{A}^T \underline{A} \underline{X}$$

Premultiplying both sides by $(\underline{A}^T \underline{A})^{-1}$

$$\underline{X} = (\underline{A}^T \underline{A})^{-1} \underline{A}^T \underline{Y} \quad (\text{E.2})$$

Where $(\underline{A}^T \underline{A})^{-1} \underline{A}^T$ is the left pseudoinverse of the matrix \underline{A} .

If $r < n$ in equation E.1, the right pseudoinverse is used.

by noting that:

$$\underline{I} = (\underline{A} \underline{A}^T)(\underline{A} \underline{A}^T)^{-1}$$

then equation E.1 could be written as:

$$\begin{aligned} \underline{A} \underline{X} &= \underline{A} \underline{A}^T (\underline{A} \underline{A}^T)^{-1} \underline{Y} \\ \underline{X} &= \underline{A}^T (\underline{A} \underline{A}^T)^{-1} \underline{Y} \end{aligned} \quad (\text{E.3})$$

Where $\underline{A}^T (\underline{A} \underline{A}^T)^{-1}$ is the right pseudoinverse of \underline{A}

equation E.2 and E.3 both reduce to the conventional inverse equation when $r=n$.

APPENDIX F

The discrete system is more useful in this thesis than the continuous system. To transfer a system from the time domain to the frequency domain, either the Laplace transform (continuous) or the Z-transform can be used. It is efficient to use Laplace transform (i.e S-transform) for continuous signals and Z-transform for sampled signals. Because if a continuous signal is to be transferred to Z-domain, it must be transferred first to S-domain and then to Z-domain and vice-versa.

The differences, which are our concern here, between S-domain and Z-domain are listed below:

First, for the S-domain:

1. Uses differential equations.
2. Signals are continuous.

Second, for the Z-domain:

1. Uses difference equations.
2. Signals are sampled.
3. $Z = e^{sT}$ in terms of S.